SYNTHESIS, CHARACTERIZATION AND CATALYTIC PROPERTIES OF SOME TITANIUM AND ZIRCONIUM CONTAINING MOLECULAR SIEVES

A Thesis
Submitted to

THE UNIVERSITY OF PUNE

for the degree of

DOCTOR OF PHILOSOPHY
(IN CHEMISTRY)

By

D. P. SABDE
CATALYSIS DIVISION
NATIONAL CHEMICAL LABORATORY
PUNE - 411 008, INDIA

AUGUST-2000

CERTIFICATE

Certified that the work incorporated in the thesis entitled "**Synthesis, Characterization and Catalytic Properties of some Titanium and Zirconium containing molecular sieves**" submitted by **Mr. D. P. Sabde** for the degree of Doctor of Philosophy was carried out by the candidate under my supervision in the National Chemical Laboratory, Pune. Such material as has been obtained from other sources has been duly acknowledged in the thesis.

Dr. M. K. Dongare
(Research guide)

ACKNOWLEDGEMENTS

I wish to express my deep sense of gratitude to my research guide, Dr. M. K. Dongare, for his valuable guidance, support and encouragement throughout the course of the investigation.

I am deeply indebted to Dr. S. G. Hegde for his inspiring discussions, guidance, constant help and support.

I am greatful to Dr.A.V. Ramaswamy, the head of catalysis division, for his constant help, advice and encouragement during my research work.I owe enormous debt of gratitude to Dr S. Sivasanker for his valuable support and motivation.

I am grateful to Dr. C. Gopinathan, Dr.(Mrs.) Gopinathan, Dr.(Mrs.) Veda Ramaswamy, Dr. H. S. Soni, Dr.S. P. Mirajkar, Dr. P. R. Rajamohanan and Dr. Sainkar for their help co-operation and encouragement.

I also wish to thank Dr. Shaikh, Mr. Bokade, Dr.(Mrs) Belhekar, Ms. Agashe, Ms.Awate, Dr.(Mrs.) Kamble, Dr.(Mrs.)Pardhay, Mr.Sahapure, Ms. Violet, Mr. K. Ramakrishnan and Mr. Mulla for their support and encouragement.

I take this opportunity to thank Dr. Kalkote, Dr. Bhawal, Dr.Wadgaonkar, Dr.A. Sudalai and Mr. Dahibhate for their valuable support and guidance.

I sincerely thank Ms. Sharda, Mr. Vijay, Ms. Jainy, Mrs. Sushma Kale, Mr. Gore, Mr. Joshi, Mr Tope and Mr. Kuriyawar for their whole-hearted cooperation and help that made it possible to complete my research work.

My most heartfelt thanks are due to Mr. Khatke, Mr. Gote, Mr. Mali, Mr. Anand Rai Mr. Vivek Bulbule, Mr Mahesh Patil, Mr. Santosh Birajdar and Mr Nandkumar Patil for their whole-hearted cooperation and help.

I sincerely thank my friends, Dr. Tapas Sen, Dr. Kannan, Dr Katdare, Dr. Sinha. Dr. P. Mukherjee, Dr. K. Choudhary Dr. Shevde, Dr. Vinod, Mr. Waghmode, Ms.Sindhu, Mr.Rajaram Bal, Mr Anand, Mr Siju, Mr Thomas, Mr. Laha, Mr Mandal, Mr Patra, Ms. Vandana and Ms. Jaimol for their cooperation and constant support, which gave me the necessary inspiration to fulfil my task.

Those who have helped me in different ways are far too numerous to mention by name but I would like them to accept my sincere thanks.

I am indebted to my brothers Adv. Bharat and late. Dinesh, and all other family members for their cooperation and constant encouragement. I specially thank my wife Rupali, for her inspiration and cooperation.

I thank the Director, National Chemical Laboratory for his kind permission to submit my work in the form of thesis. I also take this opportunity to pay my gratitude towards CSIR, for extending financial assistance by awarding me senior research fellowship.

(D. P. SABDE)

CONTENTS

1.1 INTRODUCTION

Catalyst technology has increasingly played a key role in the economic development of countries around the world during the 20th century. The catalytic production of chemicals and fuels contributes to the worldwide economy by over 10 trillion dollars per year[1]. Today, most of the chemicals, polymers, drugs, dyes and fabrics are prepared by using catalysts; the success of these chemical industries is based purely on catalyst technology. Nearly 95 % of all the processes used in the chemical industry are catalytic in nature.

Catalyst technology, in principle, was in vogue for centuries on a small scale to produce foodstuff, wines and beverages. It was in the early part of the nineteenth century, that Berzelius first discovered the catalysis phenomenon. Since then the field of catalysis has been an intriguing and continuing area of development and efforts have been on to understand and utilize it for practical purposes. The discovery of new catalysts and their applications has historically led to major innovations in chemical processing. Some of the major catalytic processes developed during the last 50 years are given in Table-1.1.

The beginning of catalyst technology in the modern sense was the large-scale production of sulfuric acid on platinum catalyst in 1875, which was followed by the production of nitric acid and the synthesis of ammonia. The Fischer-Tropsch technology, which was developed later, made possible the efficient utilization of CO for the production of hydrocarbons, liquid fuels and other chemicals. With the discovery of Ziegler-Natta catalyst in 1955, the polymer industry came into its own.

Then came another significant process- catalytic cracking, using solid acid catalysts, which boosted the petroleum industry by increasing the gasoline yield and efficiently using petroleum feedstock. Other catalytic processes, such as naphtha reforming and hydrotreating,

also contributed to the prosperity of the petroleum industry.

Table 1.1

The development of important industrial catalytic processes in last 50 years

Year	Process	Catalyst	Area of industry
1950	Mono-metallic reforming	$Pt\text{-}Al_2O_3$	Petroleum
1955	Polymerization	$TiCl_3$ / $Al(R)_3$	Chemicals
1960	Wacker process	$PdCl_2$	Chemicals
1962	Steam reforming	$Ni\text{-}K\text{-}Al_2O_3$	Petroleum
1964	Cracking on zeolites	X, Y zeolites	Petroleum
1967	Multi-metallic reforming	Pt-Re, Pt-Ir-Cu	Petroleum
1974	Carbonylation	Rh-I	Chemicals
1976	Auto emissions control	Pt, Pd or Rh/Al_2O_3	Auto-emission control
1980	Selective catalytic reduction	VO_x-TiO_2, Zeolites	Environmental control
1988	Selective oxidation	Ti- Silicalite	Chemicals
1988	Chiral catalysts	Cinchonidine-Pt; BINAP	Chemicals
1991	Polymerization	Metallocenes	Chemicals
1980-95	Shape selective reactions	ZSM-5, New zeolites	Chemicals
1980-2000	Organic Chemicals	Various heterogeneous catalysts	Chemicals

Together with the solid acid catalysts, processes utilizing homogeneous catalysts were also developed, they were applicable in hydrogenation, disproportionation, carbonylation, oxidation, polymerization and many other processes.

The development of crystalline alumino-silicate (zeolites) and its applications in the petroleum industry was very significant as it affected the global economy. Zeolites were found useful in detergents due to their ion exchange capacity, in catalysis due to their acid-base properties and in adsorption and separation processes due to their molecular sieving properties. The increasing assemblage of different zeolite catalysts along with multiplicity of new reactions were explored in many industrial applications. The new zeolite based catalytic processes are making efficient use of energy and raw materials with minimal impact on the environment. Such catalysts are also contributing to solve the environmental problems such as removal of hydrocarbons, carbon monoxide and nitrogen oxides from waste and exhaust gases.

Zeolites are crystalline hydrated alumino-silicates, possessing a rigid three- dimensional framework constituted by corner sharing of all the four oxygen atoms of SiO_4 and AlO_4^- tetrahedral primary building units[2]. According to the Lowenstein's rule, two Al atoms cannot share the same oxygen, i.e., two Al tetrahedra are not near neighbors. The framework contains channels or interconnected voids that are occupied by the cations and water. Each AlO_4^- unit in the framework bears a net negative charge, which is balanced by a cation. These cations are

mobile and can undergo ion exchange. The water may be removed reversibly leaving the crystalline framework structure unaltered. Depending on the type of zeolites, the pore size and connectivity pattern varies[2]. The crystallographic unit cell of a zeolite[3] may be represented as $M_{x/n}$ $[(AlO_2)_x$ $(SiO_2)_y].zH_2O$, where 'M' is the cation of valence 'n', x and y are the moles of AlO_2 and SiO_2 units respectively and z is the number of water molecules. Zeolites are classified according to their morphological characteristics[2-5], crystal structure[3,4,6], effective pore diameter[3,4,7], chemical composition[3,4,8] and natural occurrence[3,4].

The formation of porous crystalline material is not restricted to Si and Al oxides, but can also be formed by the oxides of a number of other elements (for example, P, Ti, V, Cr, Zr, B, Ge, Ga etc). The compositional and structural range of molecular sieves are significantly increased by the discovery of crystalline alumino-phosphate based frameworks[9]. Such materials are denominated by their inventors with the acronym AlPO-n. The AlPO-n molecular sieves are composed of AlO_4^- and PO_4^+ tetrahedra, which are linked to form different three-dimensional neutral frameworks. Incorporation of Si or some other metal in the AlPO-n framework gives rise to silico-aluminophosphate (SAPO-n) and metal-aluminophosphate (MeAPO-n) frameworks, having the chemical compositions $(Si_xAl_yP_z)O_2$ and $(Me_xAl_yP_z)O_2$, respectively, where x, y and z are moles of the respective oxides. The simultaneous incorporation of both Si and metal in aluminophosphate framework (MeAPSO-n) further extends the structural diversity and compositional variations.

AlPO-n molecular sieves have many similarities to silicates. (i) They are iso-electronic with SiO_2, (ii) The average ionic radii[10] of Al^{3+} (0.39nm) and P^{5+} (0.17nm), i.e., 0.28nm is very close to that of Si^{4+} (0.26nm), and, (iii) They can form isomorphic dense phases like α and β quartz, crystobalite and α, β and γ tridymite. These molecular sieves are classified, on the basis

of the effective pore diameter, into major groups such as small pore, medium pore, large pore and ultra large pore with respect to the ring with maximum number of oxygen atoms.

No systematic nomenclature has been developed for molecular sieve materials. The discoverer of these novel materials characterized them based on X-ray diffraction study and chemical composition, and assigned trivial symbols. Milton, Breck and other workers used the Arabic alphabets (e.g., zeolite A, L, X and Y). Mobil and Union Carbide scientists initiated the use of Greek alphabets (e.g., zeolite alpha, beta and omega). Some are named after the center of invention (e.g., UTD-1, NCL-1, EU-1, VPI-5, etc.). Many of the synthetic zeolites whose topology resembles that of mineral zeolites are assigned the name of the mineral (synthetic Mordenite, Chabazite, Erionite, etc.). In 1979 the International Zeolite Association (IZA) and International Union of Pure and Applied Chemistry (IUPAC) assigned[11] a three-letter code for the known topologies, irrespective of composition, e.g., 'MFI' for ZSM-5, 'MEL' for ZSM-11, 'AFI' for AlPO-5 and 'AEL' for AlPO-11. Some of the most important structure types with their physical properties are listed in Table-1.2.

1.2 SYNTHESIS OF MOLECULAR SIEVES

1.2.1 Zeolite-based molecular sieves

The remarkable catalytic and adsorption properties of certain natural zeolites were recognized already in the middle of the nineteenth century, but were not available in quantities large enough for the industrial applications. Therefore, Barrer & coworkers[3], in the early 1950's, found a synthetic method for the preparation of zeolites in large quantities. The process of zeolite synthesis involved the formation of an intermediate aluminosilicate gel, which after an induction period under hydrothermal conditions formed zeolite crystals. Sand[12] has summarized the important steps in zeolite crystallization. It consists of precipitation of gel phase, dissolution of gel,

nucleation of zeolite structure, crystallization and crystal growth of the final crystalline phase.

Apart from the above factors, the structure directing agents (organic templates) also play an important role in the crystallization of many of the known zeolite molecular sieve structures. These organic species get trapped inside the pores of the zeolite after crystallization and act as structure directing templates, besides being void fillers.

Table 1.2

Classification of some molecular sieves according to the size of pore opening.

Type of molecular sieve	Type of structure	Framework composition	Ring size[a]	Pore opening (Å)	Channel dimension
Small pore					
Linde type A	LTA	Alumino-silicate	8-8-8	4.1	3
Erionite	ERI	Alumino-silicate	8-8-8	3.5 x 5.1	3
AlPO-34	CHA	Alumino-phosphate	8-8-8	3.8	3
Medium pore					
ZSM-5	MFI	Alumino-silicate	10-10-10	5.3 x 5.6	3
ZSM-11	MEL	Alumino-silicate	10-10-10	5.3 x 5.4	3
AlPO-11	AEL	Alumino-phosphate	10	3.9 x 6.3	1
Large pore					
Faujasite X/Y	FAU	Alumino-silicate	12-12-12	7.4	3
Beta	BEA	Alumino-silicate	12-12	7.6 x 6.4	3
Mordenite	MOR	Alumino-silicate	12-8	6.5 x 7.0	2
AlPO-5	AFI	Alumino-phosphate	12	7.3	1

Ultra large pore					
AlPO-8	AET	Alumino-phosphate	14	7.9 x 8.7	1
VPI-5	VFI	Alumino-phosphate	18	12.1	1
Cloverite	CLO	Gallo-phosphate	20-8	13.2	3
MCM-41	-	Alumino-silicate	>18	>20 to 100	1

a: Number of T or O atoms comprising largest rings in channel

The organic species can interact physically with the gel components and thereby alter the gelling process, solubility of the various species, aging characteristics, crystallization time, transport properties and interactive energies. The templates may be charged or neutral, Moretti et al[13] has reported a wide variety of neutral and ionic organic amines for the synthesis of various zeolites having different structures. The role of the template may be to act as a donor of the hydroxyl ion, increase the solubility of aluminate, silicate and other metal ions, organize the water molecule, stabilize the structures with meta-stable state and balance the framework charge.

1.2.2 Aluminophosphate based molecular sieves

The aluminophosphate molecular sieves, like zeolites are also synthesized hydrothermally. However, the initial pH of the reactive gel is weakly acidic to moderately acidic in contrast to alkaline medium for the aluminosilicate. The lower pH facilitates the incorporation of other elements in the lattice of these materials than in the case of zeolites[14, 15]. They are synthesized in the range of 100 to 250^{0}C from a reactive gel containing sources of aluminum, phosphorous and

an organic amine or quaternary ammonium salt, which gets entrapped within the crystalline products. The typical molar gel composition used is 1-3R: Al_2O_3: P_2O_5: 40-100 H_2O, where R is template. The synthesis procedure involves aluminophosphate gelation, nucleation of active gel and crystallization.

The entrapped template species are removed by thermal decomposition. Most of the aluminophosphate molecular sieves remain crystalline after calcination at around 400-600^{0}C, i.e. the temperature required to burn out the template. The removal of the template is necessary for making the intra-crystalline void volume available for adsorption and catalysis. A single template can give rise to many aluminophosphate structures and a variety of templates can be used to synthesize a single structure type. For example, AlPO-5 and AlPO-11 structure types are synthesized by using a large variety of organic templates; a single template like tetrapropyl ammonium hydroxide can produce various structure types like AlPO-5, SAPO-5 and SAPO-40. Not only the template, but variables such as gel composition, pH, temperature and time also influence the crystallization of a particular structure.

1.3 ISOMORPHOUS SUBSTITUTION

In recent years the isomorphous substitution in zeolite and alumino-phosphate materials by other elements has been extensively studied and reviewed[16-18]. Isomorphous substitution of elements in these materials is carried out in order to modify their catalytic and shape selective properties. Different ways to perform such substitutions are well established, either during hydrothermal synthesis or by post-synthesis method in liquid and vapor phase. Generally, hydrothermal synthesis is preferred over post synthesis because it leads to better incorporation of a wide variety of metal ions. The post synthesis method of Fe^{3+} and Ti^{4+} incorporation in the liquid phase into the framework of various zeolites is reported using corresponding metal salts[19].

In the vapor phase method the zeolite is subjected to dealumination and then treated with vapors of a volatile compound of the metal to be incorporated[20].

It has been found that the di-, tri-, tetra- and pentavalent metal ions can all replace the framework tetrahedral sites in molecular sieves. They can also occupy one or more of the following positions in the zeolite, such as, defect sites, cation exchange sites, inside the pores or on the external surface as finely dispersed metal oxides and as bulk oxide on external surface. This results in different catalytic properties and may even lead to bifunctional catalysis.

In the case of zeolites, the isomorphous substitution is mainly for Al but in aluminophosphates, it can happen in three different ways.[14,21].

a) Substitution for only Al atoms (SM1),

b) Substitution for only P atoms (SM2) and

c) Substitution for a pair of Al and P atoms (SM3)

The partial substitution of P^{5+} with Si^{4+} by SM2 mechanism results in the formation of Al-(OH)-Si type linkages wherein the bridging hydroxyl groups are formed generating Brönsted acidity in the resulting aluminophosphate. The SM3 type of substitution is observed in silico-aluminophosphates (SAPO-n), wherein two Si atoms replace the isolated pair of adjacent Al and P atoms. This type of substitution results in the formation of Si(1Si 3Al) and Si(1Si 3P) environments. SM1 mechanism is unlikely to form, as it involves the formation of Si-O-P linkages, which is unstable in hydrothermal conditions.

The possibility of isomorphous substitution and stability of a particular metal ion in the zeolite tetrahedral framework is governed by Pauling's theory[22]. According to this, for cations whose ρ (radius ratio of cation to oxygen) is out of the specific range ($0.414 > \rho > 0.225$) the substitution is either impossible or should take place to a lesser extent. However metal ions such

as Fe^{3+}, Ti^{4+}, Ga^{3+}, Sn^{4+} and V^{5+} whose ρ values are out of this range have been successfully incorporated into the framework. Probably the geometrical parameters become less important than other factors under such crystallization conditions. For this reason it is difficult to identify simple criteria for predicting the ability of a given element to be incorporated in the silica or aluminophosphate framework. The critical values of the parameter ρ (ρ_{crit}) for selected cations are listed in Table-1.3 and some of the Ti and Zr containing molecular sieves are listed in Table-1.4[23-43].

1.4 STRUCTURE OF MOLECULAR SIEVES

The framework topology of a particular molecular sieve is described on the basis of the size of the pore opening and dimension of the channel system. The pore opening is described by the size of the ring defining the pore, which is designated as n-rings, where 'n' is the number of T atoms (or oxygen atoms) in the ring.

Table-1.3

Pauling's critical values (ρ_{crit}) for various coordination numbers for selected ions.

Critical values (ρ_{crit})	Coordination number	Cations with the expected coordination number
$\rho_{Crit} > 0.732$	8	Bi^{3+}, Ce^{2+}, Ce^{3+}, Nd^{3+}, Pb^{2+}, Sn^{2+}, Tl^{3+}.
$0.732 > \rho_{crit} > 0.414$	6	As^{3+}, Bi^{5+}, Co^{2+}, Cr^{3+}, Cr^{2+}, Fe^{2+}, Fe^{3+}, Ga^{3+}, Hf^{4+}, In^{3+}, Mn^{2+}, Mn^{4+}, Mo^{6+}.,Sb^{5+}, Sn^{4+}, Ta^{5+}, Ti^{3+}, Ti^{4+}, V^{4+}, V^{5+}, Zn^{2+}, Zr^{4+}
$0.414 > \rho_{crit} > 0.225$	4	Al^{3+}, As^{5+}, Be^{2+}, Cr^{6+}, Ge^{4+}, Mn^{2+}, P^{5+}, Se^{6+},

		Si^{4+}.
$0.225 > \rho_{crit} > 0.147$	3	B^{3+}

Table-1.4

Silicates, aluminophosphates and silico-aluminophosphates with Ti and Zr as heteroatoms in the framework

Element	Metallo-silicate or Metal-aluminophosphate (Structure code)	References
Titanium		
	Silicates	
	ZSM-5 (MFI)	[23] Taramasso et. al.
	ZSM-11 (MEL)	[24] Reddy et. al.
	ZSM-12 (MTW)	[25] L. Yu et. al.
	ZSM-48	[26] Dartt et. al.

Beta (BEA)	[27] Camblor et. al
ETS-10	[28] Anderson et. al
UDT-1	[29] Balkus et. al.
HMS	[30] Tanev et. al.
MCM-41	[31] Blasco et. al.
MCM-48	[32]Corma et. al.
Aluminophosphates	
AlPO-5 (AFI)	[33] Ulagappan et al
AlPO-11(AEL)	[33] Ulagappan et al
AlPO-34(CHA)	[34] Marchese et. al
SAPO-34(CHA)	[34] Marchese et. al
AlPO-36(ATS)	[35] Zahedri et. al.
Zirconium Silicates	
ZSM-5 (MFI)	[36] Dongare et. al.
ZSM-11(MEL)	[37] Sabde et. al.
Beta (BEA)	[38] Rakshe et. al.
M14S	[39] Tuel et. al.
Zr-MCM-41	[40] Vercruysse et. al.
Aluminophosphates	
AlPO-5 (AFI)	[41] Dongare et. al.
SAPO-11(AEL)	[42] Meriadeau et. al.
AlPO-11(AEL)	[43] Sabde et. al.

1.4.1 Zeolite based molecular sieves: Structure of ZSM-5 and ZSM-11

ZSM-5 and ZSM-11 are two important types of high silica zeolites. Their building blocks are formed from pentasil units linked through edges to form chains and these chains are connected to form corrugated sheets. These sheets link to form a three-dimensional framework. Unlike others, these zeolites have pores of uniform dimension and have no large super cages.

ZSM-5 consists of two intersecting channels formed by rings of 10 Oxygen atoms[44-46].

These two channels have slightly different pore dimensions. One runs parallel to the a-axis of the unit cell, which is sinusoidal and nearly of circular dimension (5.4 x 5.6 Å). The other runs parallel to the b-axis and has a straight but elliptical opening with dimensions 5.1 x 5.5 Å. These channels intersect to form a three dimensional 10 ring channel system. As the pore opening of ZSM-5 is different compared to large pore zeolites (FAU and Beta), the shape-selectivity, sorption capacity and catalytic activity are distinctly different. The less-deactivating characteristic of ZSM-5 is one of the important factors useful in industrial applications.

ZSM-11 contains two straight elliptical channels, intersecting at right angles to each other[47,48]. Both the channels are of dimension 5.1 x 5.5 Å. ZSM-5 and ZSM-11 can be conveniently differentiated through X-ray diffraction profiles, which are discussed later in detail. The topological details of the ZSM-5 and ZSM-11 are illustrated in the Figs. 1.1 and 1.2, respectively.

STRUCTURE OF ZSM-5 (MFI)

Chemical Composition	$Na_n[Al_nSi_{96-n}O_{192}] \sim 16\ H_2O$
Symmetry	Orthorhombic
Unit cell constants	a = 20.1, b = 19.9 and c = 13.4 Å
Space Group	Pnma
Pore Structure	10 membered ring structure ; 5.1 x 5.5 Å [100]
	5.6 x 5.3 Å [010]

Channel System Three dimensional

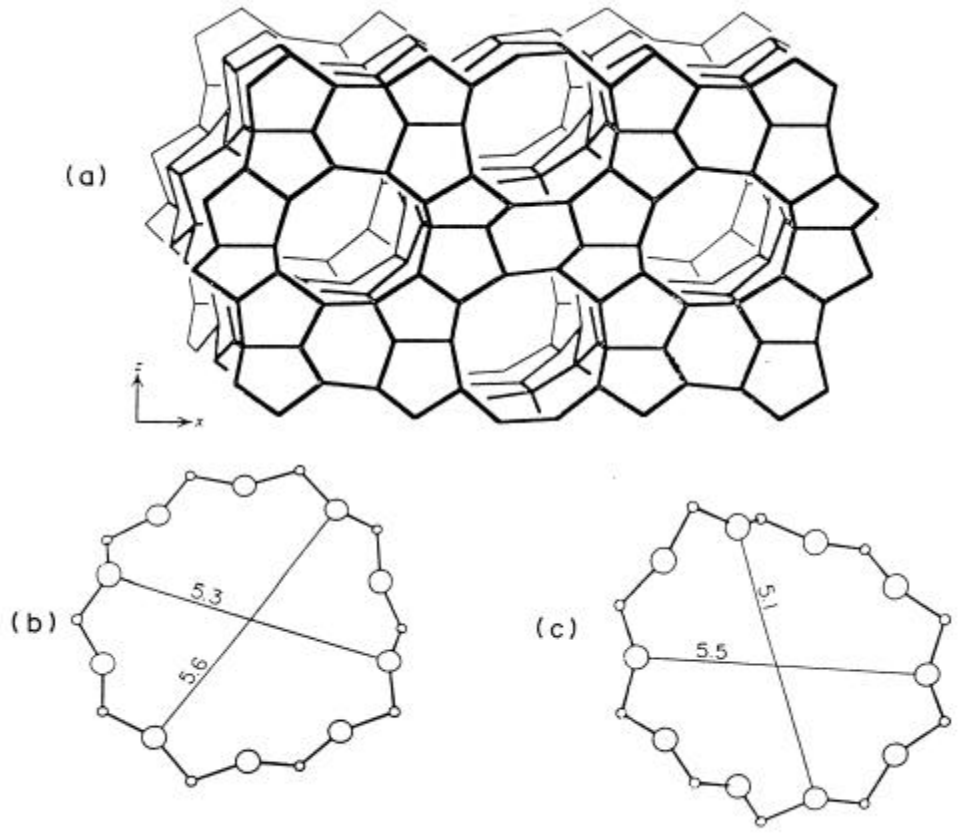

Fig. 1.1 Structure of ZSM-5 a) The MFI framework topology b) 10-ring viewed along [010] (Straight channel) and c) 10-ring viewed along [100] Sinusoidal Channel

STRUCTURE OF ZSM-11 (MEL)

Chemical Composition	$Na_n[Al_nSi_{96-n}O_{192}] \sim 16\ H_2O$
Symmetry	Tetragonal
Unit cell constants	a = 20.1 and c = 13.4 Å
Space Group	I4m2
Pore Structure	10 membered ring structure ; 5.3 x 5.4 Å [100]

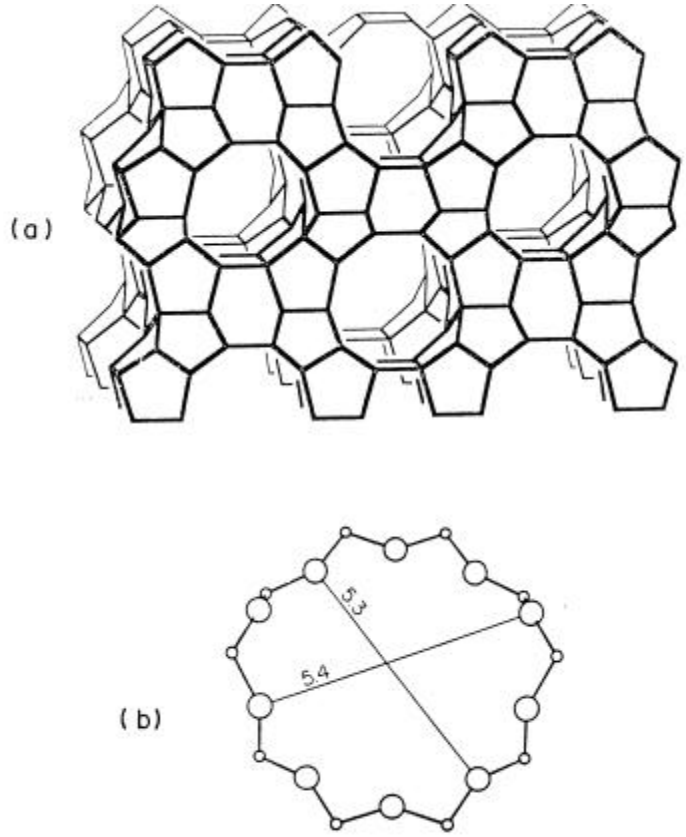

Channel System Three dimensional

Fig. 1.2 Structure of ZSM-11 a) The MEL framework topology and b) 10-ring viewed along [100]

1.4.2 Structure of AlPO-5 and AlPO-11

The AlPO-5 structure consists of alternating Al and P atoms forming 4- and 6- member rings. The pore system consists of non-connecting parallel channels of 12-member rings[49,9].

The AlPO-11 topology consists of sheets of 6-ring-6-ring-4-ring units[50,51]. Three vertices ofeach

tetrahedron are linked to form sheets containing 4-, 6- and 10-rings. By linking the remaining vertices, which project alternately up and down normal to these sheets, a three-dimensional framework is produced. The 10-membered straight channel has side pockets, which are double 6-membered channels. The structural features of the AlPO-5 and AlPO 11 are illustrated in Figs. 1.3 and 1.4, respectively

STRUCTURE OF AlPO-5 (AFI)

Chemical Composition $Al_{12}P_{12}O_{48}$

Symmetry	Hexagonal
Unit cell constants	a = 13.726, c = 8.484 Å
Space Group	P6cc
Pore Structure	12 membered ring structure ; 7.3 Å [001]

(a)

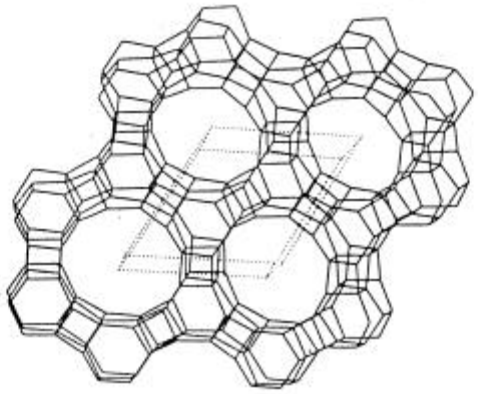

(b)

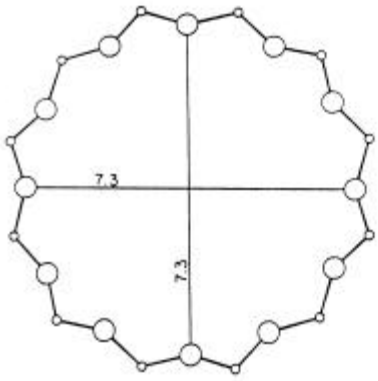

Channel System	One dimensional

Fig. 1.3 Structure of AlPO-5 a) The AFI framework viewed along [001] and b) 12-ring viewed along [001]

STRUCTURE OF AlPO-11 (AEL)

Chemical Composition	$Al_{20}P_{20}O_{80}$
Symmetry	Orthorhombic
Unit cell constants	a = 8.4, b = 18.5 and c = 13.5 Å
Space Group	Imma
Pore Structure	[100] 10 membered ring structure ; 3.9 x 6.3 Å

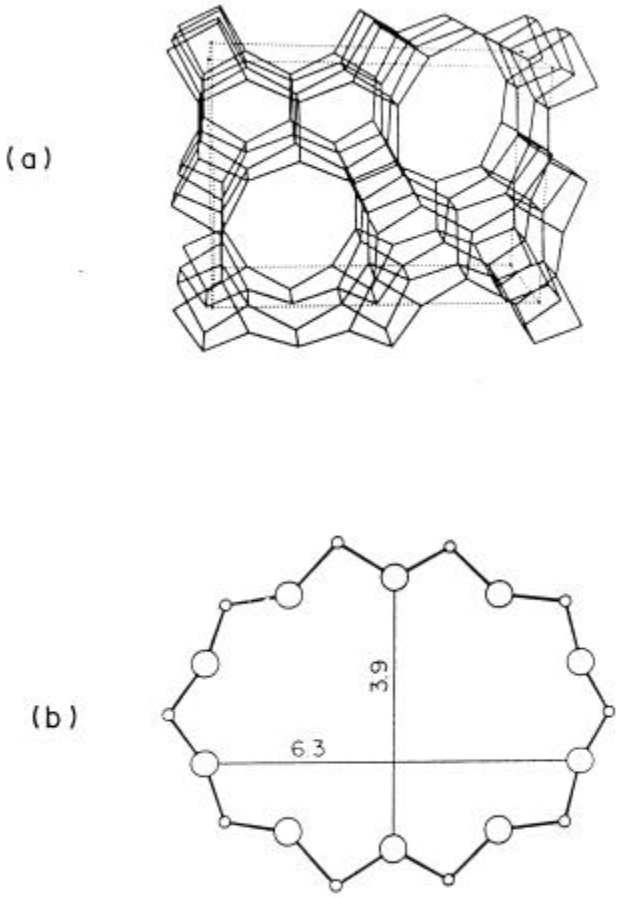

Channel System — One dimensional

Fig. 1.4 Structure of AlPO-11 a) The AEL framework topology viewed along [100] and b) 10-ring viewed along [100]

1.5 SHAPE SELECTIVITY IN MOLECULAR SIEVES

Zeolites have a well-defined pore structure with confined active sites responsible for catalysis. The pore size and shape of the zeolites are responsible for shape selectivity in different reactions. Shape selective catalysis provides specific, desired pathways leading to desired products in hydrocarbon processing and synthesis of chemicals. P.B. Weisz et al[52] coined the term "shape selective catalysis" to describe the catalytic properties of molecular sieves. A number of comprehensive reviews and discussions on the principles and applications have been reported[53-57]. Csicsery[58] has categorized the three main shape selective effects; the first two are related to mass transfer limitations and the third is concerned with spatial limitation of transition-state.

1.5.1 Reactant shape selectivity

When the operative pore size of the zeolite is such that it excludes larger molecules present in the reactant and admits only certain smaller molecules, only such small molecule react within the pore. This preferential transformation of the smaller molecules is called reactant shape selectivity. This type of selectivity is observed during the dehydrogenation of mixed alcohols, cracking of n-butanes and branched butanes over small pore zeolites[52,59] and the hydrogenation of cyclo-hexene and cyclodecene over a zeolite supported catalyst[60]

1.5.2 Product shape selectivity

This type of selectivity occurs when some of the compounds formed within the pores are too bulky to diffuse out as products. The bulky product molecules may undergo secondary reactions to smaller molecules or may block the catalyst pores resulting in the deactivation of the catalyst. The products formed in this case are due to restricted diffusivity of the products during the course of the reaction, thus creating selectivity towards the product of a certain dimension. A

classical example of this type of selectivity is the preferential formation of p-xylene during the reaction of methylation of toluene[61-62] and the monomolecular isomerization of alkyl aromatics over ZSM-5 catalysts.

1.5.3 Restricted transition state selectivity

When the reaction occurs inside a confined micropore of a catalyst, the geometry of the pore imposes a steric restriction on the transition state, which is too bulky to be accommodated within the pores/ cavities of the zeolites. In such cases, neither the reactants nor the products are restricted from diffusing through the pores of the zeolite. Examples of this type of selectivity are the trans-alkylation of dialkyl benzenes[63,64] and alkylation of naphthalene over mordenite catalyst[65].

Different researchers have proposed various other types of shape selectivities. Derouane et. al[66] proposed a shape selectivity, referred as molecular traffic control type, which occurred in zeolites containing intersecting channels of different diameters. In this type of selectivity the reactants enter preferentially through one set of channels and the products diffuse out through the other, thus minimizing counter diffusion.

Recently Guisnet et. al[67] reported tunnel type of shape selectivity. This type of selectivity is observed only in mono-dimensional molecular sieves like MCM-41 type. The reactant molecule before desorption undergoes various successive reactions in regular, non-connecting long channels. In addition to the above-mentioned selectivities, there are a few other common effects responsible for selectivity in zeolites, such as concentration effect[68], molecular circulation[69], nest effect[70] and energy gradient selectivity[71].

1.6 THE CATALYTIC PROPERTIES OF MOLECULAR SIEVES

The commercial introduction of crystalline molecular sieves as adsorbents in 1954 is

considered as the onset of the zeolite industry. At present zeolites are produced in very large quantities (worth ~$ 1.48 billion) to meet the requirements for various applications[72-73]. The greater part of the production is intended for ion exchange in the detergent industry and only a small amount is used as catalysts in acid, bifunctional and oxidation catalysis. In the petrochemical industry zeolites are used for cracking, hydrocracking, isomerization and alkylation reactions. Owing to their importance in oil refining most of the work in zeolite catalysis is concentrated on their acid and metal stabilizing properties. Compared to their wide applicability in hydroprocessing, their use in the synthesis of organic intermediates and fine chemicals is limited (Table-1.5). However with the shift from homogeneous catalysis to heterogeneous catalysis, solid catalysts have gained importance in the synthesis of intermediates and fine chemicals[74-75].

Zeolite based catalysts, which are commonly used in acid catalyzed reactions, are also used in oxidation reactions. A titanium containing zeolite with the MFI structure (TS-1) was developed[76], which together with hydrogen peroxide replaced conventional stoichiometric oxidants in various oxidation processes. TS-1 based processes are very eco-friendly and offer many advantages because of their non-corrosive nature, the absence of waste and disposal problems, easy set-up in continuous processes and high thermal stability.

The potential of shape selective catalysis is further amplified by the added dimensions of isomorphous substitution and the availability of a large variety of AlPO-n, SAPO-n and MeAPO-n type compositions. Especially the Silico-aluminophosphates (SAPO-n) are very active and selective catalysts for a variety of important hydrocarbon conversions. As acid catalysts they promote olefin isomerization and oligomerization. The low coking tendency of medium pore aluminophosphate has resulted in a viable approach to skeletal isomerization of n-butenes to isobutenes[77]. In conventional catalytic dewaxing, zeolites typically crack the paraffins to lighter

olefinic materials. Aluminophosphate compositions show outstanding selectivity in catalytic dewaxing of heavy petroleum products[78]. They isomerize the long chain paraffins to non-waxy hydrocarbons of similar molecular weight. Another application of Me-APSO-n compositions is found in methanol conversion to lower olefins. Ethylene and propylene are produced at very high selectivity[79]. A process for lube

Table 1.5

Some catalytic processes in the synthesis of organic chemicals and hydrocarbon processing

Process	Objective	Molecular Sieve
Catalytic processes for synthesis of organic chemicals		
Benzene Ethylation Isopropylation	Production of ethyl benzene Production of isopropyl benzene and Diisopropyl benzene	ZSM-5 Mordenite
Toluene Ethylation Ethylbenzene Ethylation	Production of p-Ethyl toluene Production of p-Diethyl benzene	ZSM-5 ZSM-5
Biphenyl Isopropylation Toluene acylation	Production of 4,4' diisopropyl biphenyl Production of p-acylated toluene	Mordenite Acidic zeolites
Benzoylation of Naphthalene Methanol Conversion (MTO)	Production of 2-benzoyl naphthalene Production of Olefins	Acidic zeolites Me-SAPO-n
Phenol Oxidation Benzene Oxidation	Production of Catechol and hydroquinone Production of Phenol	TS-1 Modified MFI type
Dehydrocyclization of Lower paraffins Chlorination of toluene	Production of Aromatics Production of p-chloro-toluene	Ga-ZSM-5 Acidic zeolites
Catalytic processes in hydrocarbon processing		
Selectoforming M-forming Fluid Catalytic Cracking	Increase antiknock quality of gasoline Increase antiknock quality of gasoline Increase antiknock quality of gasoline	ERI ZSM-5 ZSM-5

(ZSM-5)		
Distillate Dewaxing	Improve low temperature properties of gas oils and lube oils	ZSM-5
Lube Dewaxing	Improve low temperature properties of gas oils and lube oils	ZSM-5
Wax Isomerization	Production of low viscosity lube oil	AlPO-11
Cyclar Process	Synthesis of Ethyl benzene	ZSM-5

dewaxing by wax isomerization is developed using Pt loaded SAPO-11 catalyst at Cheveron[80]. Many excellent reviews are also available in the literature on the applications of zeolites and aluminophosphate molecular sieves in hydroprocessing and organic synthesis[81-86].

1.7 PHYSICO-CHEMICAL CHARACTERIZATION

To know the physico-chemical properties of the molecular sieves, a number of characterization techniques are employed. Powder X-ray diffraction, UV-Vis, FTIR, ^{27}Al, ^{31}P and ^{29}Si MAS-NMR, SEM, TEM and XRF are the important spectroscopic techniques used. There are many review articles, books and chapters devoted to the applications of spectroscopic techniques in catalysis[87-89].

Powder X-ray diffraction is the single most powerful technique applied to characterize any crystalline sample. In zeolite molecular sieves the XRD pattern provides information on the degree of crystallinity of the sample as well as its phase purity[90]. Lattice spacing 'd' can be calculated from the measured 2θ by Bragg's equation $n\lambda = 2d \sin\theta$ (where λ is the wavelength of $CuK\alpha$), which is further used to calculate the unit cell volume.

Infrared spectroscopy is used to obtain information about the zeolite structure, acid-base

properties[91] and to determine the incorporation of certain elements in the lattice[92].

UV-Visible spectroscopy is used to study the bulk properties of the catalyst, like the d-d transitions of the transition elements. This technique is also used to investigate the oxidation states and coordination number of the element present in the catalyst[93].

NMR spectroscopy is used to obtain information about the surrounding of certain elements in the pores or in the lattice of molecular sieves[94]. ^{29}Si Liquid NMR is used to characterize the nature and the amount of silicate species in precursor reactive solutions during the synthesis of zeolites.

With the help of SEM and TEM one can visualize the particle size and the morphology of the sample[95].

X-ray fluorescence spectroscopy (XRF) is used for the quantitative analysis of chemical composition of the material prepared[96].

The adsorption and desorption behavior of different molecules is studied to obtain information about the pore volume, surface area and acidity[97].

Temperature programmed desorption (TPD) of ammonia gives the information about the total strength of acidity associated with the catalyst[98-99].

1.8 OBJECTIVES AND SCOPE OF THE WORK

ZrO_2 and TiO_2 are the most interesting and useful catalysts and catalyst support materials because of their pronounced catalytic behavior in spite of their almost neutral surface properties. The co-operation of weakly acid sites and weakly basic sites, of which acid-base pair sites are suitably oriented on the surface, is surprisingly powerful for specific reactions with good selectivity and long catalyst life[100-102]. However, because of the inherent problems associated with these catalysts, such as low dispersion and less number of active sites, their industrial applications are

limited[103]. Owing to the difficulty in preparation of ZrO_2 and TiO_2 catalysts in highly dispersed state with high surface area, incorporating them in molecular sieve materials offers various advantages like large number of dispersed active sites, high thermal stability and molecular shape selectivity. Attempts have been made to incorporate Ti and Zr in the framework of various micro- and mesoporous materials. They have been found to be active in many oxidation reactions. As a result, titanium silicalite-1 catalyst (TS-1) is being employed on industrial scale for various oxidation reactions[81].

TS-1 can be synthesized using various silicon alkoxides as silica source, but among them, only tetraethyl orthosilicate (TEOS) was reported[104] to yield good quality TS-1. But the high cost of TEOS makes the cost of TS-1 prohibitive. Therefore it is desirable to search for an alternative cheaper silicon source to prepare pure TS-1 for industrial use.

As compared to titanium containing molecular sieves, the isomorphous substitution of zirconium has not been studied extensively. Although there are only a few reports on Zr substitution in ZSM-5, ZSM-11 and mesoporous M41S in the literature[36,39,105,106], they undoubtedly demonstrate that Zr enhances the catalyst life in isomerization reactions[38,42]. Whereas the incorporation of Ti in AlPO- molecular sieves is already established, the studies on Zr incorporation are limited and need further attention.

The objectives of the present investigation are;

1. To study the incorporation of Titanium and Zirconium in microporous zeolites, with MFI and MEL structures, and aluminophosphates with AFI and AEL structures.
2. To characterize these materials using various techniques such as XRD, XRF, FT-IR, MAS-NMR, electron microscopy (TEM/SEM), TPD of ammonia, UV-visible, and adsorption of probe molecules.

3. To study the catalytic activity of these materials in some industrially important reactions like hydroxylation of aromatics and isomerization.

This investigation is described in the following chapters.

The various experimental techniques used in the hydrothermal synthesis and characterization of the samples prepared in this study are described in Chapter 2. The methods adopted for the catalytic evaluation of the samples are also described here.

The results on the synthesis of TS-1 using Ethyl Silicate-40 (ES-40), a new source of silica and tetraethyl orthosilicate (TEOS), are presented in Chapter 3. The physico-chemical characterization of the samples by using XRD, XRF, FT-IR, ^{29}Si Liquid NMR, MAS-NMR, SEM, UV-visible and adsorption of probe molecules is presented, and the samples have been compared. The catalytic activity in the hydroxylation of phenol and anisole using dilute hydrogen peroxide is also presented.

Chapter 4 describes the synthesis of zirconium containing ZSM-5, Silicalite-1 and Silicalite-2 molecular sieves. The preparations of the samples prepared by using different zirconium sources and characterization by different physicochemical methods are described. The catalytic activity in phenol hydroxylation using dilute hydrogen peroxide as oxidant, and in ortho-toluidine isomerization is also presented.

Chapter 5 contains the synthesis of zirconium containing alumino-phosphate molecular sieves with AlPO-5 and AlPO-11 structures. They are further modified by platinum for catalytic evaluation. The results of the characterization by various physico-chemical techniques and the results of m-xylene isomerization and n-hexane hydroisomerization are described. A summary of the total work is presented in the end.

1.9 REFERENCES

1. a) R. J. Farrauto and C. H. Bartholomew in *Fundamentals of Industrial catalytic processes*, Published by Blackie Academic and Professional (Chapman & Hill) Boundry Row London UK (1997) 7., b) Jens Hagen in *Industrial catalysis: A practical approach* Published by Wiley-VCH D-69469 Weinheim, Germany (1999) 1.

2. a) R. M. Barrer, in *"Zeolite and Clays Materials as Sorbents and Molecular Sieves"*, Academic press, London, (1978), b) W. M. Meier, D. H. Oslon, in *"Atlas of Zeolite Structure Types"*, Butterworth-Heinemann, London, (1992).
3. R. M. Barrer, in *"Hydrothermal chemistry of zeolites"*, Academic press, New York, (1982).
4. D.W. Breck, in *"Zeolite Molecular Sieves"*, Wiley Publ. New York, (1974).
5. W. L Bragg., in *"The Atomic Structure of Minerals"*, Cornell Univ. Press, Ithaca New York, (1937).
6. W. M. Meier., in *"Molecular Sieves"*, Soc.Chem.Ind., London, (1968) 10.
7. L.B. Sand, in *Econ. Geol* (1967) 191.
8. E. M. Flanigen., in *"Proceedngs of the fifth international zeolite conference"*, Ed. L.V.C. Rees, Heydon, London, (1980) 760.
9. S. T. Wilson, B. M. Lok, C. A. Messina, T. R. Cannan and E. M. Flanigen. *J. Am. Chem. Soc.,* 104, (1982)1146.
10. R. D. Shannon Atca. Cryst. 32 A, (1976), 751.
11. R. M. Barrer, *Pure and Appl. Chem* 51, (1979) 1091.
12. L.B. Sand, *Pure and Appl. Chem*, 52, (1980) 2105.
13. Moretti E, Lontesa S, and Padoan M *Chim. Ind* 671, (1985).
14. S. T. Wilson in *Introduction to zeolite science and practice* (Eds. H. Van. Bekkum, E. M. Flanigen and J. C. Jansen). *Stud. Surf. Sci. and Catal.,* 58 (1991) 138.
15. E. M. Flanigen, B. M. Lok, R. L. Patton and S. T. Wilson, in *New Developments in Zeolite Science and Technology* Eds. Y. Murakami, A. Ijima and J. W. Ward. Kondansha, elsevier, Amsterdam, Oxford, New York, *Proc. 7th Int. Zeol. Conf.*, Tokyo (1986) 103.
16. Jean-Louis and Henry Kessler (Chapter I) and Johan-A. Martens and Pierre A. jacobs (Chapter II) *Catalysis and Zeolites: Fundamentals and applications* (Eds. J. Weitkamp and L. Puppe) Springler, (1999).
17. Bellussi, G.; Fattore, V. *Stud. Surf. Sci. Catal., 69,* (1991) 79-92.

18. Weckhuysen, Bert M.; Rao, R. Ramachandra; Martens, Johan A.; Schoonheydt, Robert A., *Eur. J. Inorg. Chem.,* 4, (1999) 565-577.

19. G. W. Sheels and E. M. Flanigen., in *ACS Sym. Ser. 398,* Washington D.C (1989) 420.

20 A. Carati, S. Contarini, R. Millini and G. Bellusi., *Pro. Mat. Res. Soc.* extended abstracts (EA-42). (1990).

21. E. M. Flanigen, R. L. Patton and S. T. Wilson, in *Innovation in zeolite Materials Science*, Eds. P. J. Grobet, W. J. Mortier, E. F. Vansant and G. Schultz-Ekloff, Stud. Surf. Sci. Catal. Elsevier, Amsterdam, 37, (1988), 13.

22. L. Pauling, "*The Nature of the Chemical Bond*", Cornell Univ. Press, Ithaca, (1960).

23. M. Taramasso G. Perigo, B, Notari, U.S Patent 4, 410, 501 (1983)

24. J. S. Reddy and R. Kumar *Zeolites* 12, (1992) 95.

25. L. Yu, H. Jiang and W. Pang, *Huaxue Xuebao,* 51 (1993) 780.

26. Dartt, C. B., Khouw C. B., Li H. X. and Davis M. E. *Micro. Mater.* 2(5) (1994) 425.

27. M. A. Camblor, A. Corma, A. Martinez and J. Parez-Pariente. *J. Chem. Soc. Chem. Commun.* (1992) 589.

28. M. W. Anderson, O. Terasaki, T. Ohsuna, A. Phlippou, S. P. Mackay. A. Ferreira, J. Rocha and S. Lidin. *Nature* 367 (1994) 347

29. K. J. Balkus, A. Khanmamedora. A. G. Gabrielov and S. I. Zones. *Stud. Surf. Sci. Catal.* 101, (1996) 1341

30. P. T. Tanev, M. Chibwe and T. J. Pinnavaia, *Nature* 368, (1994), 321.

31. Blasco T. Corma A. Navarro M. T and Perez Pariente. *J. Catal.* 156(1) (1995) 65.

32. Corma A. Kan Quibin, and Rey Fernando. *J. Chem. Soc. Chem. Commun* 5, (1998) 579.

33. N. Ulagappan, V. Krishnasamy, *J. Chem. Soc. Chem. Commun* (1995), 373

34. L. Marchese, A. Frache, S. Coluccia and J. M. Thomas. Proceedings of *12th Inter. Zeol. Conf.* (Eds: M. M. J. Treacy, B. K. Markus, M. E. Bisher and J. B. Higgins

Materials Research Society Warrendale, Pennsylvania, USA) 1909 (1999).

35. Zahedri-Naki, M. Hassan, Joshi P. N. Kaliaguine S. *J. Chem. Soc. Chem. Commun* (1) 1996, 47.
36. M. K. Dongare, P. Singh, P. P. Moghe, and P. Ratnasamy. Zeolites 11, (1996) 690.
37. D. P. Sabde, S. G. Hegde and M. K. Dongare *J. Mater. Chem,* (Communicated).
38. B. Rakshe, V. Ramaswamy, S. G. hegde and A. V. Ramaswamy. *Proceedings of 12th Inter. Zeol. Conf.* (Eds: M. M. J. Treacy, B. K. Markus, M. E. Bisher and J. B. Higgins Materials Research Society Warrendale, Pennsylvania, USA) 1909, (1999).
39. A. Tuel, S. Gontier and R. Teissier, *J. Chem. Soc. Chem. Commun.* (1996) 651
40. Vercruysse K. A, D. M. Collin g, T. Klingeleers and Jacobs P. A. *Stud. Surf. Sci. Catal.* 117, (1999) 469.
41. M. K. Dongare, D. P. Sabde, R. A. Shaikh, K. R. Kamble and S. G. Hegde. *Catal. Today* 49, (1999) 267.
42. Meriadeau, V. A. Yuan. L. N. Hung, F. Lefebvre, H. P. Nguyen, *J. Chem. Soc. Fara. Trans.* 93 (23) (1997), 4201.
43. D. P. Sabde, K. R. Kamble, S. G. Hegde and M. K. Dongare *J. Mater. Chem* (Communicated)
44. S.L. Meisel, J.P. McCullough, C.H. Lechthaler and P.B. Weisz, *Chemtech*, 6 (1976) 86.
45. G. T. Kokotailo, S. L. Lawton, D. H. Olson and W. M. Meier *Nature* 272 (1978) 437.
46. D. H. Olson, G. T. Kokotailo, S. L. Lawton and W. M. Meier, *J. Phys. Chem* 85 (1981) 2238.
47. G.T. Kokotailo, P. Chu, S.L. Lawton and W.M. Meier, *Nature*, 275 (1978) 119.
48. C. A Fyfe, H. Gies, G. T. Kokotailo, C. Pasztor, H. Strobl and D. E. Cox *J. Am. Chem. Soc.* 111 (1989) 2470.
49. J. M. Bennett, J. P. Cohen, E. M. Flanigen, J. J. Pluth and J. V. Smith *ACS Symp. Series* 218 (1983) 109.
50. J. W. Richardson Jr. J. J. Pluth and J. V. Smith, *Acta Crystallogr*,44 (1988) 367.
51. J. M. Bennett, J. W. Richardson, Jr. J. J. Pluth and J. V. Smith. *Zeolites* 7 (1987) 160
52. P.B. Weisz and V.J. Frilette, *J. Phys. Chem.* 64 (1960) 382.
53. Paul. B. Venuto in *ACS series book* (1999)

54. Hoelderich W. F, Hesse M. Naumann F. *Angew. Chem. Int. Ed. Engl.*, 27 (1988) 226

55. Hoelderich W. F, van Bekkum H. *Stud. Surf. Sci. Catal.* 58 (1991) 631.

56. a) S. M. Csicsery, *Zeolites*, 4, (1984) 202., b) E. G. Derouane *Stud. Surf. Sci. Catal.,* 5, (1985) 5., c) S. M. Csicsery, *Pure and Appl. Chem.* 58, (1986)841., d) P. B. Weisz *Pure and Appl. Chem.* 52, (1980) 2091.

57. N. Y. Chen, W. E. Garwood and F. G. Dwyer, in *"Shape Selective Catalysis in Industrial Applications"*. 2nd edition, Marcel Dekker, New York (1996), 282.

58. S. M. Csicsery, in J. A. Rabo (Ed.) *"Zeolite Chemistry and Catalysis"*, ACS Monograph, Washington D.C. (1976), 171, 680

59. P.B. Weisz and V.J. Frilette Maatman. R. W. and Mower E. B. *J. Catal.* 1 (1962) 307.

60. Augustine R. L. *Heterogeneous Catalysis for the Synthetic Chemist,* Marcel Dekker, New York, (1996) 93.

61. Chen N. Y and Garwood W. E., *J. Catal.* 52, (1978) 453

62. Chen N. Y Kaeding W.W and Dwyer F. G., *J. Am. Chem. Soc.* 101 (1979) 6783.

63. Csicsery S. M. *J. Org. Chem.*, 34 (1969) 3338.

64. Weitkamp, J. Nerst, S. *Catal. Today,* 19 (1994) 107.

65. Song C, Ma. X, Schmitz A. D, Schobert H. *ACS Symp. Ser.*, 738 (2000) 305.

66. E.G. Derouane and Z. Gabelica, *J. Catal.*, 65 (1980) 486.

67. M. Guisnet, S. Morin and N. S. Gnep., *Shape Selective Catalysis: Chemical Synthesis and Hydrocarbon Processing,* ACS Symposium Series; 738, Washington D.C (1999) 334.

68. J. A. Rabo, R. Bezman and M. L. Poutsma., *Acta phys. Chem.* 24 (1987) 39.

69. C. Mirodatos and D. Barthomeuf, *J. Catal.* 57 (1979) 136

70. Eric. G. Derouane. *J. Catal.* 100, (1986) 541

71. C. Mirodatos and D. Barthomeuf, *J. Catal.* 93 (1985) 246.

72. Armor J. N. *Appl. Catal.*, 139 (1996) 217.,

73. News. *Ind. Catal. News*, 1, (1998) 3.

74. R. A. Sheldon, in G. Centi and F. Trifiro (Editors), *New Development in Selective Oxidation,* Elsevier Science Publishers (1990) 1.

75. W. F. Hoelderich. P. A. Jacobs and R. A. van Santen (Editors*), Zeolites: Facts, Figures and Future* Elsevier Science Publishers (1989), 69.

76. M. Taramasso G. Perigo, B, Notari, U.S Patent 4, 410, 501 (1993)

77. Pellet R. J. Coughlin, P. K., Long G. N and Rabo. J. A., U.S. Pat. 4 859 314, UOP (1989)

78. Gortesema F. P. Springer A. R. and Long. G. N U.S Pat. 4 880 700 UOP (1989).

79. Pellet R. J. Coughlin, P. K., Stainiulis M. T. Rabo J. A and Long G. N., U.S. Pat. 4 791 083 UOP (1988).

80. S. J. Miller. *Microporous Materials.* 2 (1994) 439.

81. P. B. Venuto *Microporous Materials* 2, 1994, 297

82. a) Corma A. Garcia H. *Catal. Today* 38 (1997) 257, b) Van der Waal, J. C, van Bekkum, H. *J. Porous Mater* 5 (1998) 289.

83. Murugavel, Ramaswamy; Roesky, Herbert W. *Angew. Chem., Int. Ed. Engl.*, 36(5), 1997, 477-479.

84. Sugi, Y. Kubota Y. C*atalysis-Specialist Periodical Report* 13 (1997) 55.

85. Song. C. *Stud. Surf. Sci. Catal.* 113, (1998) 163.

86 a) Maxwell I. E and Stork, W. H. J *Stud. Surf. Sci. Catal.* 58 (1991) 571.
John C. S. Clark, D. M. Maxwell I. E. *New Insights into Zeolite Catalysis. In Perspectives in catalysis,* Ed. By J. M. Thomas and K. I. Zamaraev. Blackwell Scientific Publications,

87. H. G. Karge, M. Hunger and H. Beyer in *Catalysis and Zeolites: Fundamentals and Application* (Eds: Weitkamp J. Puppe L., Springer: Berlin, Germany) (1999) 200.

88. Delgass W. Nicholas, Haller Gary L, Kellerman Richard and Lunsford, Jack H. *Spectroscopy in Heterogeneous Catalysis.* Academic Press: New York, N. Y. 341, (1979)

89. Ertl G, Knoezinger H, (Editors, Wiley-VCH: Weinheim, Germany) *Handbook of Heterogeneous Catalysis* 2, (1997) 427.

90. R. Szostak in *Molecular sieves: Principles of Synthesis and Identification,* Van

Nostrand Reinhold New York (1989)

91. J. G. Post and J.H.C van Hooff, *Zeolites,* 4 (1984) 9

92. A. Zecchina, S. Bordiga, G. Spoto, L. Marchese, G. Petrini, G. Leofanti and M. Pondavan. *J. Phys. Chem.*, 96 (1992) 4985.

93. a) Boccuti, K. M. Rao, A. Zecchier, G. Leofanti and G. Pefrini, *Stud. Surf. Sci. Catal.,* 48 (1989) 133. b) T. Sen, Ph.D., thesis submitted to "University of Pune", India, June 1997.

94. a) Lippmaa E, Magi M, Samoson, A., Engelhardt A and Grimmer A. R., *J. Am. Chem. Soc*. 102, 4889, (1980)., b) Nagy J. B and Derouane A. E. G, *ACS Sym. Series* 368, 2, (1988)., c) Lippmaa E, Magi M, Samoson, A., Tarmak M and Engelhardt G , *J. Am. Chem. Soc.* 103, (1981) 4992.

95. A. J. P. van der Pol, A. J. Verduyn and J. H. C. van Hooff. *Appl. Catal*. 92(2), (1992) 113.

96. J. Scherzer, *ACS Symp*. 248 (1984) 157.

97. Derouane E. G and Gabelica Z., *J. Catal.*, 65 (1980) 486.

98. Topsoe, N., Penderson , R. K. and Derouane, E.G., *J. Catal.*, 70 (1981) 41. 110.

99. Borade, R. B., Hegde, S. G., Kulkarni, S. B. and Ratnaswamy, P. *Appl. Catal.*, 13 (1984) 27.

100. a) Moles, Peter. *Spec. Chem.*, 15(4), 192, 194, 197-8, (1995)., b) Moles, Peter. *Spec. Chem.,* 14(3), 217-18, 220-1, (1994), c) Moles, Peter. *Spec. Chem.*, 14(2), 84,87-8, (1994)., d) Moles, Peter. *Spec. Chem.*, 12(6), 382, 384, 387-8, (1992)., e) Moles, Peter. *Spec. Chem.*, 18(5), 220-222, (1998).

101. Sabu, Kuzhunellil Raghavan Pillai, Rao, Kalur Vijayachandra C, Nair, Chandrathil Govindan Ramachandran, *Bull. Chem. Soc. Jpn.*, 64(6) (1991) 1920.

102. K. Tanabe, M. Misono, Y. Ono and H. Hattori, *New Acids and Bases*, Kondansha-Elsevier, Tokyo-Amsterdam, (1989), Chapter-4.

103. T. Yamaguchi *Catal.Today* 20 (1994) 199.

104. A. Tuel and Y. Ben Taarit. *Appl. Catal.-A*, 110 (1994) 137.

105. K. Eichler, E. I. Leupold, H. Arpe, H. Baltes. U. S. Patent 4 720 583 1988.

106. G. Wang. X, Wang, X, Wang, S. Yu. *Stud. Surf. Sci. Catal.* 83 (1993) 67.

2.1 INTRODUCTION

The synthesis of titanium and zirconium containing silicate and aluminophosphate molecular sieves were carried out using reactive sources listed in Table-2.1. The synthesis procedures adopted, precursors involved and the different instrumental techniques used in characterizing the structural features of catalysts are discussed in this chapter.

2.2 SYNTHESIS

2.2.1 Synthesis of Titanium Silicalite-1 (TS-1)

Two different methods for the synthesis of titanium silicalite (TS-1) were used. In the first method, titanium tetrabutoxide (TBOT) in isopropyl alcohol (IPA) and Ethyl silicate-40 (ES-40) were mixed together and stirred for few minutes. Then aqueous tetrapropyl ammonium hydroxide (TPAOH) solution was added slowly to the above solution. In the second method, similar quantities of all the reactants were used, but the order of their addition was different. The ES-40 was first hydrolyzed with TPAOH solution and then TBOT in IPA was added. The solutions obtained in both the methods were further stirred at 60-70^{0}C for about two hours to partially remove the alcohol. Then the required amount of water was added. Finally the solutions were placed in an autoclave (Fig.2.1) for hydrothermal crystallization in the range of 130 to 170^{0}C for 2-3 days. The solids were recovered by centrifugation, washed with deionised water and dried overnight at 100^{0}C in an oven and then calcined at 550^{0}C in presence of air for 8-10 h. The samples with different Si/Ti ratios were prepared by varying the amount of TBOT. For comparison, TS-1 and ZrS-1 (zirconium silicalite-1) were also prepared using TEOS as per the reported procedure[1,2]. The details of the reaction compositions and temperature of hydrothermal crystallization are described in Chapter 3.

In order to study the influence of the temperature on the rate of crystallization on TS-1using ES-40, the reactant compositionwas kept as SiO_2:0.03 TiO_2: 0.33 TPA:35 H_2O.

Table-2.1

Specifications of the reactants used in the synthesis

Sr. No.	Reactants used	Specifications
1.	Titanium(IV) butoxide, $Ti(OBu)_4$	Aldrich, 99 %
2.	Tetraethyl orthosilicate, $Si(OEt)_4$	Aldrich, 99 %
3.	Ethyl Silicate-40, Polymeric silicon alkoxide	Chemplast, 99 %
4.	Zirconium (IV) Propoxide, $Zr(OPr)_4$	Aldrich, 70 wt% in IPA
5.	Zirconium Nitrate, $ZrO(NO_3)_2\ xH_2O$	Loba, 99 %
6.	Zirconyl Oxychloride, $ZrOCl_2.H_2O$	Loba, 99 %
7.	Aluminum Isopropoxide, $Al(OPr^i)_3$	Aldrich, 98 %
8.	Orthophosphoric acid, H_3PO_4	S.d fine, 85 % (15% H_2O)
9.	Tetrapropyl ammonium Hydroxide, $(C_3H_7)_4NOH$	22 wt % in H_2O
10.	Tetrabutyl ammonium Hydroxide, $(C_4H_9)_4NOH$	40 wt % in H_2O
11.	n-Dipropyl Amine, $NH(C_3H_7)_2$	Aldrich, 99 %
12.	Triethyl Amine, $N(C_2H_5)_3$	Ranbaxy, 99 %
13.	Isopropyl Alcohol, C_3H_7OH	S.d fine, 99 %
14.	Tetraammine platinum(II) chloride, $Pt(NH_3)_4Cl_2$	Aldrich, 99 %

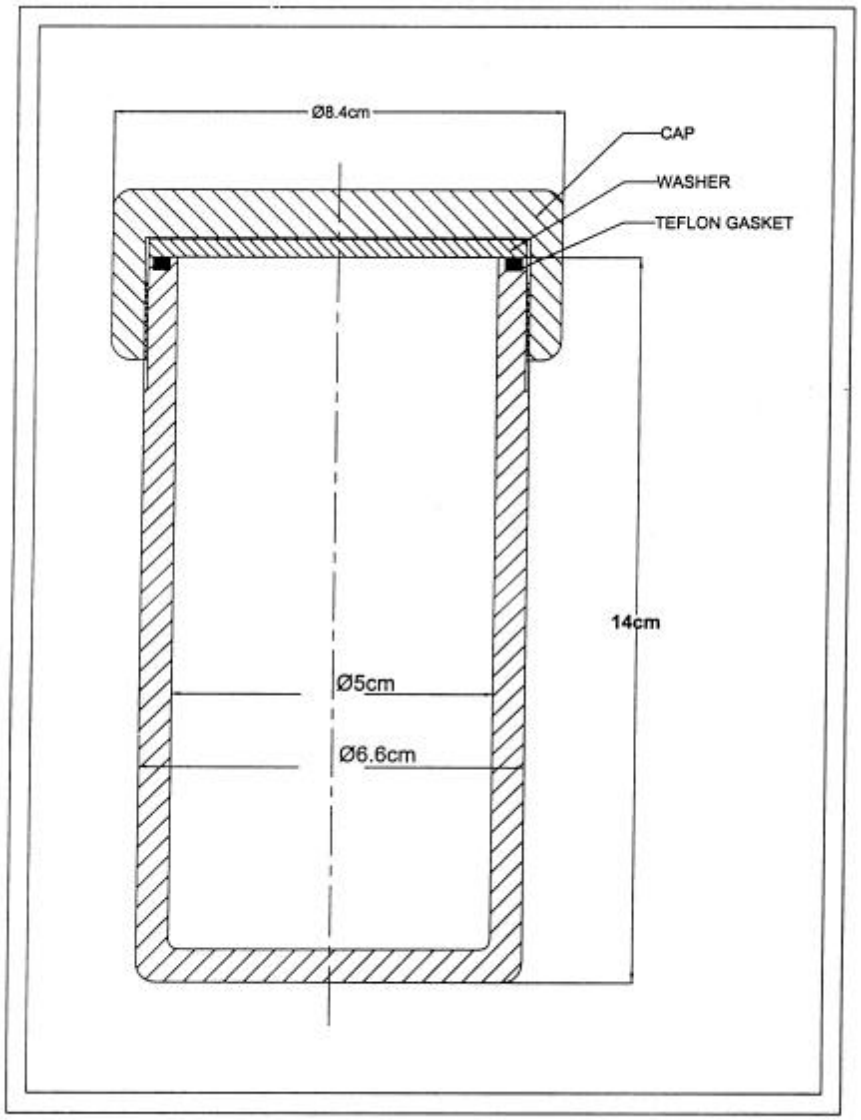

Fig. 2.1 Stainless steel autoclave for hydrothermal synthesis

The precursor solutions were placed in several identical autoclaves. The autoclaves were stirred while heating at temperatures 130, 150, 160 and 170^{0}C for hydrothermal crystallization. The synthesis was interrupted at various stages at different time intervals, to isolate the intermediate phases. To study the influence of SiO_2/TiO_2 and SiO_2/TPAOH ratio, the reactant composition was varied.

2.2.2 Synthesis of Zirconium Silicalite-2 (ZrS-2)

Zirconium containing molecular sieve with MEL topology was prepared using zirconium propoxide(ZrP), TEOS and alcoholic solution of tetrabutyl ammonium hydroxide(TBAOH). TEOS and ZrP were hydrolyzed with alcoholic solution of TBAOH, warmed at about 60^{0}C to remove excess of alcohol. Requisite amount of water was added to the above solution while stirring. The final reaction solution was then crystallized hydrothermally in an autoclave at 170^{0}C for 60-72 h. The product was centrifuged/ filtered, washed, dried and calcined in air at 550^{0}C for 10 hours. The samples with different Si/Zr ratios were prepared by varying the amount of zirconium propoxide. For comparison, Ti-MEL (TS-2) and ZrS-1 samples were prepared using reported procedures[3,2]. The details of the reaction compositions and temperature of hydrothermal crystallization are described in Chapter 4.

2.2.3 Synthesis of Zirconium containing alumino-Silicate-1 (AlZrS-1)

Zirconium containing alumino-silicalite with MFI topology (AlZrS-1) were prepared from gel compositions 0.1 NaOH: SiO_2: x ZrO_2: yAl_2O_3: 0.33 TPAOH: 35 H_2O, where x and y were varied to obtain samples with different Si/Zr and Si/Al ratios. The AlZrS-1 samples were prepared using zirconium propoxide as zirconium source, sodium aluminate as aluminum source, TEOS and aqueous tetrapropyl ammonium hydroxide (TBAOH) solution.

TEOS was added to a mixture of NaOH and TPAOH solution in a beaker. Zirconium propoxide in IPA was added to the above mixture while stirring followed by the addition of sodium aluminate in water. The above mixture was heated to remove alcohol, requisite amount of water was added and stirred for an hour. Finally the mixture was transferred in an autoclave for hydrothermal crystallization at 170^{0}C for 4-5 days.

After the hydrothermal crystallization, the product was centrifuged / filtered, washed, dried at 100^0C and calcined overnight in presence of air at 550^0C. The samples with different Si/Zr and Si/Al were prepared by varying the amount of zirconium and aluminum source. All the calcined Al-ZrS-1 samples were treated with 1M ammonium nitrate solution and subsequently calcined at 500^0C in air for 8-10 hours. The samples are represented as H-AlZrS-1 (X,Y), where X and Y represent Si/Zr and Si/Al mole ratios respectively in the final sample. The details of the reaction compositions and temperature of hydrothermal crystallization are described in Chapter 4.

2.2.4 Synthesis of Zirconium containing AlPO-5 (Zr-AlPO-5)

A series of zirconium containing AlPO-5 samples were prepared hydrothermally using an aluminum, zirconium and phosphorous source. In a typical synthesis procedure, aluminum isopropoxide was added to dry isopropyl alcohol in a beaker. Zirconium isopropoxide in IPA was added to the above solution, stirred and warmed to 60-70^0C to remove alcohol partially. Then orthophosphoric acid along with the required amount of water and template (Triethyl amine) was added and stirred for another few hours. The homogeneous gel was transferred into a Teflon lined stainless steel autoclave and kept for hydrothermal crystallization at 200^0C for 4 to 5 days. After complete crystallization, the white solid was recovered by filtration, washed several times with deionised water and dried in an oven. The samples thus obtained were calcined in air to remove the template by heating slowly to 600^0C and holding it for 8 h. The details of the reaction compositions and temperature of hydrothermal crystallization are described in Chapter 5.

2.2.5 Synthesis of Zirconium containing AlPO-11 (Zr-AlPO-11)

Aluminum isopropoxide and isopropyl alcohol were mixed together in a polypropylene beaker and stirred for an hour. Zirconium propoxide in IPA was added and stirred for some time. The mixture was heated under stirring at 60-70^0C for 1-2 h to

remove excess of alcohol. Required amount of phosphoric acid and water was added slowly to the above solution in ice cold conditions. Finally, the white gel obtained was stirred for another 1 h and then dipropyl amine was added. The resulting gel was kept for hydrothermal crystallization at 180^0C for 4-5 days in a stainless steel autoclave. After hydrothermal crystallization, the sample was recovered by filtration, washed, dried and then calcined at 560^0C in air for 8 to 10 h. Zirconium free AlPO-11 and SAPO-11 samples were prepared using a standard procedure[4,5]. Platinum was loaded on Zr-AlPO-11, SAPO-11 and pure AlPO-11 samples by wet impregnation with an aqueous solution of $Pt(NH_3)_4Cl_2$. The resulting materials were dried and reduced in flowing hydrogen prior to catalytic testing. The details of the reaction compositions and temperature of hydrothermal crystallization are described in chapter-5.

2.3 PHYSICOCHEMICAL CHARACTERIZATION

2.3.1 Chemical composition by XRF

During the present study a Rigaku 3700 X-ray fluorescence spectrophotometer with rhodium target energized at 50 uv and 40 mA was utilized for the analysis of the samples. Borate fusion method was used for preparing the samples and standards.

2.3.2 X-ray diffraction

All the samples synthesized in the present investigation were characterized using Rigaku, D-Max III VC model X-ray diffractometer, with nickel filtered CuKα radiation, λ = 1.5404. Data was collected in the 2θ range of $5\text{-}50^0$ at the scan rate of 1^0/min. The interplanar spacing 'd' was corrected with respect to silicon standard and then used for the determination of the unit cell parameters.

2.3.3 Scanning Electron Microscopy (SEM)

The SEM of the samples was taken using a JEOL JSM-500 electron microscope. The samples were mounted on a specimen grid and then coated with a film of gold to

prevent the surface charging and protect from thermal damage by electron beam. A uniform thickness of about 0.1 mm was maintained for all the samples.

2.3.4 FT-IR Spectroscopy

The samples were characterized by IR spectroscopy (Nicolet, 60 SXB model) in the framework as well as in hydroxyl region. The FTIR spectra in the fundamental vibrations region of structural framework was taken by KBr pellet technique. For insitu studies, the samples were activated in a sample cell shown in Fig 2.2 for four hours and then cooled to room temperature before recording the spectra. For acidity determination, these activated samples were exposed to probe molecules such as ammonia and pyridine for half an hour. The physically sorbed molecules were removed by evacuation at different temperatures and subsequently spectrum was recorded.

2.3.5 NMR spectroscopy

^{27}Al, ^{31}P and ^{29}Si MAS-NMR spectra were recorded at room temperature on a Bruker MSL 300 NMR spectrometer. The ^{29}Si liquid NMR spectra were also recorded at 59.6 MHz using the same instrument. In order to avoid the signal arising from the glass background, the measurements were carried out in a conventional wide line probe using a 10-mm o.d plastic tube having tight fitting cap. The free induction decays (FIDs) were collected with a 30^0 flip angle. The ^{29}Si signals during the TEOS and TBOT hydrolysis reaction were monitored with one seconds recycle delay.

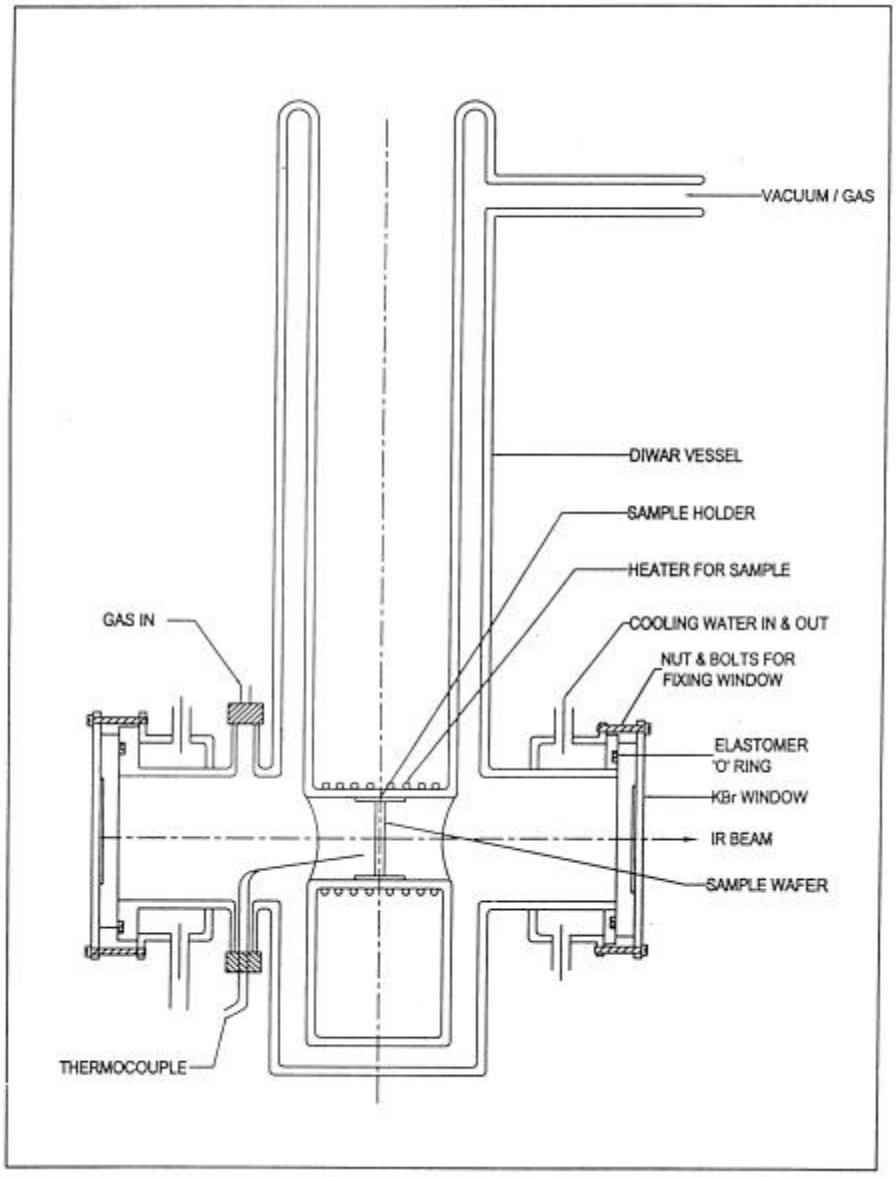

Fig. 2.2 FT-IR sample cell

2.3.6 UV-Visible spectroscopy

The UV-Vis diffuse reflectance spectra was recorded using UV-Vis scanning spectrophotometer, model Shimadzu 2101 PC.

2.3.7 Temperature programmed desorption of ammonia

The temperature programmed desorption (TPD) of ammonia measurements were carried out using Sorbstar (Model 200, Institute of Isotopes, Budapest). 200 mg. of the sample was loaded in the 'U' shaped silica sample holder and activated at 500^0C for 4 h in an argon flow. The sample was cooled to room temperature in argon and ammonia was adsorbed on the sample for half an hour. The sample was flushed with argon for one hour to remove the physically sorbed ammonia. The sample was then heated in the argon flow of 40 ml/min at the rate of 10^0C/min upto 540^0C. Thermal conductivity detector was used to record the concentration of desorbed ammonia at various temperatures.

2.3.8 Adsorption measurements

Adsorption studies were carried out using all glass gravimetric apparatus with McBain-Baker type silica spring (sensitivity 83 cm/g) connected to a high vacuum system (Fig.2.3). 30 to 40 mg of the sample was hand pressed into a pellet and weighed in an aluminum holder, which was attached to the spring. Initially the sample was evacuated in low vacuum and then in high vacuum at 10^{-6} torr. The sample was activated at 400^0C in vacuum till a constant weight was obtained. It was then cooled to the adsorption temperature and exposed to the adsorbate vapor at the desired vapor pressure. The changes in the weight due to desorption and adsorption was noted using a cathetometer.

2.3.9 The surface areameasurements

The surface area of the samples was determined by N_2 adsorption (Coulter 100CX Omnisorb). The samples were heated to 400^0C for 2 h in high vacuum. After the treatment, the anhydrous weight of the sample was taken at room temperature. The sample was then cooled to 77K using liquid nitrogen. Then the sample was allowed to adsorb nitrogen gas. Finally the surface area was calculated by BET method.

2.4 CATALYTIC PROPERTIES

During the course of this investigation, different chemicals used in the catalytic reactions are presented in Table-2.2.

2.4.1 Hydroxylation of aromatics

Phenol and anisole hydroxylation reactions were carried out in liquid phase in a batch reactor. Dilute H_2O_2 was added to the reactor vessel by using a syringe pump with a constant feed rate. The reaction was carried out for 5-8 h at 80^0C, with phenol to hydrogen peroxide ratio of 5:1. The products were analyzed by GC (HP 5880A) equipped with a capillary column (50 m x 0.25 mm, cross-linked methyl-silicon gum).

2.4.2 m-Xylene isomerization

The catalytic experiments for m-xylene isomerization were performed in an all silica vertical fixed bed down flow reactor (Fig. 2.4) taking 2 g. of the catalyst particles of 10-20 mesh. The catalyst was activated at 500^0C prior to reaction and m-xylene was fed to the reactor using a syringe pump (Sage Instruments, USA). The reaction was carried out at 350-550^0C keeping WHSV-$2h^{-1}$. The Products were analyzed by GC (Shimadzu - 15A) using xylene master column with FID detector.

2.4.3 Isomerization of ortho-toluidine

The ortho-toluidine isomerization reactions were also performed in identical manner. The catalyst was activated at 500^0C in air and then in presence of nitrogen prior to reaction. O-toluidine was fed to the reactor by using a syringe pump. The reaction was carried out at different temperatures in presence of nitrogen gas. The products were analyzed by GC (5889 A) using megabore column with a FID detector.

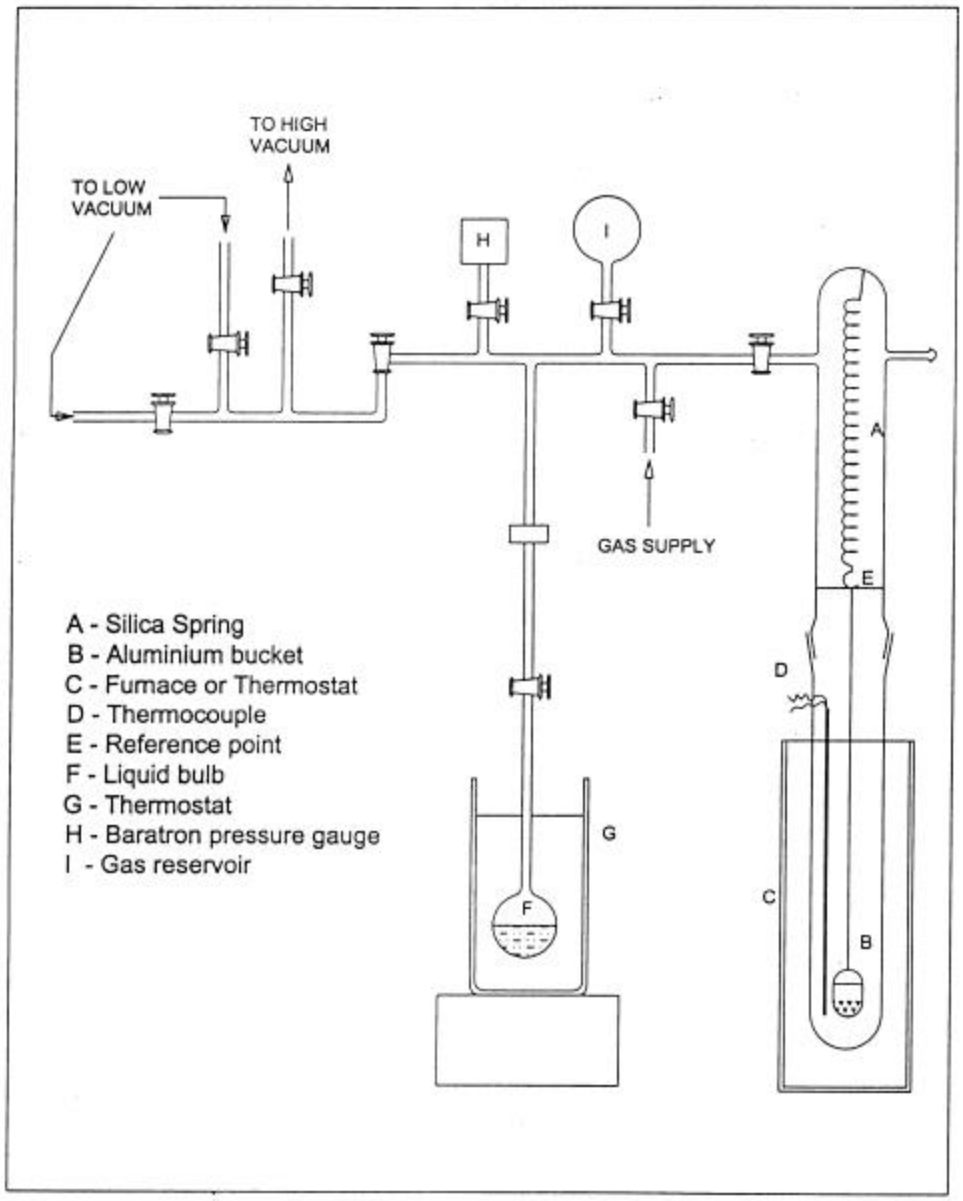

Fig. 2.3 McBain spring balance

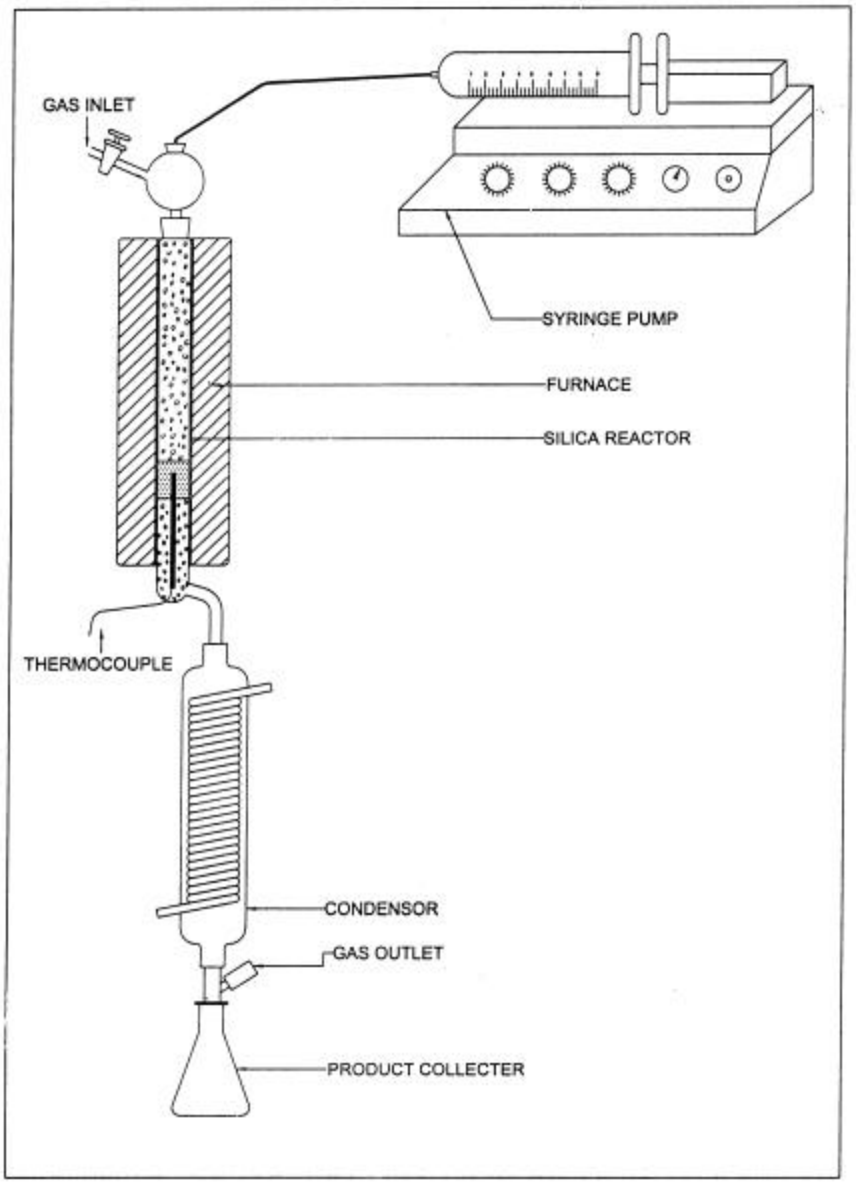

Fig. 2.4 Fix bed down flow reactor set-up for gas phase reactions

2.4.4 Hydroisomerization of n-hexane

The hydroisomerization of n-hexane was carried out in a similar reactor at the temperatures of 300-325^{0}C with H_2/n-hexane ratio of 4. The pellets of catalyst powder was made, crushed, sieved to 10 to 20 mesh size and then 2 g of it was loaded into the reactor. It was activated at 400^{0}C in presence of hydrogen and n-hexane was fed to reactor by using a syringe pump. The products were analyzed by gas chromatograph (HP 5880 A) with a FID detector and a capillary column (50 x 0.2 mm; HP-1, cross-linked methyl silicon gum)

Table - 2.2

The reagents used in various catalytic reactions

Sr. No.	Reactants used	Specifications
1.	Phenol, C_6H_5OH	S.d. fine, 98 %
2.	Anisole, $C_6H_5OCH_3$	Aldrich, 99 %
3.	m-xylene, $C_6H_4(CH_3)_2$	Aldrich, 99 %
4.	n-Hexane, C_6H_{14}	S.d. fine, 99 %
5.	Ortho-toluidine, $C_6H_4(NH_2)CH_3$	Aldrich, 99 %
6.	Hydrogen peroxide, H_2O_2	(Asian Peroxide) 28 % in H_2O

2.5 REFERENCES

1. A. Thangaraj, M. J Eapen, S. Sivasankar and P.Ratnasamy. *Zeolites* 12 (1992) 943

2. M.K. Dongare, P. Singh, P.P. Moghe and P. Ratnasamy, *Zeolites* 11 (1991) 690.

3. J.S. Reddy, R. Kumar and P. Ratnasamy, *Appl. Catal.* 58, (1990) L1.

4. B. M. Lok. C. A. Messina, R. L. Patton, R. T. Gajek, T. R. Cannan and E. M. Flanigen U.S. 440 871 (1984)

5. Alfonzo, M., Goldwasser, J., Lopez, C. M.; Machado, F. J.; Matjushin, M.; Mendez, B and Ramirez de Agudelo, M. M. *J. Mol. Catal. A: Chem.*, 98(1), (1995) 35.

3.1 INTRODUCTION

Heterogeneous catalysts are playing a key role in the preparation of bulk and fine chemicals, and in the development of eco-friendly processes. Particularly in the oxidation reactions the choice of the catalyst and the oxidant are very important, as they determine the amount of waste. The traditional stoichiometric oxidation processes are environmentally unacceptable, as they are associated with many problems such as corrosion, waste disposal, difficulty in continuous operation, low thermal stability etc. Considering the increasing stringent environmental constraints, the processes involving heterogeneous oxidation catalysts and environ-friendly reagents offer many advantages.

Titanium containing zeolite catalyst with MFI structure[1] (Ti-ZSM-5 or TS-1) was developed by Enichem in 1983, which catalyzed wide variety of oxidation reactions using hydrogen peroxide as oxidant. This catalyst offered uniform microenvironment and site location for Ti(IV) and high selectivity in oxidation reactions. As a result of extensive research, TS-1 based processes for the production of hydroquinone, catachol and caprolactam were commercialized[2]. Subsequently other titano-silicate molecular sieves like Ti-ZSM-11, Ti-ZSM-12, Ti-ZSM-48 and Ti-beta were also developed[3-6], which broadened the scope of oxidation catalysis with molecular sieves. All these materials being microporous with an average pore less than 1 nm imposed a constraint on the size of the organic substrate that can be oxidized. Therefore, mesoporous molecular sieves came in the focus of research. For example, Tanev et. al[7] synthesized titanium containing hexagonal mesoporous silica (Ti-HMS) with a pore diameter of around 2.8 nm possessing significant catalytic activity in the oxidation for bulky molecules like 2,6 ditert-butyl phenol. Blasco et. al[8] and Corma et. al[9] reported the preparation and properties of Ti containing MCM-41 and MCM-48 respectively. But among all these Ti-containing molecular sieves, TS-1 was the most interesting as it selectively oxidized wide variety of

organic substrates. Recently, Kumar et. al[10] reported chemo-selective oxidation of organic halides under solvent-free triphasic conditions using TS-1 catalyst. TS-1 was also employed in regioselective cyclization of unsaturated alcohols to furan and pyran derivatives[11], selective oxidation of alkenes to epoxides[12], α-olefins via epoxidation to 1,2-diols[13] and styrene oxide to phenylaldehyde[14]. Apart from the above reactions, TS-1 was also used in the manufacture of epichlorohydrin[15], NN-disubstituted hydroxylamine[16] and glycidyl methacrylate[17]. Various organic transformations involving TS-1 as catalyst are represented schematically in the Fig 3.1.

3.2 SYNTHESIS OF TS-1

The synthesis and catalytic properties of TS-1 catalyst are being studied extensively in the recent years because of its interesting catalytic properties in various oxidation reactions using aqueous H_2O_2 as oxidant[18-19]. The catalytic properties of TS-1 are strongly affected by the Si/Ti ratio, crystallite size and the amount of framework and extra-framework titanium content. Various silicon and titanium sources are used to synthesize TS-1 with the intention to incorporate more amount of titanium in the framework. Taramasso et al[20] reported two methods for the hydrothermal synthesis of TS-1 using tetraethyl orthosilicate (TEOS) and colloidal silica (Ludox) as the silicon source, tetraethyl orthotitanate (TEOT) as the titanium source and tetrapropyl ammonium hydroxide (TPAOH) as the organic template. The maximum mole fraction of titanium that could be incorporated was 0.025 (corresponding to Si/Ti = 39).

It is believed that the silicon source plays an important role in controlling the crystallization rate of the MFI-type zeolites. Thangaraj et al[21] used silica sol for TS-1 synthesis and found that the product was less active in oxidation reactions. Other silica sources like fumed silica and silica gel also produced TS-1, but with very less amount of Ti incorporation. The presence of Na^+ and K^+ associated with it was also found to be

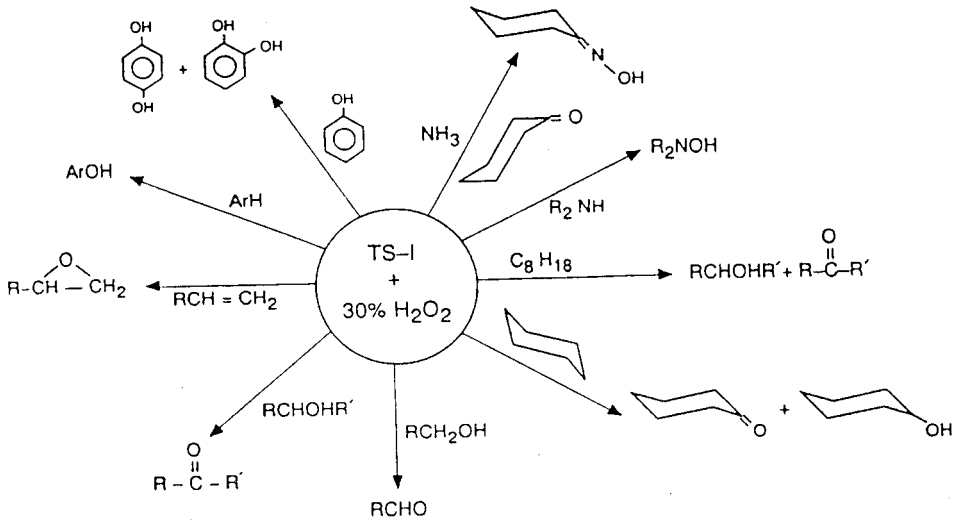

Fig. 3.1 The broad spectrum of selective oxidation using TS-1.

detrimental to the TS-1 synthesis. Therefore a different modified route was developed to incorporate higher amount of titanium (Si/Ti < 20). Tetrabutyl orthotitanate (TBOT) and TEOS were used as the titanium and silicon sources respectively. TEOS was first hydrolyzed with aqueous TPAOH to which TBOT in dry isopropyl alcohol (IPA) was added in order to avoid the precipitation of titanium dioxide.

As the titanium ions are not stable at high pH conditions normally used in zeolite synthesis, they form stable TiO_2 phase, which does not dissolve to form $Ti(OH)_4$ species. Therefore to avoid such irreversible formation of TiO_2 species, a method was also developed based on the formation of peroxytitanates[22]. Tuel[23] attempted crystallization of TS-1 in the presence of alcohol and studied the influence on Ti incorporation on the quality of the material and the catalytic activity. Various recipes in the reported literature were used retaining alcohol in the system prior to crystallization and found that, the crystallization time was considerably reduced. It was observed that when hydrolysis of the Si and Ti sources was carried out in the presence of isopropyl alcohol, all added Ti was incorporated in the zeolite lattice. Tuel et al also reported[24] the influence of the nature of the silicon and titanium sources on the rate of crystallization and the incorporation of titanium in TS-1. Various silicon alkoxides such as silicon tetraethoxide (TEOS), tetramethoxide (TMOS), tetrapropoxide (TPOS) and tetrabutoxide (TBOS) were used for the synthesis of TS-1. TPOS and TBOT were not recommended because of their low rate of hydrolysis and yielded materials with low crystallinity containing extra-framework TiO_2. The higher amount of titanium could be incorporated using TMOS, which was attributed to a very high rate of hydrolysis of the silicon source. Until now, TEOS was thought to be the most preferred silicon source for the synthesis of TS-1 because of its monomeric nature and the moderate rate of hydrolysis. But the high cost of TEOS prohibited the use of TS-1 in industrial applications. Attempts were also made to decrease

the cost of TS-1 by using small amount of TPABr instead of TPAOH[25], but the overall cost was reduced marginally. The cost of TS-1 is mainly determined by the source of silica used and therefore it was desirable to find an alternate cheaper silicon source to prepare pure TS-1 for industrial use. In the present investigation, a new silicon source Ethyl silicate-40 (ES-40) was used for the synthesis of TS-1 for the first time.

Ethyl silicate-40[26] (ES-40, CAS. Registry No. 18954-71-7) is a mixture of linear, branched and cyclic ethoxysiloxanes and gives 40wt % silica after hydrolysis. It is a partially hydrolyzed product of TEOS, which is manufactured from the industrial alcohol containing 7-10% water, whereas the TEOS is manufactured using absolute alcohol and it gives only 28 wt% silica on hydrolysis. Therefore the ES-40 is cheaper silicon source compared to TEOS.

The synthesis, characterization and catalytic properties of TS-1 prepared using ES-40 and TEOS are discussed in this chapter. The influence of synthesis parameters, like temperature, SiO_2/TiO_2 and $TPAOH/SiO_2$ ratios were also studied.

3.2.1 Synthesis of TS-1 using Ethyl Silicate-40

Two different methods for the synthesis were followed as shown schematically in the Fig.3.2. In a typical synthesis by method-I, 1.98 g of TBOT in 20 g. of dry IPA was mixed with 30g of ES-40 at 25^0C and stirred for 10 minutes. A clear solution was obtained. Then 56 g of aqueous TPAOH (22.2 wt %) was added slowly to the above solution while stirring. The resulting solution still remained clear. Whereas in the method-II, the quantities of all the reactants were the same, but the order of their addition was different. The ES-40 was first hydrolyzed with TPAOH solution and then TBOT in IPA was added. The solutions obtained in both the methods were further stirred at 60-70^0C for about two hours to remove the alcohol. The required amount of water (80g.) was added to the above solution. The solution still remained clear which was further stirred for one

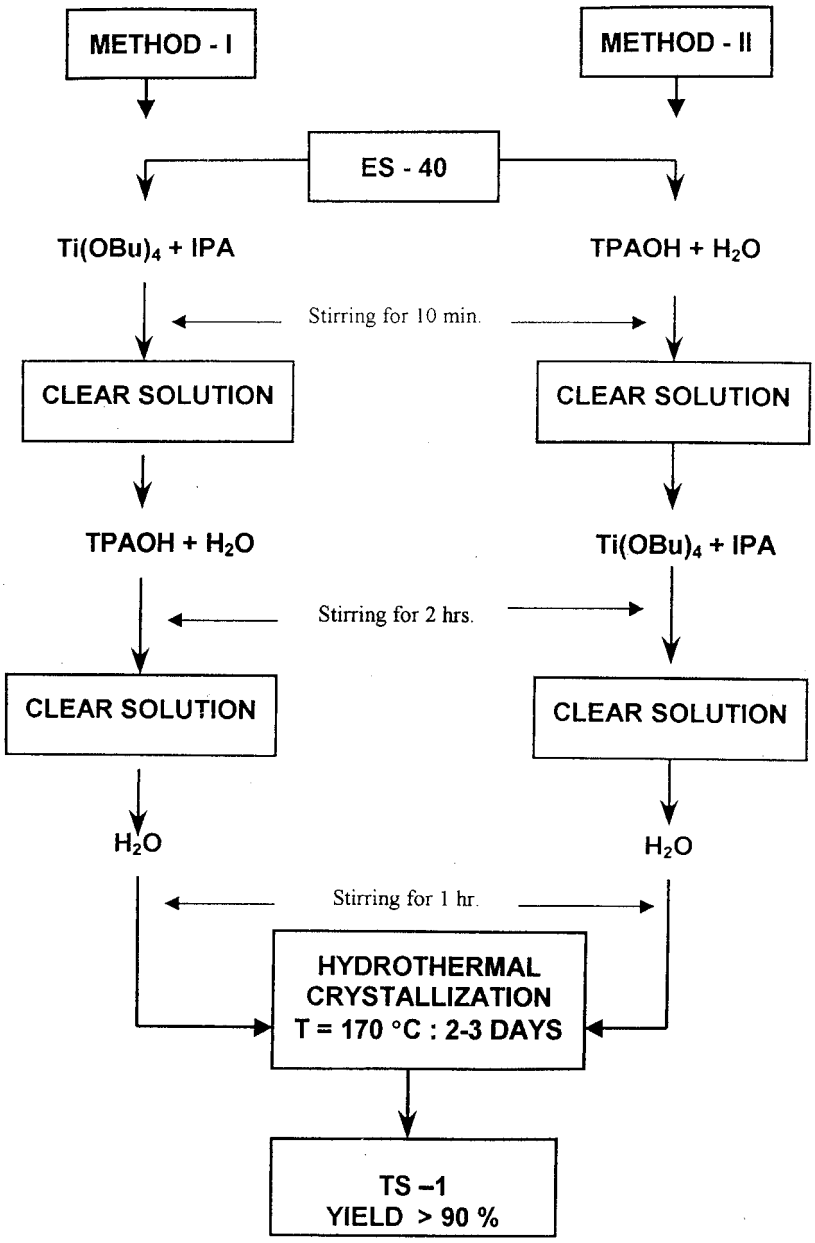

Fig. 3.2 Schematic representation of two different methods for TS-1 synthesis.

ES-40: Ethyl Silicate-40, $Ti(OBu)_4$: Titanium tetrabutoxide, IPA: Isopropyl alcohol and TPAOH: Tetrapropyl ammonium hydroxide.

hour. The chemical composition of this reactive solution was SiO_2: 0.03 TiO_2: 0.33 TPA: 35 H_2O. This solution was placed in an autoclave at 170^0C for 2-3 days for hydrothermal crystallization. After the reaction the solid was recovered by centrifugation, washed with deionized water, dried overnight at 100^0C in an oven and then calcined at 550^0C in presence of air for 8-10 h. The samples of different Si/Ti ratios were prepared by varying the amount of TBOT. For comparison, TS-1 and Zr containing silicalite-1 (ZrS-1) were also prepared using TEOS as per the reported procedure[21,27].

3.3 PRECURSOR CHARACTERIZATION

3.3.1 Structure of ES-40 and TEOS

The ^{29}Si and ^{1}H liquid NMR spectroscopic techniques were used to understand the structure of Ethyl silicate-40. ^{29}Si liquid NMR was used to characterize the type and quantitative distribution of $Si(O^-)_{4-n}$ $(OSi)_n$ structural units (designated as Q^n) in the solution.

A typical ^{29}Si liquid NMR spectrum of TEOS and ES-40 are shown in Fig.3.3 (a and b respectively). The spectrum of TEOS relative to that of TMS, shows a sharp single peak at chemical shift of -82.3 ppm, indicating that all the Si atoms in TEOS have same environment, which are all monomeric in nature. On the contrary, spectrum of ES-40 shows four different peaks with chemical shifts at around -82.1, -89.1, -96.5 & -104.2 ppm, suggesting that ES-40 contained a variety of silicate species, including polymeric species essentially containing Si-O-Si linkages.

The ^{1}H NMR spectra of TEOS and ES-40 are shown in Fig.3.4 (a and b respectively). A typical ^{1}H NMR spectra of TEOS shows two chemical shifts at δ = 3.7-3.9 (2H, q, C*H*$_2$), δ = 1.2 –1.35 (3H, t, C*H*$_3$) suggesting that TEOS contained -O-CH_2 and -CH_3 groups. The ^{1}H NMR spectra of ES-40 also shows two chemical shifts

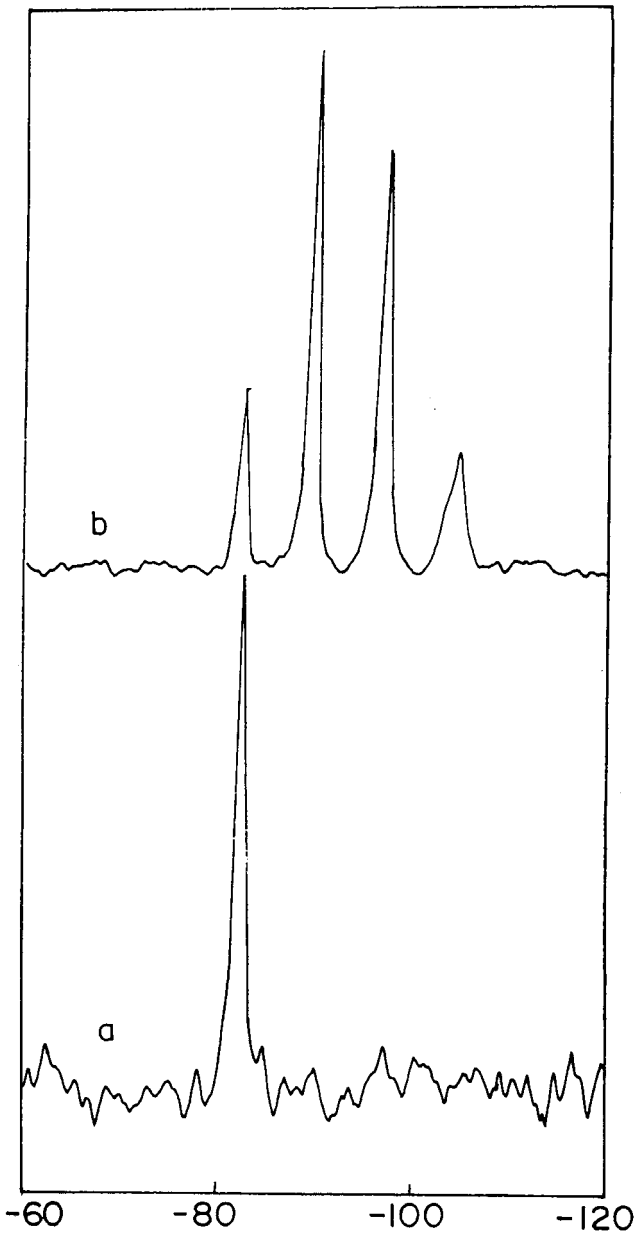

Fig. 3.3 ^{29}Si liquid NMR spectrum of TEOS and ES-40 (a and b respectively)

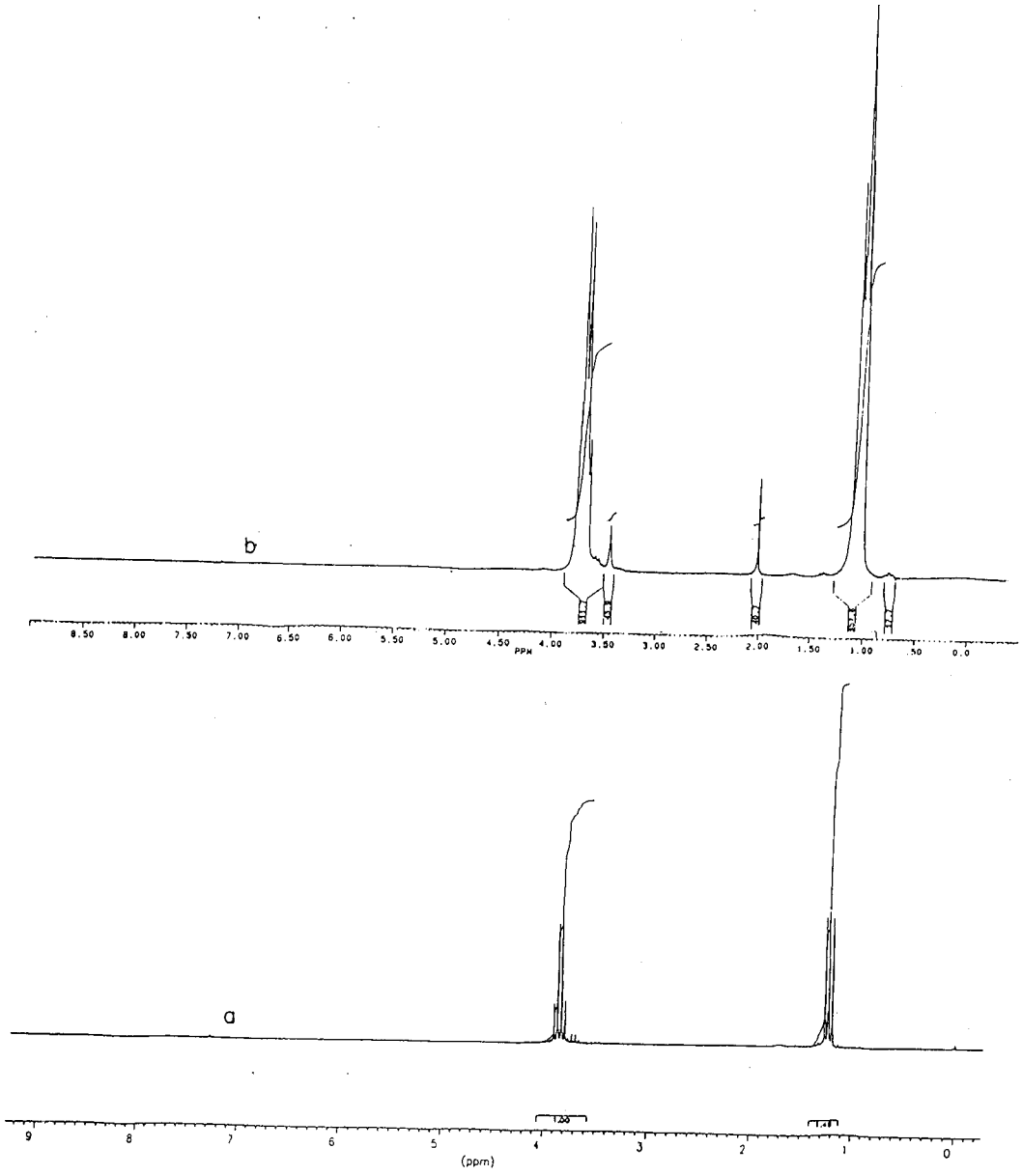

Fig. 3.4 ^{1}H NMR spectrum of TEOS and ES-40 (a and b respectively)

and is identical to that of TEOS, except that in the case of ES-40 the lines are broader as expected for a polymeric species.

It is inferred form ^{29}Si and ^{1}H liquid NMR studies that in ES-40, Si atoms are not only bonded to another Si through oxygen (Si-O-Si), but also to -O-C_2H_5 groups at remaining valence positions.

3.3.2 ^{29}Si liquid NMR studies of precursor solutions

In order to characterize the nature and the amount of silicate species in the precursor reactive solutions, the high resolution liquid ^{29}Si NMR spectroscopy was used. During the synthesis of TS-1 following both of the above methods, ^{29}Si liquid NMR spectra of precursor solutions at different stages of preparation were recorded.

The ^{29}Si liquid NMR spectra of the precursor solutions at different stages in method-I are shown in the Fig.3.5. A typical ^{29}Si liquid NMR spectrum of ES-40 is shown in Fig.3.5a. The addition of isopropyl alcohol to ES-40 did not change the nature of the spectrum (Fig. 3.5b) and the relative concentrations of Q^1, Q^2, Q^3, and Q^4 species also remained unchanged.

The concentration of Q^3 and Q^4 species also remained unchanged after the addition of TBOT in IPA to the above solution (Fig.3.5c), indicating the absence of any significant interactions in the solution. When aq. TPAOH was added to the same solution, the spectrum was obtained as shown in Figure 3.5d. The Q^1, Q^2, Q^3 and Q^4 species showed broader bands around -80, -89, -98.3 and -108.3 ppm respectively. In addition, the relative concentration of Q^3 species increased significantly. This kind of immediate increase in the concentration of Q^3 species indicated oligomerization in the solution through the formation of -Si-O-Si- and -Si-O-Ti- linkages. Tuel[23] studied the crystallization of TS-1 in the presence of IPA and observed its influence on Ti incorporation and time of crystallization. When both Si and Ti sources were hydrolyzed in the presence of isopropyl

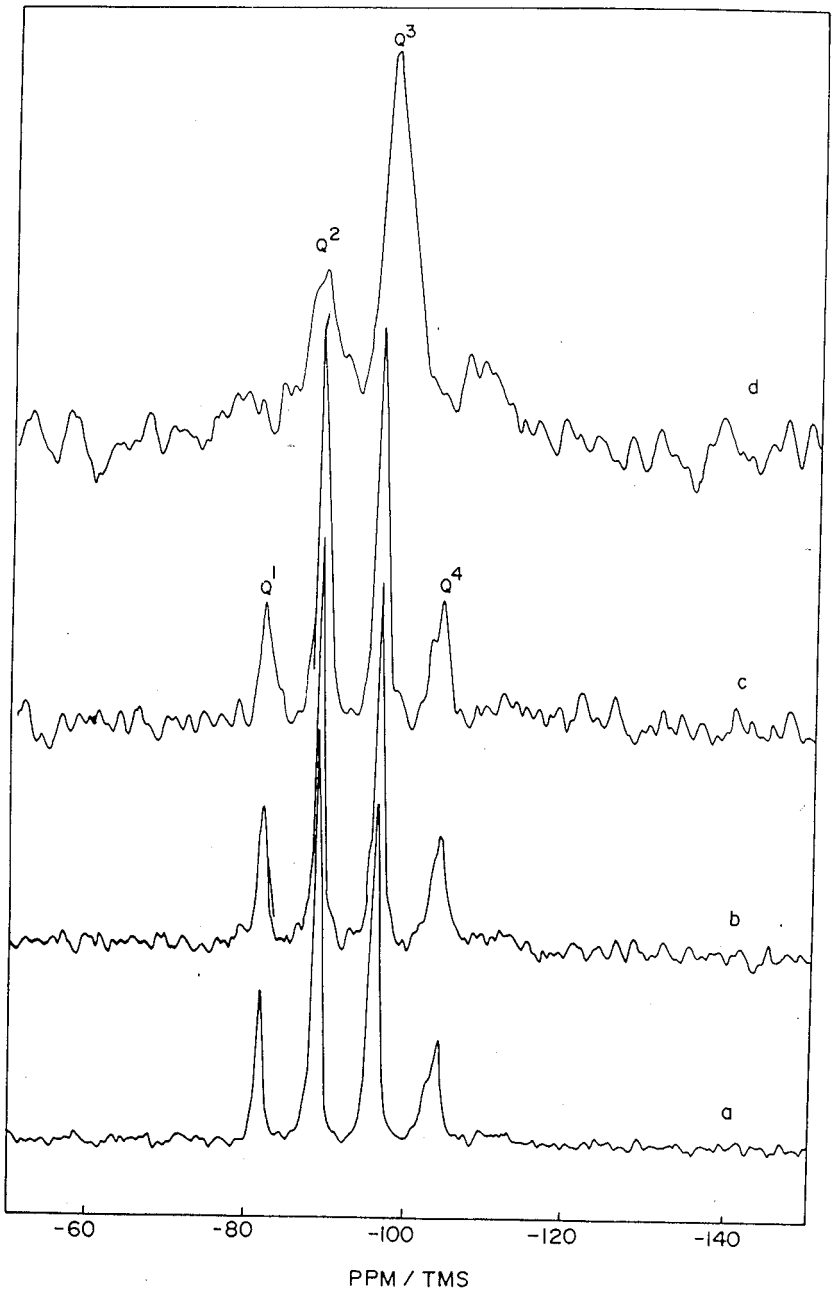

Fig. 3.5 ^{29}Si liquid NMR spectra of solutions in method-I.

a) ES-40, b) a + IPA, c) b + $Ti(OBu)_4$ and d) c + TPAOH + H_2O

alcohol, the rapid increase in Q^3 species was observed and all the available Ti was incorporated in the zeolite lattice.

It is well known that the rate of hydrolysis of different metal alkoxides $M(OR)_n$ are different and depends on the type of metal ion and alkyl group associated with it. Accordingly the rate of hydrolysis of titanium tetraethoxide (TEOT) is very high compared to that of TBOT and TEOS. In our own experiments, we observed that TBOT hydrolyzed faster than ES-40. When TPAOH solution was added to the mixture of ES-40 and TBOT in IPA, both the alkoxides were partially hydrolyzed to form $(EtO)_nSi$-OH and $(BuO)_3$-Ti-OH species respectively. This resulted in the reaction between them forming the metallo-siloxanes (Si-O-Ti linkages) through the following possible reactions, where ES-40 is represented as $Si(EtO)_n$.

$$(BuO)_3\ Ti\text{-}OH + Si(OEt)_n \longrightarrow (BuO)_3\ Ti\text{-}O\text{-}Si(OEt)_{n-1} + EtOH.$$

$$(EtO)_{n-1}\ Si\text{-}OH + Ti(OBu)_4 \longrightarrow (EtO)_{n-1}\ Si\text{-}O\text{-}Ti(OBu)_3 + BuOH.$$

These types of reactions are very well described in the literature[28]. Schmidt[29] observed that when a small quantity of water is added to the mixtures of Si and Ti alkoxides, Si alkoxide is partially hydrolyzed to produce -Si-OH, which immediately reacts with $Ti(OR)_4$ forming bimetallic alkoxide and thus preventing it from uncontrolled hydrolysis and precipitation. Tuel[30] also observed that the formation of such linkages promoted the incorporation of Ti in the lattice preventing the formation of extra-lattice TiO_2 species.

The ^{29}Si liquid NMR spectra of solutions obtained in the method-II are presented in Fig.3.6. In this method, ES-40 was first hydrolyzed by aq. TPAOH. The spectrum of the resulting solution (Fig.3.6a) consists of four peaks at -80.0, -89.3, -96.8 and -104.5 ppm, which are attributed to four different silicate species Q^1, Q^2, Q^3 and Q^4 respectively. Though the positions of these peaks are not very much different than those of pure ES-40,

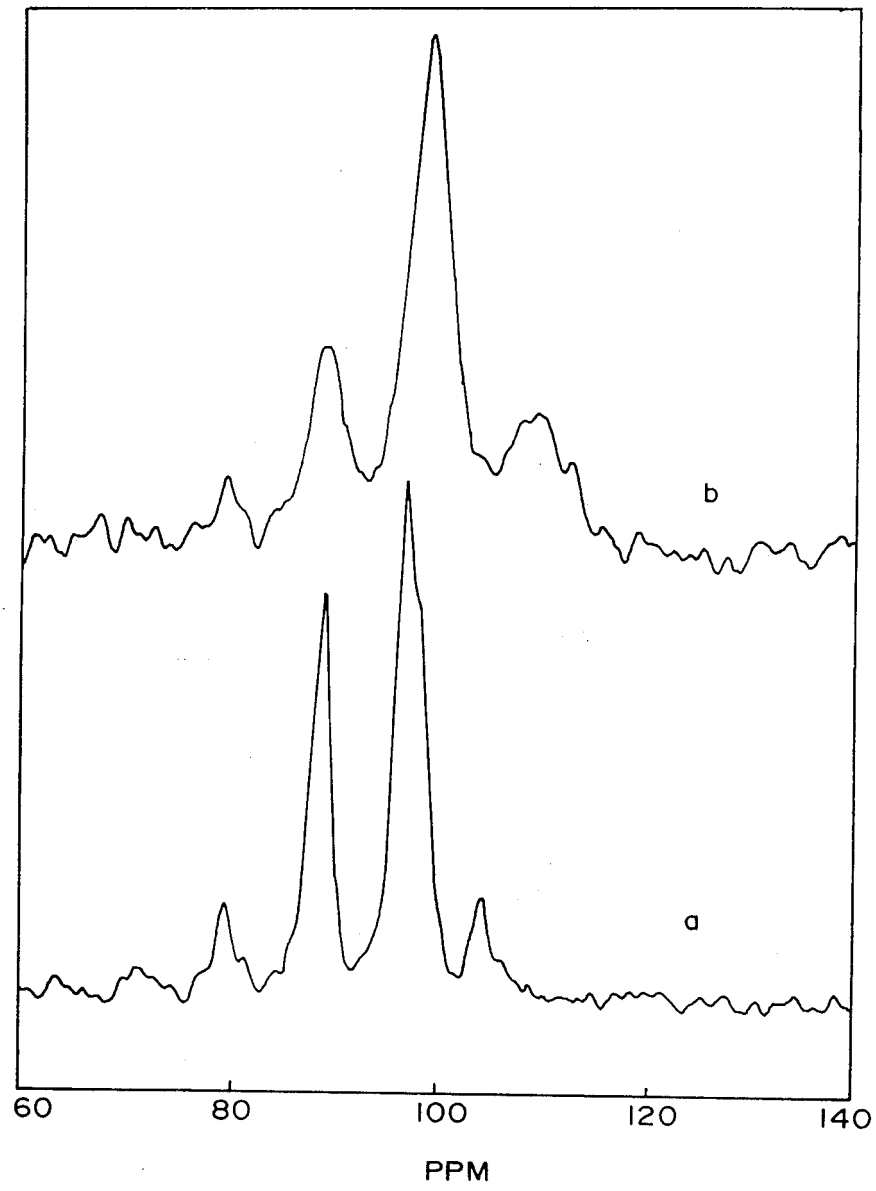

Fig. 3.6 ^{29}Si liquid NMR spectra of solutions in method-II.

a) ES-40 + aq. TPAOH and b) a + $Ti(OBu)_4$ + IPA

all the peaks are significantly broadened and the intensity of Q^3 peak increased significantly. It is due to the hydrolysis of ES-40 with aqueous TPAOH and subsequent reorganization in this highly alkaline solution to form Si-O-Si linkages. The addition of TBOT in IPA to this highly alkaline solution also leads to the rapid hydrolysis of TBOT, which condense and rearrange with silicate species. The spectrum at this stage is depicted in Fig 3.6b, wherein the relative increase in the concentration of Q^3 species is clearly observed. Booxhorn[31] and Thangaraj et al[21] also made similar observations. In this spectrum the peaks due to Q^1, Q^2, Q^3 and Q^4 species were observed at -79.7, -89.4, -97.6, -107.2 ppm respectively. Whereas the nature of this spectrum was similar to the corresponding spectrum in method-I as shown in Fig.3.5d, the chemical shifts for Q^3 and Q^4 species are relatively shifted to the lower field. Although very clear precursor solutions were obtained in both the methods, after the hydrothermal crystallization, the samples obtained by method-II were contaminated with extra-lattice TiO_2 species, which is attributed to the uncontrolled hydrolysis of both ES-40 and TBOT separately in highly alkaline solution of TPAOH. Under such conditions, the possibility of the formation of -Ti-O-Ti- linkages increases, which is responsible to the formation of dense phase TiO_2 species in the product.

Whereas in method-I, due to the simultaneous hydrolysis of both the alkoxides the titanosilicate species are formed along with silicate species, which rearrange and increase the concentration of Q^3 species. These Q^3 species are identified as soluble double five-membered ring (D_5R) as proposed by Boxhoorn[31] and are responsible for nuclei formation, which favor most efficient formation of ZSM-5 structure. However as per our observations both the methods are equally good for low amount, but the method I is preferable for higher amount of Ti incorporation.

Tuel et al[24] studied the influence of the nature of silicon and titanium alkoxides on the titanium incorporation in TS-1 and concluded that TEOS is the silicon alkoxide of choice for higher incorporation of titanium in the lattice. According to our observations for higher Ti incorporation, ES-40 is better silica source compared to TEOS.

3.4 CRYSTALLIZATION KINETICS

To study the influence of temperature, SiO_2/TiO_2 ratio and SiO_2/TPAOH ratio on the rate of crystallization, the reactant composition was kept as SiO_2: 0.03 TiO_2: 0.33 TPA: 35 H_2O. The above reactant composition was selected based on some preliminary experiments. The crystallinity of the samples was determined[32] by comparing the total area under all the peaks appearing in the 2θ range of 22-25^o with that of the standard sample prepared by the same method and confirmed by adsorption of probe molecules.

3.4.1 Influence of Temperature

In Fig.3.7 curves a-d, the XRD crystallinity of the samples prepared using ES-40, are plotted against the time of crystallization at 130, 150, 160 and 170^{0}C respectively. The curves clearly indicated that the rate of crystallization significantly depends on temperature, which strongly influences the kinetics of crystallization process. Increasing the temperature of crystallization decreased the nucleation time and increased the rate of crystallization. The rate of crystallization of TS-1 at 160^{0}C and above was very high and fully crystalline TS-1 samples were obtained within 3-4 hrs. The rate of crystallization at 160^{0}C (curve c) using ES-40 was considerably higher than that using TEOS (curve e). The fully crystalline samples were obtained at all the temperatures higher than 150^{0}C. The yield of the product was above 90 % at all the temperatures, which was also more than that obtained using TEOS (85 %). Derouane et al[33] suggested that the silica source initially containing high amount of silica monomer like TEOS, which rapidly hydrolyses to give $Si(OH)_4$ on addition of alkali, gives faster rate of crystallization of zeolite compared to

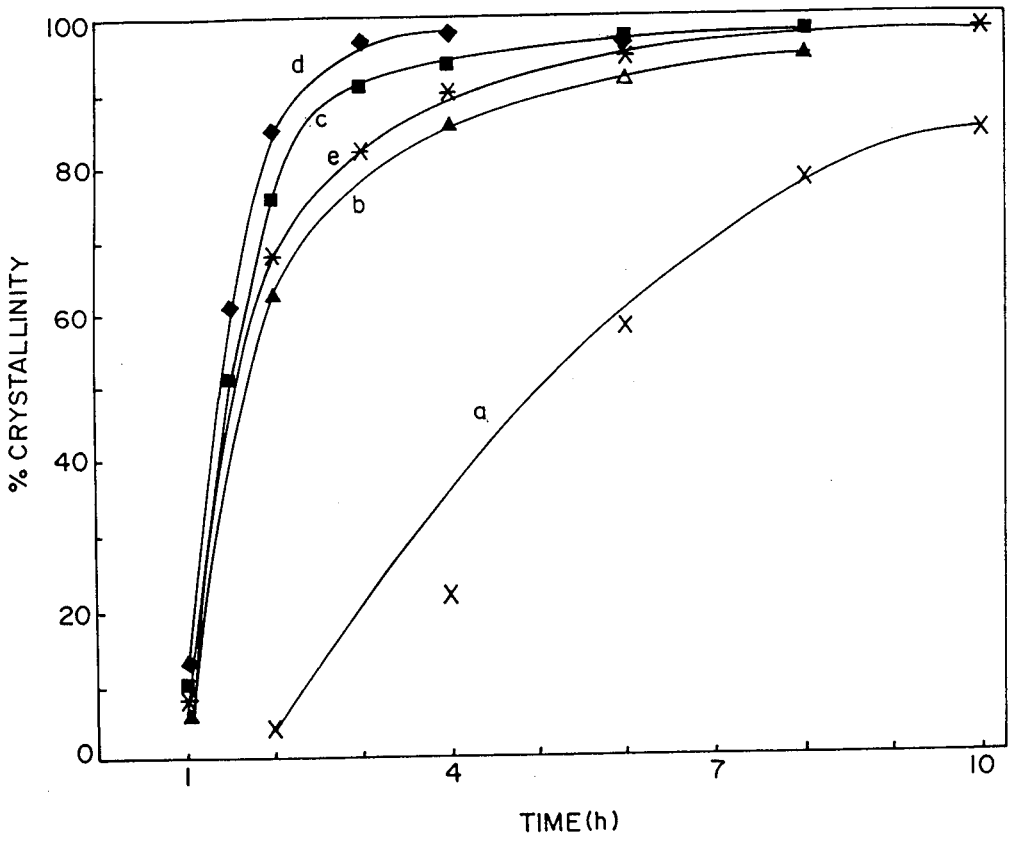

Fig. 3.7 Variation of XRD crystallinity with time of crystallization of TS-1 (Si/Ti = 33) at a) 130, b) 150, c) 160 d) 170 and e) 160°C [TEOS]

polymeric silica like silica sol, which has to de-polymerize to $Si(OH)_4$ before rearrangement. But in the case of ES-40, which already contains silica in the limited range of polymerization was able to produce TS-1 faster than that of TEOS. Even in the case of highest extent of Ti incorporation (Si/Ti=33) there is a need to insert only one Ti atom in 33 Si atoms. So it may not be necessary to completely de-polymerize ES-40 for Ti incorporation in the resulting product and therefore the rate of crystallization was faster when ES-40 was used as the silica source.

3.4.2 Influence of template concentration

Figure 3.8 (curves a-d) shows the influence of the template (TPAOH) concentration on the rate of crystallization of TS-1, when all the other parameters were kept unchanged. The $TPAOH/SiO_2$ ratio of 0.33 (curve c) was found to be the ideal, as it resulted in the fully crystalline material without any impurity phase. When the template concentration was decreased in the initial solution mixture ($TPAOH/SiO_2$= 0.1, curve a), the crystallization of the sample was not complete even after 72 h. When it was increased to 0.5, the crystallization was faster but the yield of the product was only 60-70%. The decrease in yield is attributed to the re-dissolution of nuclei. Similar results were also observed by Kraushaar et al.[34]. The template being a strong base, the pH of the initial gel mixtures was found to be high (11.5), which increased to ~12.5 on the completion of the crystallization. Earlier studies[35] have concluded that an increase in pH after complete crystallization indicates the formation of a stable and crystalline material. If the initial pH of the reactant mixture does not change or it decreases with the time of crystallization then either an unstable or amorphous product was obtained. The efficient incorporation of Ti in the MFI framework can be achieved at $TPAOH/SiO_2$ ratio of 0.33.

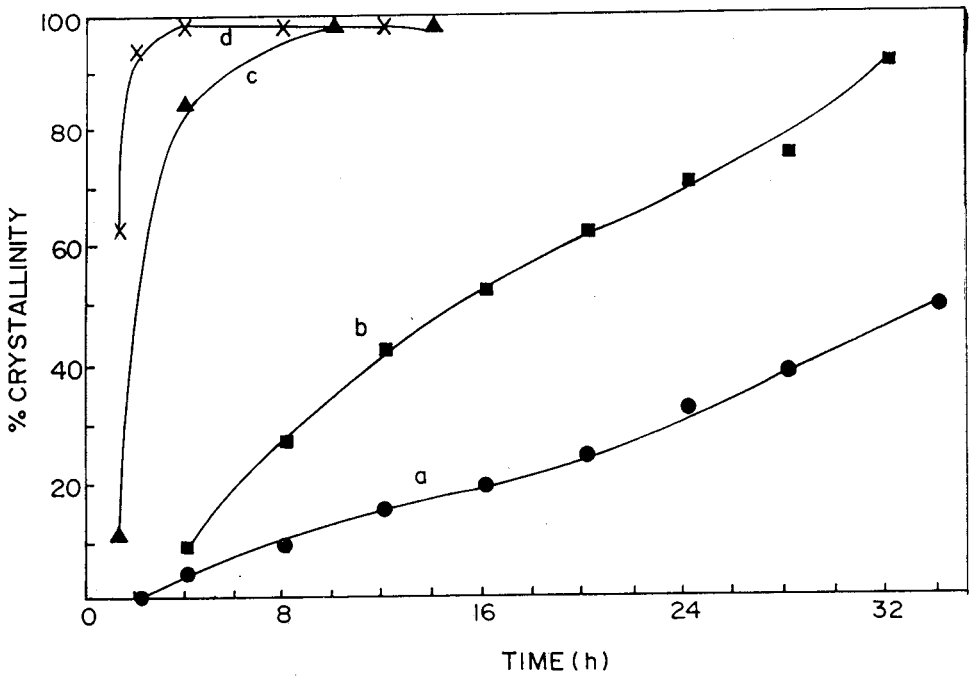

Fig. 3.8 Influence of TPAOH/SiO_2 ratio on the kinetics of crystallization of TS-1 ($SiO_2/TiO_2 = 33$) at 170 ^{0}C a) 0.1, b) 0.2, c) 0.33 and d) 0.5

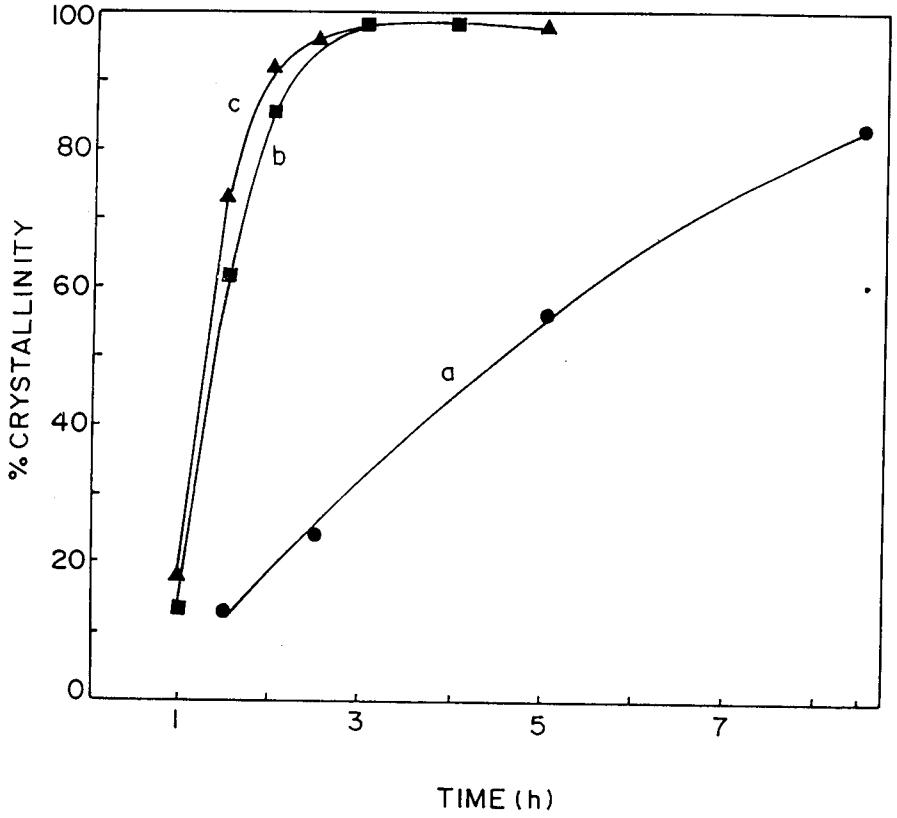

Fig. 3.9 Influence of SiO_2/TiO_2 ratio on the kinetics of crystallization of TS-1 at 170^0C a) $SiO_2/TiO_2 = 20$, b) 33 and c) 60

3.4.3 Influence of SiO_2/TiO_2 ratio

In Fig. 3.9(curves a-c), the influence of SiO_2/TiO_2 ratio on the rate of crystallization is presented while all other parameters were kept unchanged. The rate of crystallization decreased with increase in Ti content, as expected. The effect was not significant beyond Si/Ti ratio 40. The results are in good agreement with the published literature on metal substituted zeolites[36-37].

3.5 PRODUCT CHARACTERIZATION

3.5.1 Chemical analysis by XRF

The chemical composition of the product was determined using XRF and it is presented in the Table-3.1. It was observed that the Si/Ti ratio in the product was lower than that in the precursor solution. Such enrichment of titanium in the product was also observed by many authors[21,36]. Titanium source being more reactive than silicon source and unstable at high pH value of the reaction medium, it is expected to be more in the product.

3.5.2 X-Ray Diffraction (XRD)

The XRD patterns of the crystalline TS-1 samples prepared in this study are compared with the reported patterns of TS-1. The XRD patterns of the calcined TS-1 prepared using TEOS (Fig.3.10, a) and ES-40 are shown in Figure 3.10 (b-d). The samples prepared by both the methods I and II (Fig.3.10, c and d respectively) are identical to that for TS-1 prepared using TEOS and showed orthorhombic symmetry before and after calcination. The absence of symmetry change on calcination can be taken as an evidence for the incorporation of the metal in the framework[38-41]. The interplanar ‘d’ spacings are corrected with respect to silicon and were used for the calculation of unit cell parameters. The unit cell parameters calculated are tabulated in Table-3.2. It is observed

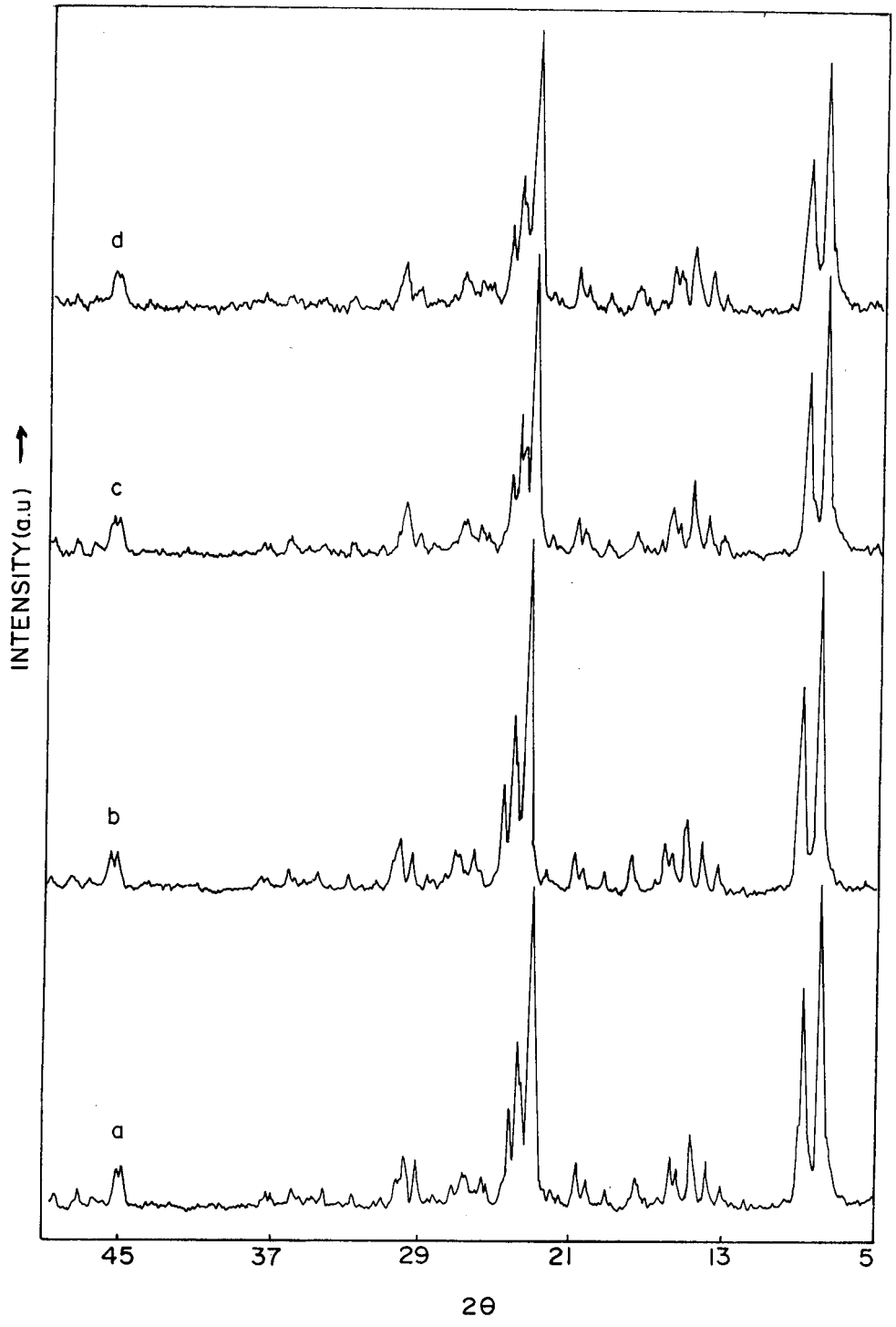

Fig. 3.10 XRD patterns of crystalline TS-1 samples

a) TS-1(50, TEOS), b) TS-1(125, M1), c) TS-1(50, M1) and d) TS-1(50, M2)

that the unit cell expands regularly with increase in titanium incorporation. This indicates the incorporation of Ti in the silicalite framework.

3.5.3 Scanning Electron Microscopy (SEM)

The SEM photographs of the samples prepared using ES-40 by both the methods are presented in Fig.3.11, photo-frame a and b respectively. The crystallites in the product obtained using ES-40 are cuboids of 0.1 to 0.2 μm, which are smaller than those of the sample (0.4 μm) obtained using TEOS[37]. Probably polymeric silicate species in ES-40 reacts with TBOT forming smaller clusters of double metal alkoxide, then rapidly hydrolyze, rearrange and crystallize in the form of smaller crystallite sizes. Whereas, TEOS completely hydrolyzes to $Si(OH)_4$ and rearranges with $Ti(OH)_4$ species facilitating the formation of bulkier moieties, which subsequently leads to the formation of crystallites of larger size.

3.5.4 Sorption of N_2 and other probe molecules

The quantities of water, n-hexane and cyclohexane sorbed by Silicalite-1 and TS-1 samples prepared using both the methods are presented in Table 3.1. The micropore volume for the above samples were calculated by N_2 adsorption applying t-plot method[42] and were found to be comparable to the reported values. The values of surface area and adsorption of water, n-hexane and cyclohexane indicate that the products are highly crystalline and they are free from occluded impurities. In many of the metallosilicate molecular sieves (Ti, V, Sn, Zr, etc.), a higher surface area compared to the parent silicalite sample has been reported[1,43-45].

3.5.5 UV-Visible Spectroscopy

The UV-Vis diffuse reflectance spectroscopic technique has been widely applied to determine the quality of Ti-containing molecular sieves, since the presence of extra-lattice TiO_2 can be detected by the observance of an absorption band at 330 nm[46]. The TS-1

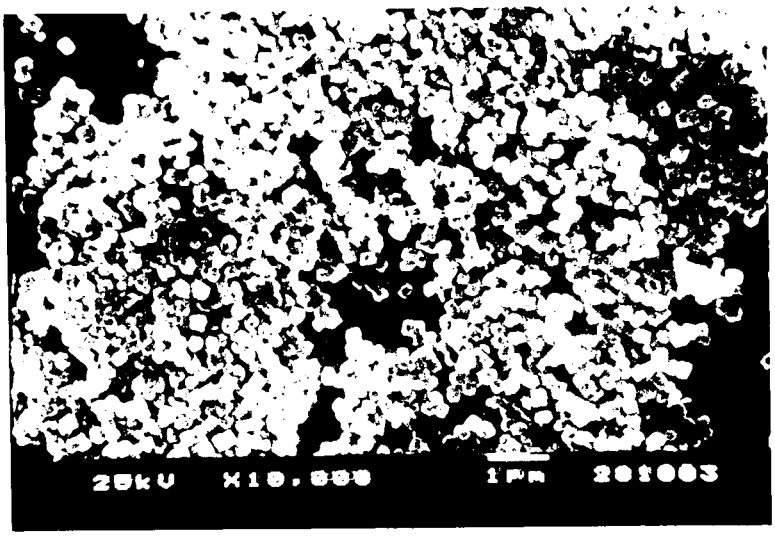

(a)

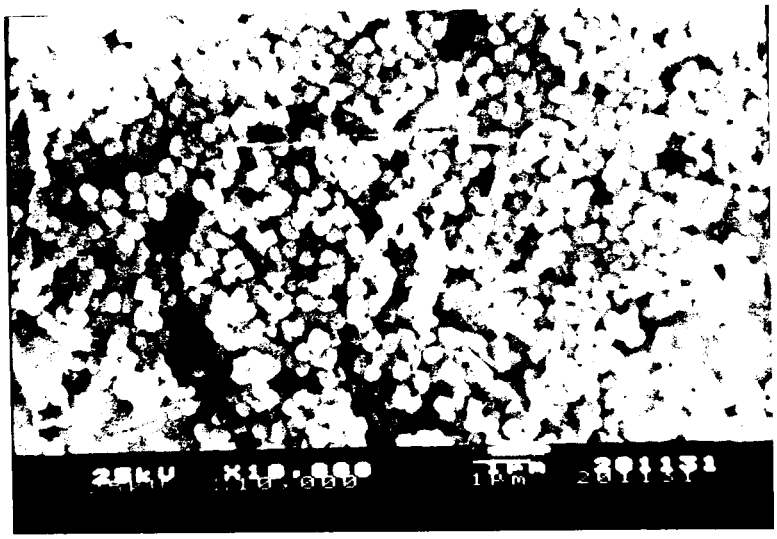

(b)

Fig. 3.11 SEM photographs of calcined TS-1 (a) method-I [TS-1(50, M1)], and (b) method-II [TS-1(50, M2)]

samples prepared by method-I (Fig.3.12b) show a strong band in the range 205-215nm and considered as an evidence of the Ti in the tetrahedral position. This band is attributed to the charge transfer character involving Ti(IV) in the [TiO_4] or [TiO_3OH] sites[47] whereas the sample prepared by method II (Fig.3.12a) shows an additional small absorption band at around 330nm indicating the presence of some extra-lattice TiO_2 species. From the figure, we may note that all the samples prepared by method-I are very pure, whereas only low Ti containing samples prepared by method-II are pure.

3.5.6 ^{29}Si MAS-NMR Spectroscopy

The solid state ^{29}Si MAS-NMR spectroscopic results (Fig-3.13,a-d) of calcined TS-1 samples by both the methods are comparable with that of TS-1 prepared using TEOS. A broad peak around -107 ppm and a small peak around -114 ppm are attributed to Si in distorted tetrahedra containing Si-O-Ti linkages and Si bonded to four siloxanes respectively[48,49].

3.5.7 FTIR Spectroscopy

The FTIR spectra of the samples in the framework vibration region are presented in Fig.3.14. The lattice vibrations for TS-1 samples revealed the presence of a band at 550 cm^{-1} due to D_5R in addition to a band at 450 cm^{-1}. All the samples show a strong absorption band at 1100 cm^{-1} attributed to internal vibrations of TO_4 tetrahedra. Although the FTIR spectrum does not give concrete evidence for the presence of Ti^{4+} ions in the TS-1 lattice, it is characterized by an absorption band[50]at 960 cm^{-1}. The FTIR spectra of the TS-1 samples prepared by method I and method II [TS-1(44, M1), TS-1(50, M1), and TS-1(50, M2) of Table-3.2, spectra b-d of Fig. 3.14 respectively) are almost identical to that of standard TS-1 (Fig. 3.14a) having characteristic band around 960 cm^{-1}. This band is believed to be due to stretching vibrations of SiO_4 tetrahedra bound to Ti atoms as Si-O-Ti linkages. The systematic increase in the intensity of this band was observed with the

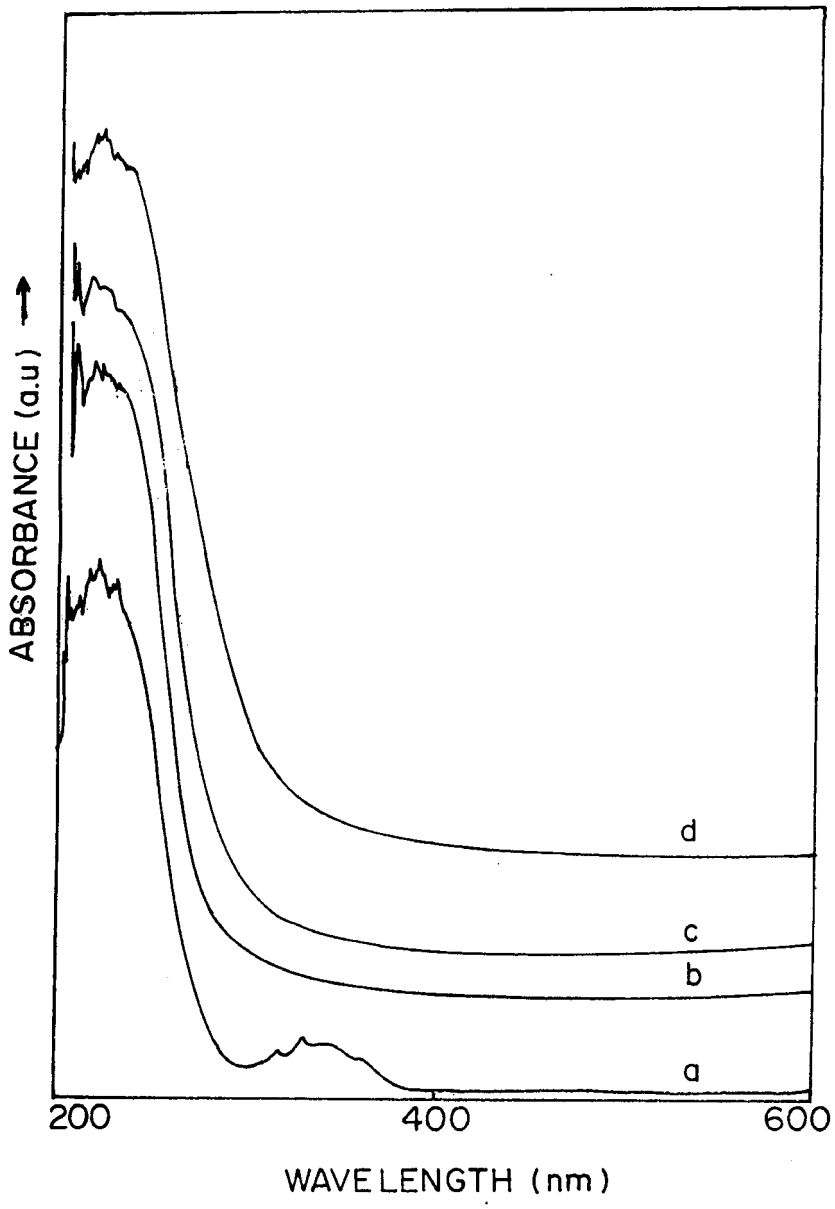

Fig. 3.12 UV-Vis diffuse reflectance spectra of TS-1 samples

a)TS-1(50, M2) b) TS-1(50, M1) c) TS-1(60, M2) and d) TS-1 (50, TEOS)

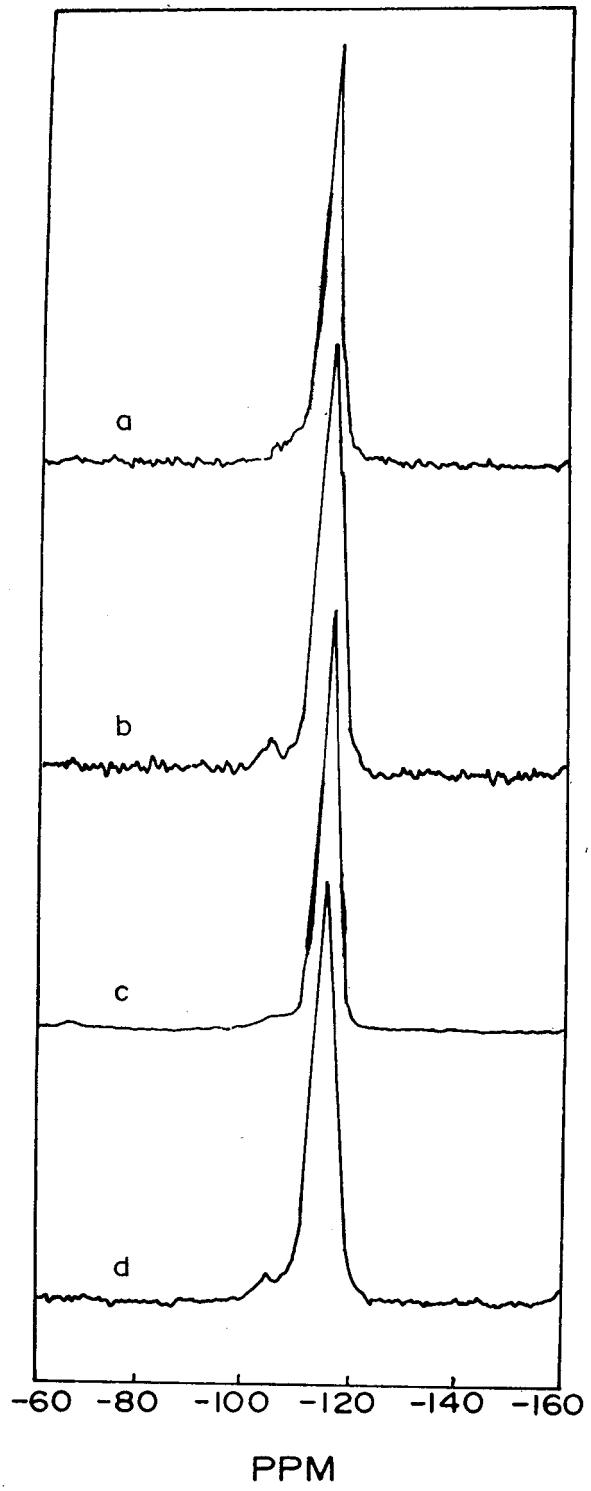

Fig. 3.13 The solid state ^{29}Si MAS-NMR spectra of calcined samples

a)TS-1(50, TEOS) b) TS-1(50, M1), c) TS-1(60, M2) and d) TS-1(44, M1)

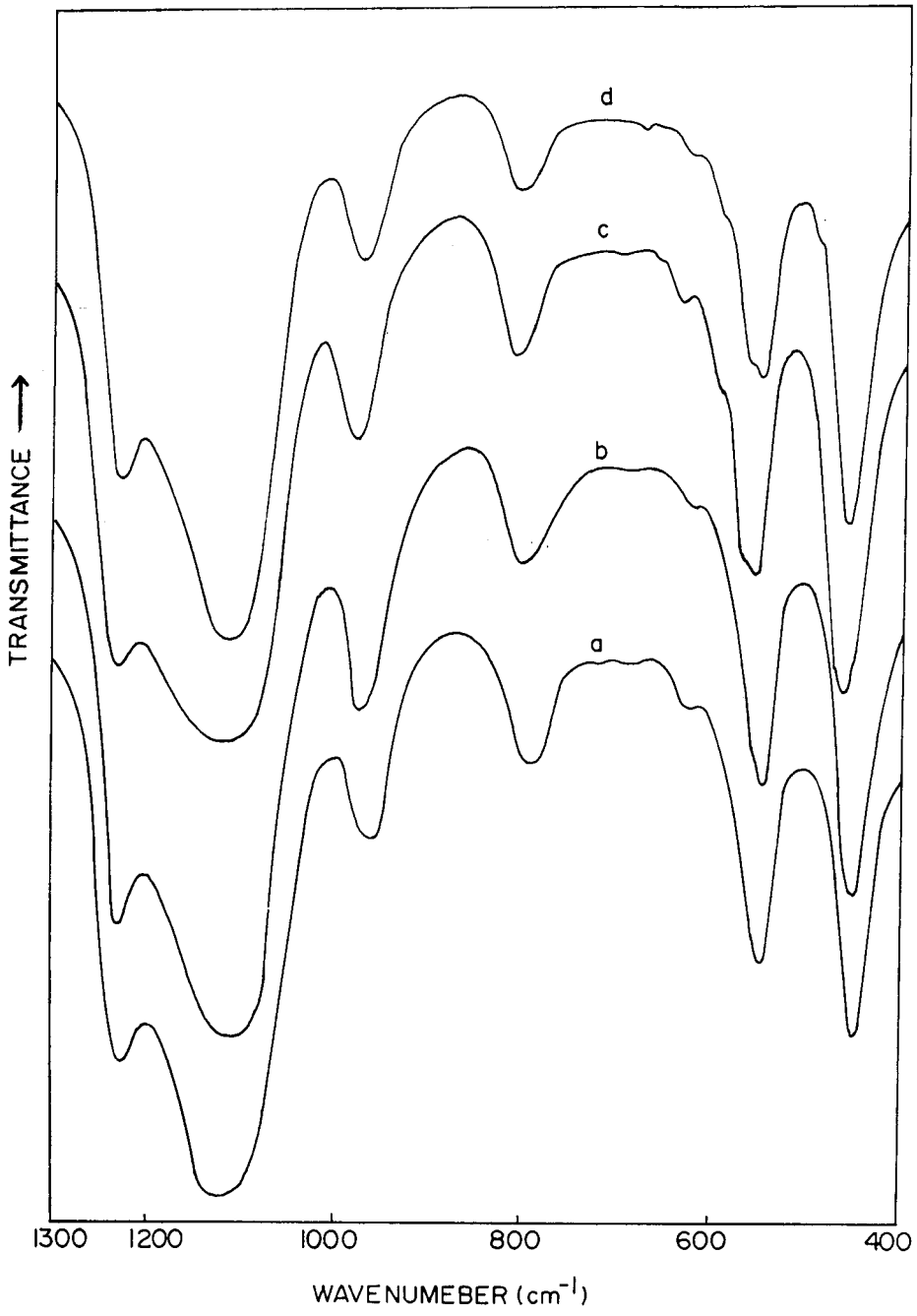

Fig. 3.14 FTIR spectra of TS-1 samples a) TS-1(50, TEOS), b) TS-1(44, M1), c) TS-1(50, M1) and d) TS-1(50, M2).

increase in the Ti content in the sample. However this band in Ti free silicalite sample was found to be very weak, which is assigned to Si-O stretching vibrations of Si-O-H linkages[51] and such bands prominently occur only in zeolite samples with lot of defect sites like beta zeolite[52]. Various possible assignments are given for this band in the literature[53]. It may be due to the stretching mode (ν_3) of a [SiO_4] unit most ir active due to the presence of adjacent Ti, local stretching mode of a [TiO_4] and/or (O_3TiOH) unit in silicalite framework, terminal Si-OH--- (HO-Ti) "defective sites" or contributions from some or all of these factors.

3.6 CATALYTIC ACTIVITY

3.6.1 Hydroxylation of phenol and anisole

The catalytic activities of various TS-1 catalysts prepared using ES-40 and TEOS in the oxidation of phenol and anisole using dilute H_2O_2 as oxidant were investigated The results are summarized in the Table-3.3.

The activity of the samples prepared by method I and II are compared with that of TS-1 and TS-2 prepared using TEOS, and Zirconium silicalite-1. It is interesting to note that in both of these aromatic oxidations, the selectivity for p- isomer was higher with the samples prepared using ES-40 than that of TEOS. Although the conversion with respect to H_2O_2 is almost the same for all samples (95-100 %) in phenol hydroxylation, the product distribution varies significantly. The sample prepared following the method II in which extra-lattice TiO_2 was detected gave rise to some p-benzoquinone. It is also observed that H_2O_2 conversion for anisole oxidation was less compared to phenol hydroxylation.

3.7 CONCLUSIONS

It is found for the first time that the TS-1 could be prepared using ES-40, which is a new silicon source for zeolite preparation.

The isomorphous substitution of Ti in to the lattice of silicalite is more efficient when silicon alkoxide and Ti alkoxide are mixed together and then hydrolyzed instead of hydrolyzing individual alkoxides before mixing.

The use of ES-40 is more advantageous compared to TEOS as the silicon source as i) the rate of crystallization is faster with ES-40 ii) the isomorphous substitution of Ti is comparable and iii) the crystallites formed are smaller.

The TS-1 prepared using ES-40 shows very high aromatic oxidation activity using dilute H_2O_2. Therefore it can also be a better source of silica for the preparation of other zeolites.

ES-40 being cheaper than TEOS, the overall cost of TS-1 is reduced to an acceptable level for commercial exploitation.

3.8 REFERENCES

1. M. Taramasso G. Perigo, B, Notari, U.S Patent 4, 410, 501 (1983)
2. Romano Ugo, Esposito Antonio, Maspero Federico, Neri Carlo, Clerici M. G. *Chim. Ind.* (Milan) 72(7), (1990) 610.
3. J. S. Reddy and R. Kumar *Zeolites* 12 (1992) 95.
4. L. Yu, H. Jiang and W. Pang, *Huaxue Xuebao*, 51 (1993) 780.
5. Dartt, C. B., Khouw C. B., Li H. X. and Davis M. E. *Micro. Mater.* 2(5) (1994) 425.
6. M. A. Camblor, A. Corma, A. Martinez and J. Parez-Pariente. *J. Chem. Soc. Chem. Commun.* 589, (1992).
7. P. T. Tanev, M. Chibwe and T. J. Pinnavaia, *Nature* 368 (1994) 321.
8. Blasco T. Corma A. Navarro, M. T. and Perez Pariente. *J. Catal.* 156(1) (1995) 65.
9. Corma A. Kan Quibin, and Rey Fernando. *J. Chem. Soc. Chem. Commun* 5, (1998) 579.
10. Kumar R, Bhaumik A. Mukherjee P. *Proc. Int. Zeolite Conf., 12th,* Eds: Treacy M. M. J. Materials Research Society: Warrendale, Pa. Vol 2, 1227-1232, (1999).
11. Bhaumik Asim, Tatsumi Takashi *Prepr. – Am. Chem. Soc., Div. Pet. Chem.,* 43(2), (1998) 231.
12. a)Chen L. Y, Chuah G. K, Jaenicke S. *J. Mol. Catal. A: Chem.*, 132(2-3), (1998), 281.,b)Huang Lin. Lee Chul Wee, Park Yong Ki, Park Sang-Eon *Bull. Korean Chem. Soc.*, 20(6) (1999) 747.
13. Ponceau Marianne, Mueller-Markgraf Wolfgang. Ger. Offen. DE 19725820 A1 24 Dec 1998.
14. Fu Zaihui, Yin Dulin. *Shiyou Huagong,* 27(7), 486, 1998
15. Strebelle, Michel; Gilbeau, Patrick; Catinat, Jean-Pierre (Solvay (S. A.), Belg.). Eur. Pat. Appl. EP 919551 A1 2 Jun 1999, 8 pp.
16. Teissier Remy, Jorda Eric Eur. Pat. Appl. EP 835688 A1 15 Apr 1998, 9 pp.
17. Kondo Osamu, Onozawa Takashi, Shimizu Yukari, Okamoto Takannobu *Jpn.*

Kokai Tokkyo Koho JP 09301966.

18. a)Notari, *B. Stucture-Activity and Selectivity Relatioship in Heterogeneous Catalysis.* (Eds. Grasselli, R. K. & Sleight, A. W) (Elsevier, Amsterdam, 1991) 243-256., b)Notari, *B.* Stud. Surf. Sci. Cata., 37 (1988) 413.

19. Huybrechts, D. R. C., De Bruycker, L., and Jacobs P. A. *Nature* 345, (1990) 240.

20. Taramasso, M., Perego, G and Notari, B. US Patent no. 4410501(1983)

21. a)Thangaraj A., M. J Eapen, S. Sivasankar and P.Ratnasamy. *Zeolites* 12 (1992) 943., b)A. Thangaraj, R Kumar, S. P. Mirajkar and P. Ratnasamy J. Catal, 130 (1991) 1.

22. De Lucas A, Rodriguez L, Sanchez P. *Appl. Catal., A,* 180(1-2) (1999) 375.

23. Tuel, A. *Catal. Lett.,* 51(1,2) (1998) 59.

24. A. Tuel and Y. Ben Taarit. *Appl. Catal.-A*, 110 (1994) 137.

25. Wang Xiang-sheng, Guo Xin-wen. *Catal. Today,* 51(1) 1999, 177.

26. a) W. Graf, V. Frey, P.John, and N. Zeller. *Wacker Chimie*, US 4209454 (1978).

    b) *Encyclopedia of Chem. Technology,* Kirk-Othmer-Vol.22, page 72, fourth edition, John Wiley & Sons, Editor-Mary-Howe-Grant, (1997).

27. M. K. Dongare, D. P. Sabde, R. A. Shaikh, K. R. Kamble, S. G. Hegde. *Catalysis Today* Vol 49, (1999) 267-276.

28. a) Ian M. Thomas in: *Sol-Gel Technology for thin films, fibers, preforms, electronics and specialty shapes* (Edited by Lisa C. Klein) Noyes Publications Park ridge, New Jersey U.S.A., b) Miller J. B, Tabone E. R, Ko E. I., *Langmuir* 12, (1996) 2878, c) Miller J. B, Mathers L. J, Ko E. I., *J. Mater. Chem*. 5, (1995) 1759, d) Coulton K. G, Hubert-Pfalzgraf L. G, *Chem. Rev*. 90 (1990) 969.

29. H. Schmidt in *Structure and Bonding*-77, R, Reisfield (Ed), p-119, Springer Verlag (1992)

30. A. Tuel. *Catalysis Letters* 51 (1998) 59-63

31. Gosse Boxhoorn, Olof Sudmeijer and (The late) Piet H.G.van Kasteren *J. Chem.Soc, Chem.Commun* (1983) 1416.

32 D. P. Serrano, M. A. Uguina, G. Ovejero, R, Van Grieken and M. Camacho

Microporous Materials 7 (1996) 309.

33 Derouane E, G., Detremmerie S., Gabelica Z., and Blom. *Appl. Catal*. 1, 201 (1981)

34 Kraushaar B. Ph.D. Thesis "*Charaterization and Modification of Zeolites and related Materials*" The Technical University of Eindhoven, Eindhoven, The Netherlands.

35 J.L. Casci and B.M. lowe, Zeolites, 3 (1983)186

36 Chen N. J, Tasi T. C, Chen N. S and Wang I. *J. Chem. Soc. Faraday Trans. I* 77 (1981) 547.

37 Gamami M. and Sand L. B. *Zeolites* 3 (1983) 156.

38. A. J. H. P. Van der Pol and J. H. C. Van Hooff, *Appl. Catal. A*, 92 (1992) 93.

39. R.W. Grose and Flanigen, E.M., *U.S. Pat*. 4061,724 (1977).

40 D.G. Hay and H. Jaeger, *J. Chem. Soc. Chem. Commun.,* (1984) 1433.

41. G. Perego, G. Bellusi, C. Corno, M. Taramaosso, F. Buonomo and A. Esposito, in "Developments in Zeolite Science and Technology" (Y. Murakami *et.al.*, Eds), Elseveir, Amsterdam (1986) 129.

42 S. Lowell and J.E. Shields in "Powder Surface Area and Porosity", (B. Scarlett, Eds.), Chapman and Hall, (1984) 80.

43 P.R.H.P. Rao, A.A. Belhekar, S.G. Hegde, A.V. Ramaswamy and P. Ratnasamy, *J. Catal*., 141 (1993) 595.

44 N.K. Mal, V.Ramaswamy, S. Ganapathy and A.V. Ramaswamy, *J. Chem. Commun.*(1994) 1933.

45 M. K. Dongare, P. Singh, P. P. Moghe, and P. Ratnasamy. Zeolites 11 (1996) 690.

46. F. Geobaldo, S. Bordiga, A.Zecchina, E. Gianello, G. Leofanti and G. Petrini, *Catal .Lett.*, 16 (1992) 109.

47. G. Bellussi, A. Carati, M. G. Clerici, G. Maddinelli, and R. Millini. *J. Catal* 133 (1992) 220.

48. Kraushaar B and van Hooff J. H. C., *Catal. Lett*. 1 (1989) 81.

49. Engelhardt G and Michel D., *High Resolution Solid State NMR of Silicates and Zeolites,* Wiley, New York, (1987).

50. E. Duprey, P. Beaunier, M. A. Springuel-Huet, F. Bozon-Verduraz, J. Fraissard, J. M. Manoli, and J. M. Bregeault *J. Catal* 165 (1997) 22.

51. M. Decottignies, J. Phalippon and J. Zarzycki. *J. Mater. Sci.* 13(12) (1978) 2605

52. M. A. Camblor, A. Corma and Perez-Periente. *J. Chem. Soc. Commun.* (1993), 557.

53. M. R. Boccuti, K. M. Rao, A. Zecchina, G. Leofanti, and G. Petrini. *Stud. Surf. Sci. Catal.* 48, 133 (1989)

Table 3.1

Physicochemical properties of TS-1 samples.

Sample Name[a]	Ti /(Si+Ti) molar ratio		BET surface Area (m^2/g.)	MicroporeVolume (mL/g)	Sorption Properties (Wt %)		
	Gel	Product			Water	n-hexane	Cyclo-hexane
Silicalite-1	-	-	384	0.116	5.2	12.4	4.8
TS-1(125, M1)	0.0079	0.0089	456	0.132	7.5	13.6	7.4
TS-1(77, M1)	0.0128	0.0147	434	0.120	7.9	13.9	7.7
TS-1(60, M2)	0.0163	0.0192	465	0.136	7.8	13.2	7.5
TS-1(50, TEOS)[b]	0.0196	0.0228	425	0.128	7.8	13.4	7.6
TS-1(50, M1)	0.0196	0.0232	489	0.126	7.6	13.7	8.2
TS-1(50, M2)	0.0196	0.0205	410	0.120	7.4	11.9	7.8
TS-1(44, M1)	0.0222	0.0243	449	0.124	7.2	13.4	7.8
TS-1(35, M1)	0.0277	0.0294	428	0.121	7.3	12.9	7.6

a: The number in the parenthesis indicate Si/Ti ratio and M1, M2 correspond to method-I and method II respectively
b: TS-1 prepared using TEOS as silicon source

Table 3.2

Unit Cell Parameters of TS-1 samples prepared using Method-I and II.

Sample name	Unit Cell Parameters (Å)			Unit cell volume ($Å^3$)
	a	b	c	
Sil-1	20.087	19.885	13.379	5344
TS-1(125, M1)	20.091	19.887	13.383	5347
TS-1(77, M1)	20.085	19.895	13.389	5350
TS-1(60, M2)	20.092	19.898	13.390	5353
TS-1(50, M1)	20.095	19.904	13.399	5359
TS-1(50, M2)	20.089	19.894	13.392	5352
TS-1(44, M1)	20.105	19.903	13.405	5364
TS-1(35, M1)	20.103	19.911	13.411	5368

Table 3.3

Hydroxylation of aromatics with aq. H_2O_2.

Reaction Conditions: Temp: 80°C, Phenol (Anisole) to Hydrogen peroxide: 5,
Reaction time: 5 h, Solvent: Water, Water to Phenol (Anisole): 10

Sr. No.	Sample[a]	Crystal size (μm)	Conv. H_2O_2 (%)[b]	Phenol Hydroxylation			Anisole Oxidation		
				S_{DHB}[c] (%)		p/o[e]	S_{HA}[d](%)		p/o[e]
				Phenol	H_2O_2		Anisole	H_2O_2	
1.	TS-1(50, TEOS)	0.4	99 (82)	93	89	1.41	61	76	2.8
2.	TS-1 (50, M1)	0.1 - 0.2	95 (78)	92	87	1.57	58	72	3.1
3.	TS-1 (50, M2)	0.2	100(30)	87	72	0.85	27	25	1.4
4.	ZrS-1	0.2	38(32)	34	28	1.1	24	18	1.8
5.	TS-2 (50)	0.4	82(76)	74	68	1.2	42	36	2.0

a: ZrS-1 and TS-2 are zirconium silicalite-1 and Titanium silicalite-2 samples
b: H_2O_2 Conversion; number in the parenthesis indicate H_2O_2 conversion for anisole oxidation
c: Selectivity in dihydroxybenzenes (DHB) based on H_2O_2(Phenol)
[(moles of dihydroxybenzenes formed)/(moles of H_2O_2(phenol) consumed x 100
d: Selectivity in hydroxy anisols (HA) based on H_2O_2(Anisole)
[(moles of hydroxy anisols formed)/(moles of H_2O_2(Anisole) consumed x 100
e: para/ortho ratio

4.1 INTRODUCTION

The success of titanium silicate molecular sieves[1-3] in many industrial catalytic oxidation processes stimulated search for such catalysts containing cations other than Ti^{4+} in a silica lattice. As the titanium incorporated molecular sieves widened the scope of zeolites in the area of oxidation catalysis using hydrogen peroxide, other metals like vanadium, chromium and tin containing molecular sieves were also being explored for similar applications[3-11]. Among them, zirconium incorporated zeolites have also shown promising results as oxidation catalysts. Zirconium was introduced the tetrahedral sites in the framework of microporous and mesoporous silicates[11-14] and alumino-phosphate[15] materials, and has shown interesting catalytic properties. Studies have shown that zirconium could be substituted in the ZSM-5[11a] and ZSM-11 structure. But the incorporation was reportedly low[12], which could be attributed to its large size or the nature of precursors used for the synthesis. When inorganic zirconium salts are added to the hydrolyzed solution of tetraethyl orthosilicate in alkaline medium, they precipitate out as metal hydroxide and thus limit the incorporation of zirconium into silicalite lattice.

An improved method for the preparation of ZrS-2 using various zirconium sources are described in this chapter. The influence of starting material and the method of preparation on the quality of the material is also highlighted. The material obtained using different templates and zirconium sources are characterized by XRD, SEM, chemical analysis, adsorption properties, ^{29}Si MAS-NMR and FTIR spectroscopy of adsorbed pyridine. The catalytic oxidation reaction using hydrogen peroxide was also studied.

4.2 SYNTHESIS OF ZIRCONIUM SILICATE MOLECULAR SIEVE (ZrS-2)

In a typical synthesis of ZrS-2, 31.1 g of tetrabutyl ammonium hydroxide (1 M TBAOH in MeOH) was added to a mixture of 21 g of tetraethyl orthosilicate (TEOS)

and 0.78 g of zirconium propoxide (ZrP) in 15 g dry isopropyl alcohol (IPA) to get a clear solution. The solution was warmed to remove excess of alcohol at about 60^0C for 1-2 h. 50 g of water was then added to the above solution and stirred for another one hour. The final clear solution was then crystallized hydrothermally in an autoclave at 170^0C for 60-72 h. The product was centrifuged / filtered, washed, dried and calcined in air at 550^0C for 10 h. Few samples with different Si/Zr ratios were prepared. In an another synthesis procedure, aqueous solution of zirconyl nitrate was added instead of zirconium alkoxide to the mixture of alcoholic solution of TBAOH and TEOS. After the addition of requisite amount of water, the same procedure as above was followed. Few ZrS-2 samples were also prepared using aqueous solution of TBAOH and various inorganic salts of zirconium. All the calcined samples were ion exchanged with 1M ammonium nitrate solution and subsequently calcined at 400^0C in air for 8-10 h. For comparison, a Ti-MEL (TS-2) sample was also prepared using the reported procedure[16].

4.3 PHYSICO-CHEMICAL CHARACTERIZATION

4.3.1 Hydrothermal Synthesis

During the synthesis of crystalline ZrS-2, if the mixture of TEOS and Zirconium alkoxide was hydrolyzed by adding alcoholic TBAOH, a clear solution was observed (sample A-D of Table 4.1). On the contrary, if aq. TBAOH was used for hydrolysis, the solution became turbid due to the precipitation of zirconium hydroxide. The solution was also turbid in either case when the mixture of TEOS and aq. solution of any other zirconium salts like nitrate or chloride were used (sample E-H). Rakshe et.al[12] have also reported similar observation when zirconium tetrachloride was used as the zirconium source.

Table-4.1

Physicochemical properties of ZrS-2 samples.

Sample Name	Source of Zr[a]	TBAOH	Nature of Precursor solution	Crystallite Size (μm)	State of Zr by UV-Vis[b]
Samples A-D	ZrP	Alcoholic	Clear	0.2 to 0.4	Td
Sample – E	ZrN	Alcoholic	Less clear	0.2 to 1	Td + Ex-ZrO_2
Sample – F	ZP	Aqueous	Turbid	0.1 to 0.2	Td + Ex-ZrO_2
Sample – G	ZrN	Aqueous	Turbid	0.2	Td + Ex-ZrO_2
Sample –H	ZrTC	Aqueous	Turbid	0.1	Td + Ex-ZrO_2

a: ZrP: Zirconium propoxide
ZrN: Zirconyl Nitrate
ZrTC: Zirconium Tetrachloride
b: Td: Tetrahedral zirconium, Ex-ZrO_2 : Extra lattice zirconia

4.3.2 X-ray diffraction

In Figure 4.1 the XRD patterns of crystalline ZrS-2 samples prepared using zirconium propoxide and zirconyl nitrate (sample D and E respectively of Table-4.1) are compared. The XRD patterns of ZrS-2 obtained by all the methods matched well with that of silicalite-2. The samples were found to be highly crystalline without any crystalline impurities.

The unit cell parameters of samples synthesized using different types of TBAOH and zirconium sources with varying amount of Zr contents are presented in Table-4.2. Most of the interplanar spacing for ZrS-2 samples synthesized using zirconium alkoxide and alc. TBAOH are greater than the corresponding values of silicalite-2, which is expected as the Zr-O bond length is larger than that of Si-O. The unit cell volume increased with increase in Zr content, indicating the presence of Zr in the silicalite-2 framework. The maximum unit cell expansion was observed for sample with Si/Zr ratio 58[5415 $(Å)^3$]. The samples with higher Zr content (Si/Zr< 60) did not show proportional unit-cell expansion and indicated the presence of extra-lattice zirconia by UV-Vis spectroscopy. The samples prepared using inorganic salts of zirconium showed less lattice expansion, which may be due to the hydrolysis of zirconium salts to metal hydroxide limiting the incorporation of zirconium in tetrahedral sites. The maximum amount of Zr incorporated into the silicalite framework was 1.65 Zr atoms per unit cell. The low amount of Zr incorporation in MFI was also observed by Fricke et.al[17] under similar conditions. The difficulty in the incorporation of Zr compared to titanium can be attributed to the larger size of Zr^{4+} ion than Ti^{4+} ion (0.59 Å and 0.42 Å respectively).

4.3.3 UV-Vis spectroscopy

For Zr(IV) oxo species, strong absorption due to charge transfer (CT) transitions between O^{2-} and the central Zr(IV) atoms are expected in the UV-Vis region. The

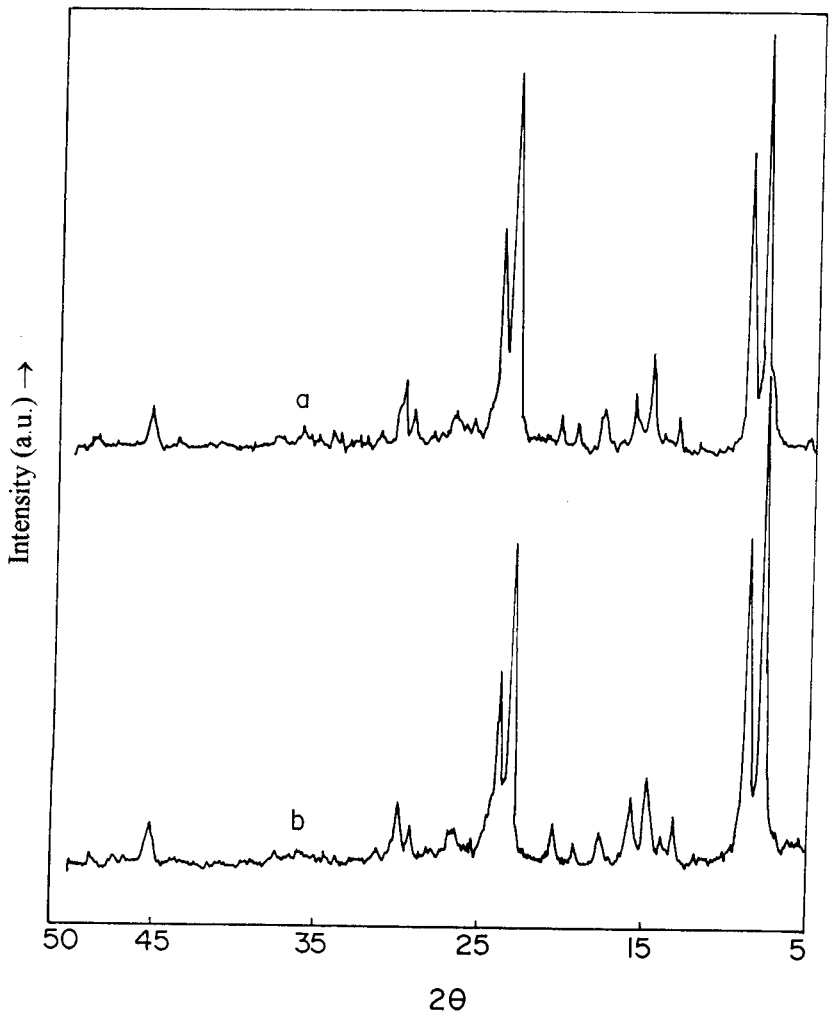

Fig.4.1 XRD patterns of crystalline ZrS-2 samples prepared using a) zirconium propoxide and b) zirconyl nitrate (samples D and E of Table-4.2 respectively.)

Table-4.2

Chemical analysis, adsorption properties and unit cell volume of different ZrS-2 samples

Sample Name	Si/Zr ratio		BET surface Area (m^2/g)	Sorption Properties (Wt %)			Unit cell volume ($Å^3$)
	Gel	Product		Water	n-hexane	Cyclohexane	
Silicalite-2	-	-	342	7.3	12.8	7.1	5341
Sample –A	250	232	482	7.5	13.6	7.4	5354
Sample –B	120	105	503	7.9	13.9	7.7	5373
Sample –C	90	82	467	7.6	13.7	8.2	5389
Sample –D	60	58	459	7.5	13.4	7.8	5415
Sample –E	90	105	418	7.1	13.2	7.4	5365
Sample –G	90	95	410	7.5	13.3	7.2	5369

UV-Visible spectra of the various samples are shown in Fig. 4.2. It is observed that the use of inorganic salts of zirconium as zirconium source or aqueous TBAOH resulted in the

samples with extra lattice species. A single strong transition band around 210 nm in the samples prepared using alc. TBAOH and zirconium alkoxide (Fig. 4.2, curve a and b) suggested that zirconium is in four-fold coordination in silicalite lattice. In titanium silicates also, such band is attributed to Ti in tetrahedral environment[18]. Whereas in the samples E and D (curves c and d) the bands are observed at around 208 and 253 nm, which are attributed to the presence of tetrahedral and extra-lattice zirconium species respectively. When the zirconium source (alkoxide, salts like nitrate or chloride) and TEOS are mixed and then hydrolyzed simultaneously by adding aq. TBAOH, the zirconium source hydrolyzed faster than the source of Si (TEOS), which inhibited the formation of Si-O-Zr linkages and favored the irreversible formation of zirconium hydroxide. This faster hydrolysis is mainly due to too much excess amount of water than stoichiometry needed to favor the formation of Si-O-Zr linkages. On the contrary, when zirconium propoxide and TEOS were hydrolyzed simultaneously with alc. TBAOH, the hydrolysis was controlled and Si-O-Zr linkages were formed in the resulting solution. Therefore the precipitation of metal hydroxide was avoided and the precursor solution remained clear and homogeneous. The formation of Si-O-Zr linkages in the solution facilitates the incorporation of zirconium in the framework during the hydrothermal crystallization and hence no extra-lattice zirconium was observed in the UV-Vis spectra. These observations on the effect of template and zirconium source on the precursor gel/solution and subsequently on purity of ZrS-2 material are presented in Table-4.1.

4.3.4 Scanning Electron Micrograph

The scanning electron micrograph of the sample prepared using zirconium alkoxide and alcoholic TBAOH shows rectangular and cubic shaped crystals ranging from

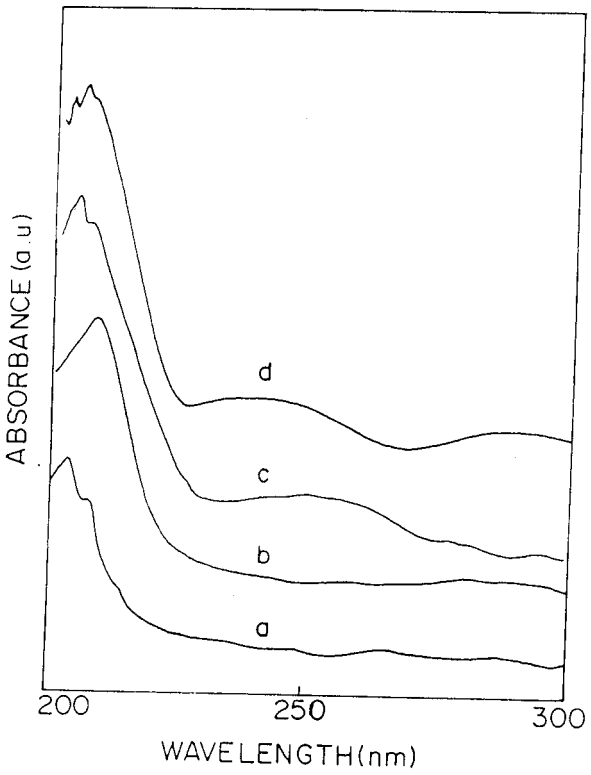

Fig.4.2 UV-Vis diffuse reflectance spectra of ZrS-2 samples, Curves a-d (samples C, D, E and G of Table- 4.2 respectively)

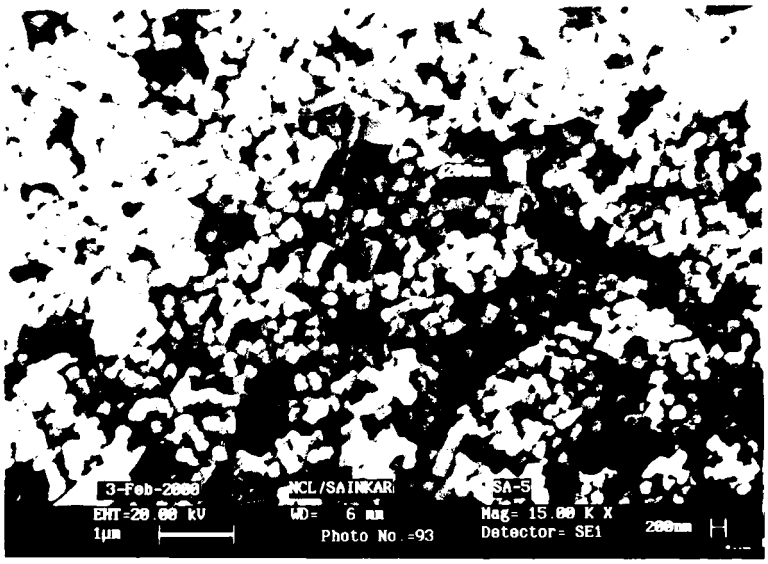

(a)

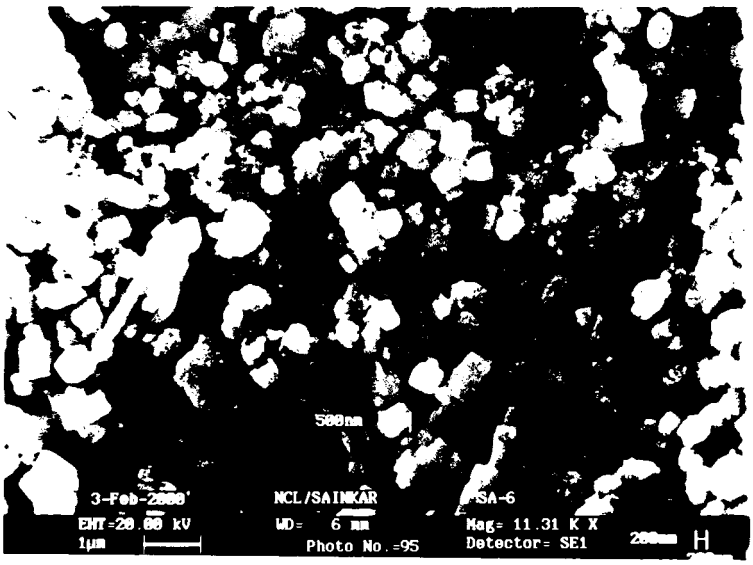

(b)

Fig.4.3 SEM of samples prepared using a) zirconium propoxide (samples D) and b) zirconyl nitrate (samples E of Table-4.2)

0.2 to 0.4 μm (Fig 4.3a), while the crystallite size of sample prepared using zirconyl nitrate varied from 0.2 to 1 μm (Fig. 4.3b).

4.3.5 FTIR spectroscopy

The IR spectra in the framework vibration region of ZrS-2 samples are shown in Fig. 4.4. The spectra exhibit a shoulder (sh) at 970 cm^{-1}, which is attributed to Si-O-Zr asymmetric stretching vibrations arising from the substitution of Zr in Si-O-Si linkages. However such band of weak intensity is also observed in pure silicalite sample, which is assigned to Si-O stretching vibrations of Si-O-H linkages[19] and such bands prominently occur only in the zeolite samples with lot of defect sites like zeolite beta[20]. In the case of titanium silicalite, the band at 960 cm^{-1} is attributed to the stretching mode of $(SiO_4)^{4-}$ bonded to $(TiO_4)^{4-}$ and considered as evidence for the presence of Ti in the framework position of zeolite[18-21]. Various possible assignments are given for this band in titanium silicates in the literature. Similar assignments may be true for Zr incorporation in silicalite-2 framework also. However a band at 945 cms^{-1} was observed in the difference IR spectra of ZrO_2 supported on silica samples, which was attributed to Si-O-Zr vibrations[22].

4.3.6 The FTIR spectra of chemisorbed pyridine

The FTIR spectra of chemisorbed pyridine at 50, 100, 150^0C on ZrS-2 (sample-D) are shown in Fig. 4.5(curves a-c). Similar spectra of TS-2 and silicalite-2 with chemisorbed pyridine at 100^0C are also shown (curve d and e) in the same figure for comparison. The bands observed at 1633, 1543 and 1492 cm^{-1} are assigned to pyridine molecules bound to Brönsted acid sites, and those at 1618, 1492 and 1447 cm^{-1} are assigned to pyridine molecules bound to Lewis acid sites. Similar type of IR bands of pyridine adsorbed on Al-MEL and Boron substituted MEL type of zeolite are reported by vedrine et. al[23] and Simon et. al[24] respectively. The spectra reveals that the intensity of the

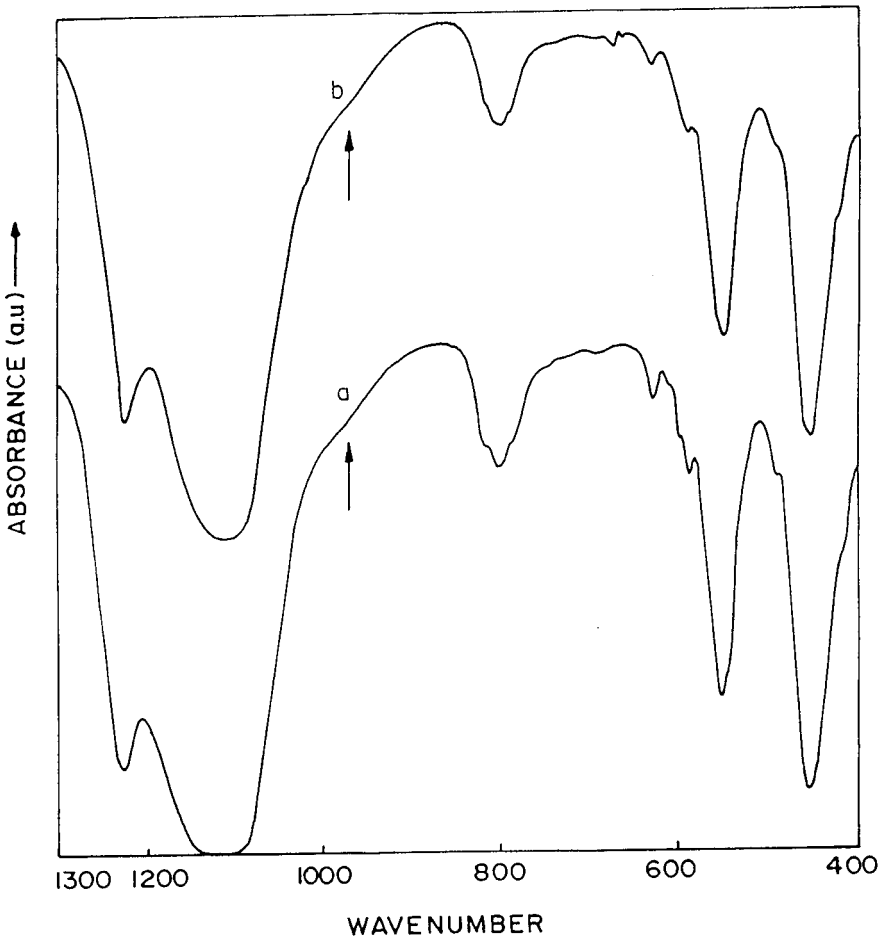

Fig.4.4 FTIR spectra of ZrS-2 samples prepared using a) zirconium propoxide and b) zirconyl nitrate (samples D and E of Table-4.2 respectively.)

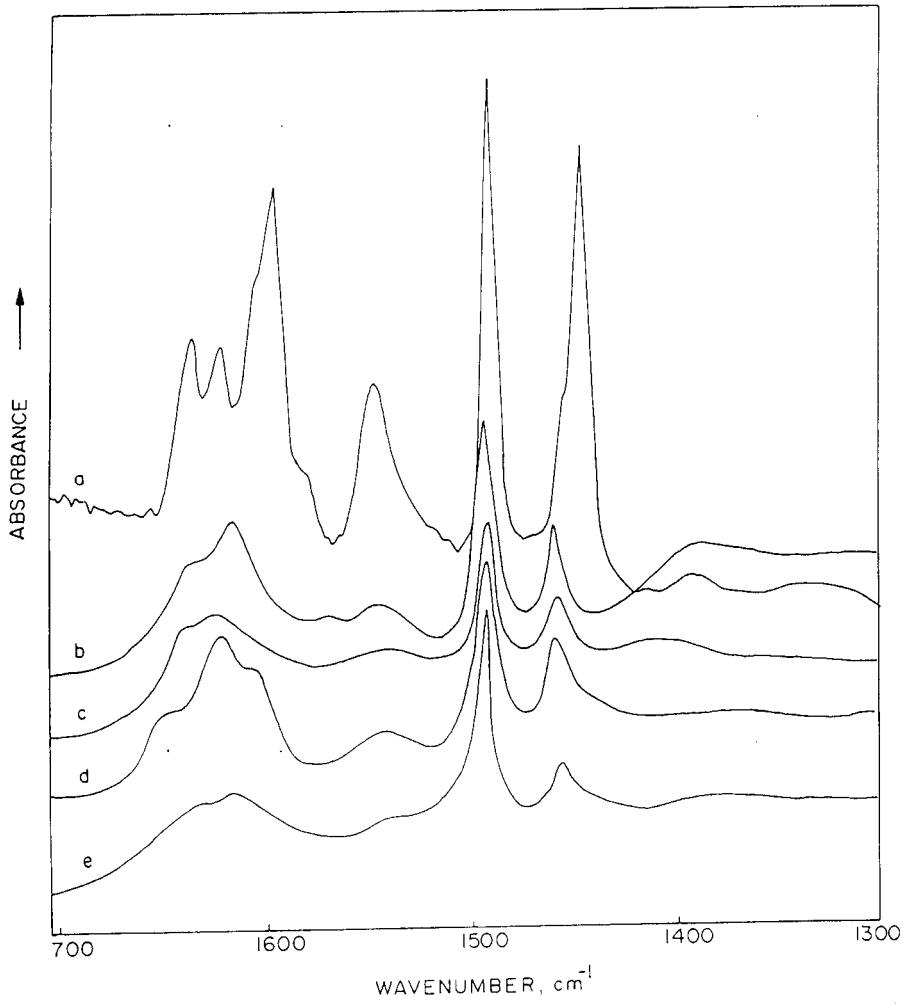

Fig.4.5 FTIR spectra of adsorbed pyridine on ZrS-2 (sample-D, Table-4.1 at a) 50, b) 100, c) 150^{0}C and d) on TS-2 at 100^{0}C and e) on Silicalite-2 at 100^{0}C.

1540 cm^{-1} band of pyridine chemisorbed at 100^0C on ZrS-2 (curve-b) is less than the corresponding band on TS-2 (curve-d), where as it is more than that on silicalite-2 (curve-e). It indicates that the Brönsted acidity of ZrS-2 is more than that of silicalite-2, but it is less than that of TS-2.

4.3.7 Adsorption studies

The adsorption capacities of ZrS-2 for water, n-hexane and cyclohexane are comparable to those of silicalite-2(Table-4.2.). The values indicate the absence of any occluded material within the channels. The BET surface area of ZrS-2 samples is found to be in the range of 410 to 503 m^2/g.

4.3.8 ^{29}Si MAS-NMR spectroscopy

The solid state ^{29}Si MAS-NMR spectroscopic results of calcined ZrS-2(sample-D) is shown in the Figure 4.6. The peaks around -108 and -114 ppm are attributed to Si in distorted tetrahedra containing Si[3(OSi),1(OZr)] and $Si(O\text{-}Si)_4$ units, indicating the presence of Zr^{4+} ions linked to siloxane group in tetrahedral co-ordination[25].

4.3.9 Catalytic activity in Phenol hydroxylation

The oxidative catalytic activity of ZrS-2 samples in the hydroxylation of phenol is shown in Table-4.3. The results of TS-2 are also included for comparison. More selective formation of hydroquinone (53 %) over ZrS-2 sample indicates that the most of the reaction takes place inside the pores. Similar results have been observed over TS-2. Although the selectivity (H_2O_2) exhibited by ZrS-2 is 26.4%, which is lower than that of TS-2 (70%), the product distribution is essentially the same. Hydroquinone to catachol ratio was 1.19 and 1.5 over ZrS-2 and TS-2 respectively. Under similar conditions, ZrO_2 impregnated silicalite-2 was found to be inactive. Probably the isolated tetrahedral zirconium ions attached to the framework of silicalite-2 are the active centers for this reaction. The catalytic activity exhibited by ZrS-2 in the hydroxylation of phenol can also

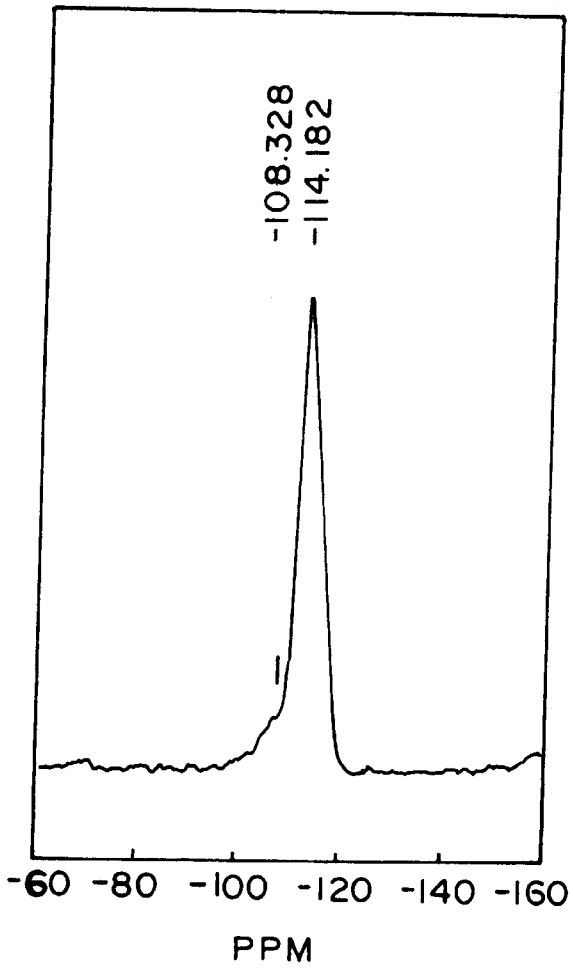

Fig 4.6 ^{29}Si MAS-NMR spectrum of ZrS-2 sample (sample D in Table-4.1).

Table-4.3

Hydroxylation of Phenol with H_2O_2

Reaction Conditions: Temp: 80 ^{0}C, Phenol to Hydrogen peroxide: 5,
Reaction time: 8hrs, Wt. of the catalyst: 0.5 g., Solvent: Water.

Catalyst	TOF[a]	H_2O_2 Selectivity	Product Distribution %		
			p-BQ[b]	Catachol	Hydroquinone
ZrS-2 (sample-D)	3.02	26.4	2.5	44.5	53
ZrS-2 (sample-E)	2.66	23.5	3.2	47.8	49
ZrO_2/Sil-2	-	3.2	55.2	43.6	1.2
TS-2	7.6	70	1.5	39	59.5

a: TOF: turn over frequency
b: p-BQ: Para-benzoquinone

be taken as evidence for the presence of Zr in the silicalite framework, either as regular tetrahedra or attached to silanol groups at defect sites.

4.4 SYNTHESIS OF Al AND Zr CONTAINING SILICALITE-1 (AlZrS-1)

The simultaneous incorporation of oxidative and acidic functions in the zeolite catalysts are emerging as the novel technique in the chemistry of zeolite catalysis. Partial incorporation of tetravalent cations like Ti^{4+} and Zr^{4+} into the zeolite lattice gives rise to such materials[26-29]. These modified bi-functional silicates are potentially active in both oxidation and acid catalyzed reactions, which has enlarged their scope as catalysts in many processes. Zirconium co-incorporation in ZSM-5 structure has been patented[30]. Moreover it has shown the advantage in prolonging the lifetime of the catalyst. However the details of the preparation, characterization, state of zirconium in the catalyst and the influence of different parameters on the purity of the sample are not described. It was therefore intended to study the synthesis and characterization of Zr containing ZSM-5 zeolite (Al and Zr ions in the framework) and study the catalytic activity for o-toluidine isomerization.

In a typical hydrothermal synthesis of Zr containing ZSM-5, 31.2 g of TEOS was added to a mixture of 0.6 g of NaOH and 41.1 g TPAOH solution in a beaker, to which a solution of 0.565 g. Zirconium propoxide in 20 g of IPA was added with constant stirring. To the above mixture, 0.3 g of sodium aluminate in 20g water was added. The above mixture was heated to remove alcohol and the requisite amount of water (42 g) was added and stirred for an hour. Finally the mixture was transferred in an autoclave for hydrothermal cystallization at 170^0C for 4-5 days. The gel composition of the reaction mixture was 0.1 NaOH: SiO_2: 0.008 ZrO_2: 0.016 Al_2O_3: 0.3 TPAOH: 35 H_2O.

After the hydrothermal crystallization, the product was centrifuged / filtered, washed, dried at 100^0C and calcined overnight in the presence of air at 550^0C. The

samples with different Si/Zr and Si/Al ratios were prepared by varying the amount of zirconium and aluminum source. All the calcined Zr-ZSM-5 samples were ion exchanged with 1M ammonium nitrate solution and subsequently calcined at 500^0C in air for 8-10 h. The samples are represented as H-AlZrS-1 (X,Y), where X and Y represent Si/Zr and Si/Al mole ratios respectively in the final sample. Zr-impregnated H-ZSM-5 was prepared by dissolving the required amount of Zr source in a minimum quantity of water. The solution was added to the required quantity of H-ZSM-5 and mixed well and then dried slowly first at 70^0C and then at 100^0C. The sample was calcined at 550^0C for 7 h in the presence of air. This sample is represented as ZrO_2/H-ZSM-5.

4.5 PHYSICO-CHEMICAL CHARACTERIZATION

4.5.1 X-ray diffraction

The XRD patterns of all the as-synthesized AlZrS-1 samples were found to match well with that of ZSM-5 framework (Fig 4.7). All the AlZrS-1 samples showed increase in the surface area compared to ZSM-5. On the contrary, the ZrO_2 impregnated ZSM-5 (112,48) and AlZrS-1 (92,78) samples shows a decrease in the surface area as can be noted in the Table-4.4.

4.5.2 UV-Vis spectroscopy

The UV-Vis spectra for the H-AlZrS-1 samples are shown in Fig. 4.8. The H-AlZrS-1(136, 62) sample showed a broad absorption band at 208 nm (curve a), where as H-AlZrS-1(92,78) samples showed absorption bands in the region of 205 and 258 nm (curves b). As discussed earlier, the absorption band at around 205 and 258 nm can be attributed to tetrahedral zirconium and extra-lattice zirconia species respectively.

4.5.3 FTIR Spectroscopy

The IR spectra in the framework vibration region of H-AlZrS-1 samples are shown in Fig.4.9. The spectra exhibited bands at 450 and 550 cm^{-1} characteristic of MFI

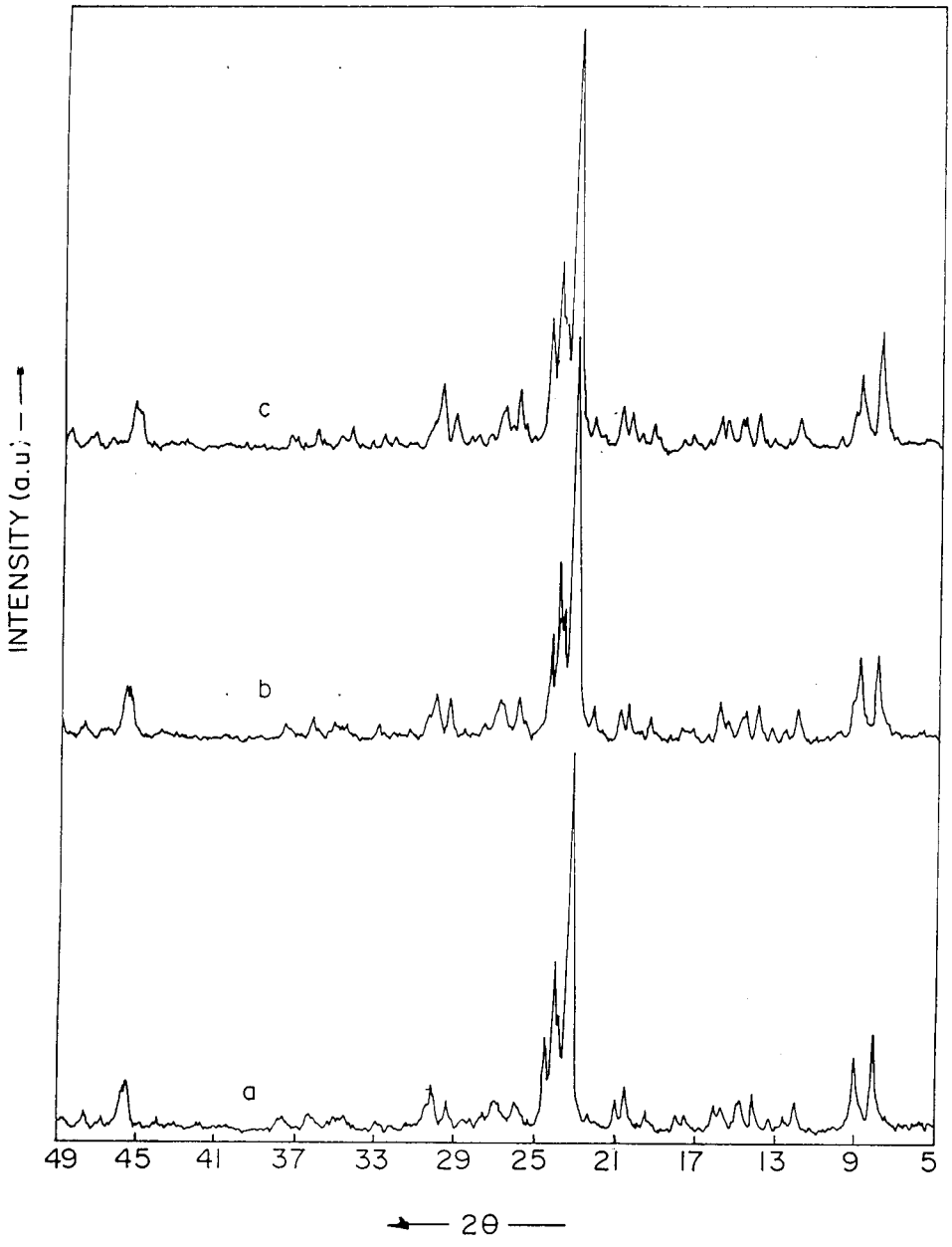

Fig.4.7 XRD patterns of as-synthesized AlZrS-1 samples a) AlZrS-1(136, 62) b) AlZrS-1(152, 124) and c) AlZrS-1(187, 42).

Table-4.4

Chemical analysis and adsorption properties of different AlZrS-1 samples

Sample*	Si/Zr	Si/Al	BET Surface Area m^2/g	Pore Volume ml/g.
H-ZSM-5	-	56	396	0.186
H-AlZrS-1(187,42)	187	42	442	0.165
H-AlZrS-1(152, 124)	152	124	454	0.182
H-AlZrS-1(136, 62)	136	62	423	0.178
H-AlZrS-1(92, 78)	92	78	416	0.153
ZrO_2/H-ZSM-5 (112, 48)	112	48	362	0.142

* Numbers in the parenthesis indicate Si/Zr and Si/Al ratio in the final solid.

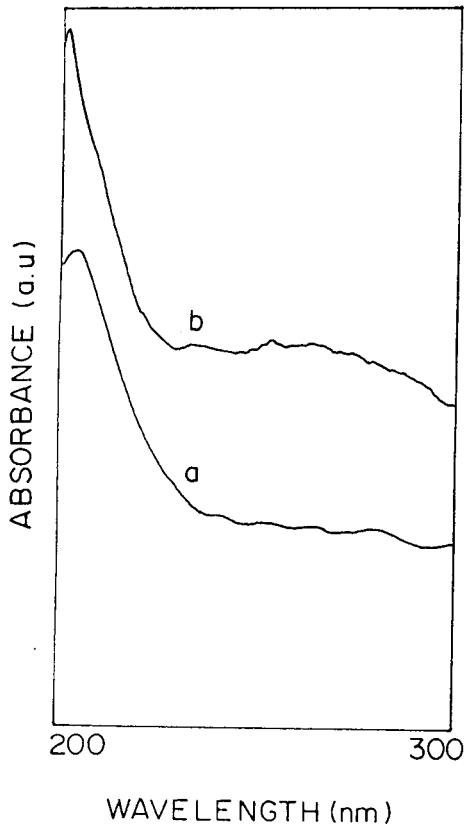

Fig 4.8 UV-Vis diffuse reflectance spectra of a) H-AlZrS-1 (136, 62) and b) H-AlZrS-1(92, 78).

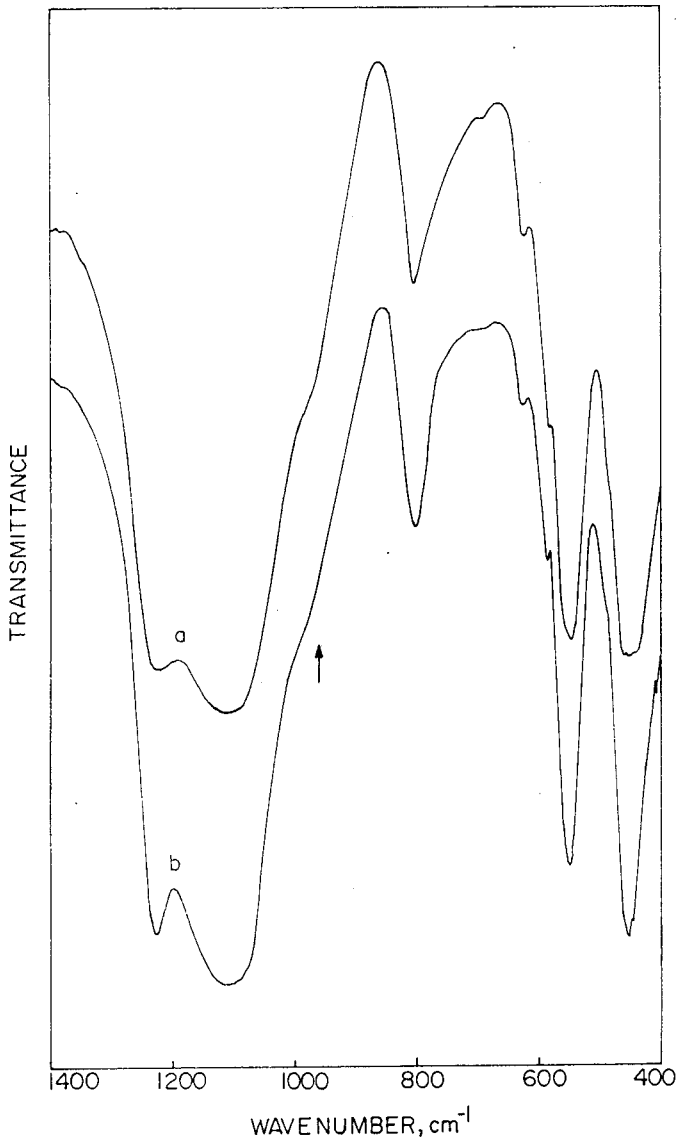

Fig 4.9 FTIR spectra of H-AlZrS-1 samples a) H-AlZrS-1(136, 62) and b) H-AlZrS-1(152, 124).

topology. In addition, a shoulder (sh) at 964 cm^{-1} is also observed in case of all Zr containing samples, which is attributed to Si-O-Zr asymmetric stretching vibrations arising from the substitution of Zr in the framework.

4.5.4 FTIR Spectroscopy of adsorbed pyridine

The FTIR spectra of chemisorbed pyridine at 50, 100 and 150^0C on H-AlZrS-1 (136, 62) sample are shown in Fig. 4.10(curves a-c). The bands observed at 1636 and 1543 cm^{-1} are assigned to pyridine molecules bound to Brönsted acid sites, and those at 1612, 1489 and 1448 cm^{-1} are assigned to pyridine molecules bound to Lewis acid sites. When the FTIR spectra of chemisorbed pyridine on pure H-ZSM-5 at 150^0C (curve d) is compared with the corresponding spectra of H-AlZrS-1(136, 62)[curve c], it is observed that the strength of acidity on the sample containing zirconium is less and also decreased with the incorporation of the zirconium in the lattice.

4.5.5 Catalytic activity in o-toluidine isomerization

The isomerization of toluidines is an industrially important reaction because only the meta-isomer is used in large quantities as an intermediate for agrochemicals and dyestuffs. Conventionally it is obtained by the nitration of toluene followed by reduction. Another method being practiced is the direct amination of meta-cresol, a relatively expensive method. In both the above cases the yield of m-toluidine is however less and the process is not cost effective.

Many zeolite catalysts have shown outstanding ability to isomerize the di-substituted aromatics to the more value added isomer. Among them, H-ZSM-5 is known to isomerize substituted toluenes, such as toluidines[31], cresols[32], halo-toluenes[33] and toluonitriles[34] with a minimum of side reactions. The activity of H-ZSM-5 for isomerization and disproportionation reactions depends on its acid strength distribution.

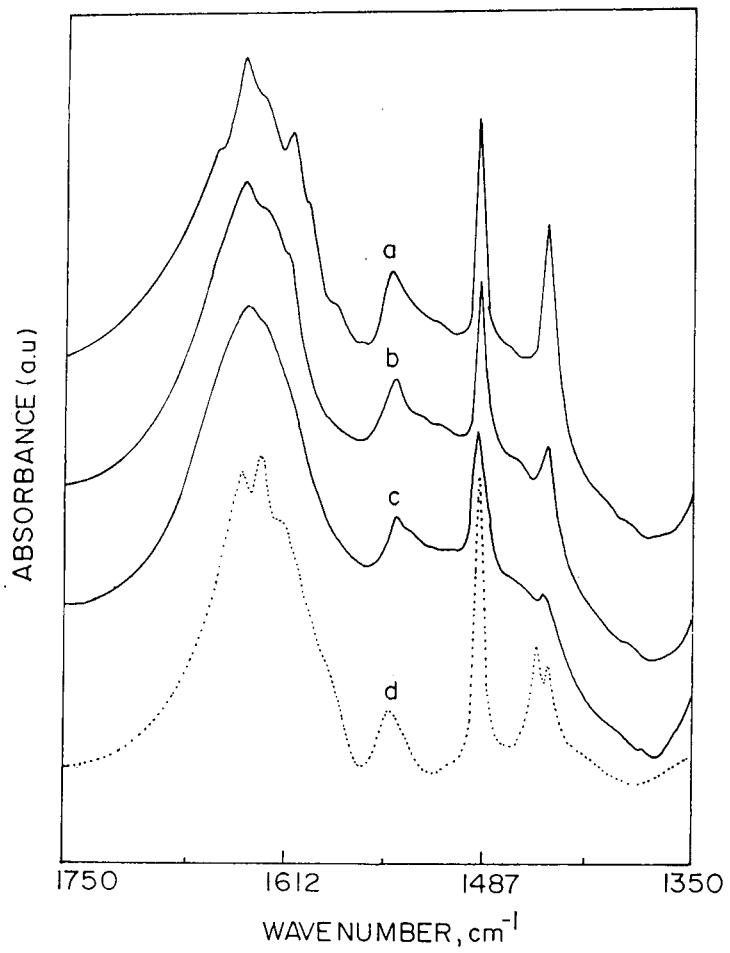

Fig 4.10 FTIR spectra of adsorbed pyridine on H-AlZrS-1(136, 62) at a) 50, b) 100 and c) 150^{0}C and d) H-ZSM-5 at 150^{0}C.

The simultaneous incorporation of the metal ions, such as Ga/B/Ti/Zr etc, in the lattice position is reported to lower the acidity of the catalyst.

It was therefore intended to study the isomerization of o-toluidine using zirconium substituted ZSM-5 zeolite (H-AlZrS-1) with varying zirconium content. The performance was compared with that of pure H-ZSM-5 zeolite. The isomerization reaction was studied in the temperature range of 320 to 470^0C. For comparison zirconium impregnated H-ZSM-5 sample was also studied.

4.5.6 Influence of temperature

The influence of temperature on the product distribution in the o-toluidine isomerization using H-ZSM-5 and H-AlZrS-1(136, 62) are illustrated in Table-4.5 and 4.6 respectively. The conversion of o-toluidine increased with increase in temperature from 320 to 470^0C. It was observed that above 420^0C, the product pattern obtained was in the thermodynamic equilibrium. As the reaction temperature was increased dealkylation and subsequent realkylation was observed, hence the concentration of undesired products such as aniline and di-methyl anilines increased with increase in temperature. At low temperature negligible amount of p-isomer was formed but with increase in temperature, the p-isomer was formed in the thermodynamic equilibrium. Therefore the selectivity towards m-isomer decreased with increase in temperature. The optimum temperature was found to be 370^0C, where in the conversion and selectivity to the desired m-isomer was maximum (79.6 %). At this temperature, the undesired products in the case of H- ZSM-5 were more compared to H-AlZrS-1.

The o-toluidine isomerization on zirconium containing samples with varying zirconium content was studied and their activity at 370^0C is summarized in Table-4.7. It was observed that all H-AlZrS-1 samples required higher temperatures as compared to the H-ZSM-5 sample of comparable ratio to give similar o-toluidine conversion. The

Table-4.5

O-toluidine isomerization on H-ZSM-5 at various temperatures.

Temperature $^0C \rightarrow$	320	370	420	470
o-toluidine conv.%	8.7	41.02	65.4	69.3
Products (Wt.%)				
Aniline	0.25	0.8	2.1	4.67
o-toluidine	91.3	58.98	34.6	30.7
p-toluidine	0.78	8.56	14.72	14.8
m-toluidine	7.29	31.07	46.58	45.86
Σ- Toluidnes	99.37	98.61	95.9	91.36
Dimethyl anilines	0.29	0.47	1.53	3.67
Others	0.09	0.12	0.47	0.21
m-toluidine selectivity	83.79	75.74	71.2	66.17

Feed: o-toluidine
Temperature: 320 - 470^{0}C,
WHSV: 1 h^{-1}
N_2 Flow rate: 20 ml/min,
Pressure: atmospheric.

Table-4.6

O-toluidine isomerization on H-AlZrS-1 (136, 62) at various temperatures.

Temperature $^0C \rightarrow$	320	370	420	470
o-toluidine conv.%	5.1	38.67	58.72	62.8
Products (Wt.%)				
Aniline	0.15	0.24	1.38	2.7
o-toluidine	94.9	61.33	41.28	37.2
p-toluidine	0.45	7.26	13.32	14.14
m-toluidine	4.3	30.8	43.25	44.49
Σ- Toluidnes	99.65	99.39	97.85	95.83
Dimethyl anilines	0.12	0.21	0.52	1.09
Others.	0.08	0.16	0.25	0.38
m-toluidine selectivity	84.31	79.64	73.65	70.84

Feed: o-toluidine
Temperature: 320 - 470^{0}C,
WHSV: 1 h^{-1}
N_2 Flow rate: 20 ml/min,
Pressure: atmospheric.

Table- 4.7

O-toluidine isomerization on various H-AlZrS-1 samples at 370^0C

Catalyst →	H-AlZrS-1 (136, 62)	H-AlZrS-1 (152, 124)	H-AlZrS-1 (187, 42)	H-AlZrS-1 (92, 78)	ZrO_2 imp (112,48)
O-toluidine conv.%	38.67	37.53	40.16	32.86	27.29
Products (Wt.%)					
Aniline	0.24	0.34	0.75	0.43	0.16
o-toluidine	61.33	62.47	59.84	67.14	72.71
p-toluidine	7.26	7.42	9.65	8.52	6.74
m-toluidine	30.8	29.45	28.78	23.42	20.16
Σ- Toluidnes	99.39	99.34	98.27	99.08	99.61
Dimethyl anilines	0.21	0.21	0.62	0.27	0.14
Others.	0.16	0.11	0.36	0.22	0.09
m-toluidine selectivity	79.64	76.35	72.49	67.18	73.84

Feed: o-toluidine
Temperature: 370^0C,
WHSV: 1 h^{-1}
N_2 Flow rate: 20 ml/min,
Pressure: atmospheric.

maximum conversion obtained using H-AlZrS-1 (187, 42) and H-ZSM-5 was 40.16 and 41.02 % respectively. But the selectivity to m-isomer was found to be marginally more on

H-AlZrS-1 samples, which can be attributed to the presence of zirconium in the lattice. It was also observed that in the case of H-AlZrS-1(92, 78) containing extra lattice zirconium species, the conversion was less (32.86) and it also deactivated faster. This may be due to the extra lattice ZrO_2 blocking the pores of the zeolite. In case of ZrO_2 impregnated H-ZSM-5 sample also the activity was found to be less (27.3%), which is attributed to the decrease in acidity of the sample and pore blockage as reflected by N_2 adsorption. As the Zr content in the lattice increases, the acid strength decreases thereby minimizing the undesired products. Thus dealkylation and disproportionation reactions are suppressed.

The isomerization of o-toluidine can be visualised on the basis of the intramolecular 1,2 methyl shift mechanism. At high temperatures the protonated benzenium ion (σ complex) is formed followed by a single or successive 1,2 methyl shifts (Fig 4.11) resulting in the formation of meta and para isomers of toluidine.

4.5.7 Effect of time on stream (TOS)

The effect of TOS on the o-toluidine conversion at atmospheric pressure for H-AlZrS-1(132, 62) and H-ZSM-5 are compared in the Figure 4.12. It was observed that the H-AlZrS-1(132, 62) sample showed better stability compared to H-ZSM-5. In the case of H-ZSM-5 the conversion continuously decreased from 41 to 24.9 % during 18 hours, whereas in case of H-AlZrS-1(132, 62) the conversion remained stable at 38.6 % initially for 9 h and then slowly decreased to 34.4 % after 18 hrs. The simultaneous incorporation of Al and Zr in the lattice substantially reduces the strength and density of acid sites. The improved stability and selectivity in case of zirconium substituted samples is attributed to the reduced acid strength, which is responsible for decrease in cracking and other secondary reactions resulting into longer catalyst life.

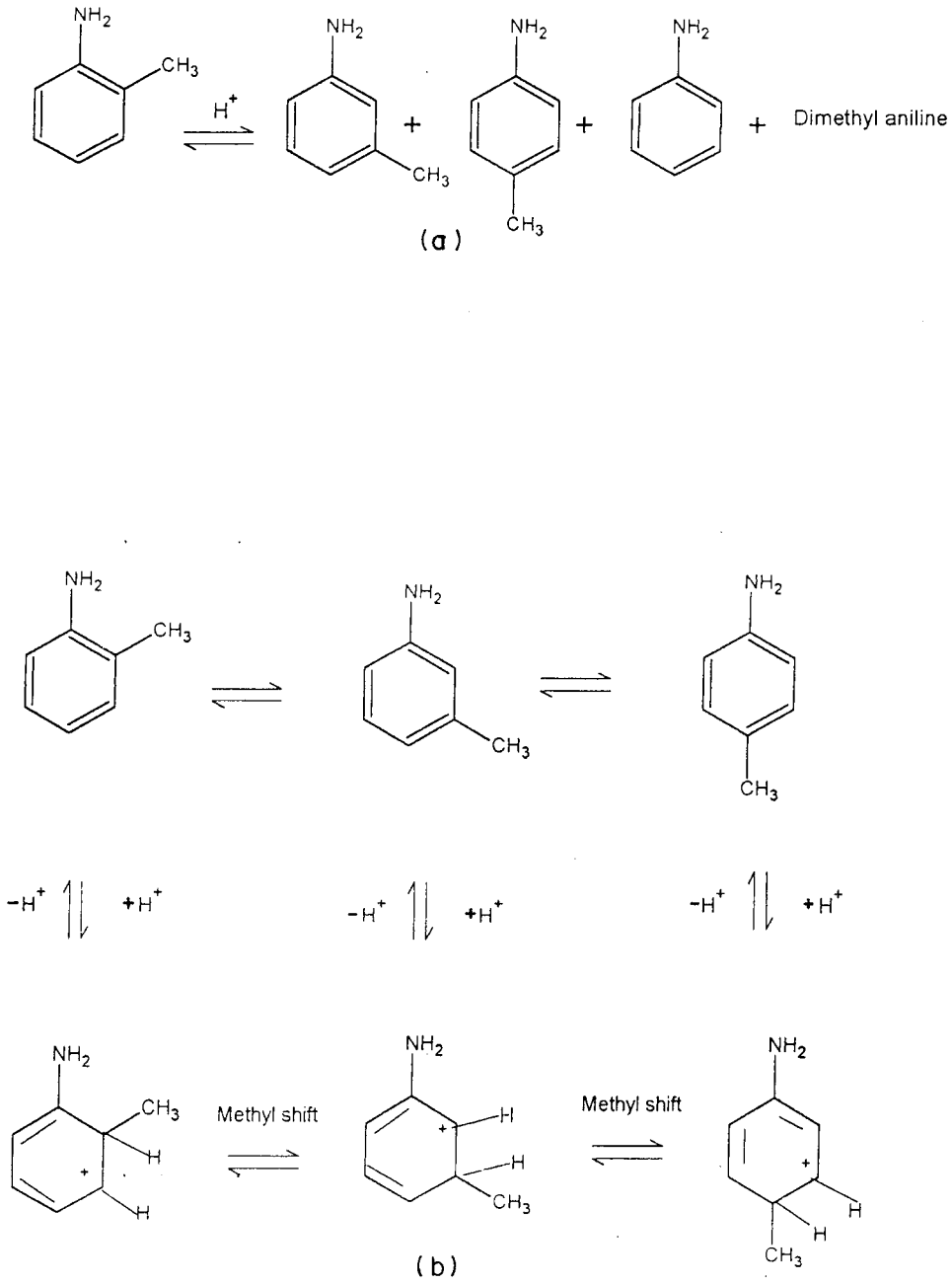

Fig 4.11 Reaction mechanism of o-toluidine isomerization on H-AlZrS-1 catalyst.
a) Schematic representation and b) 1,2 methyl shift mechanism

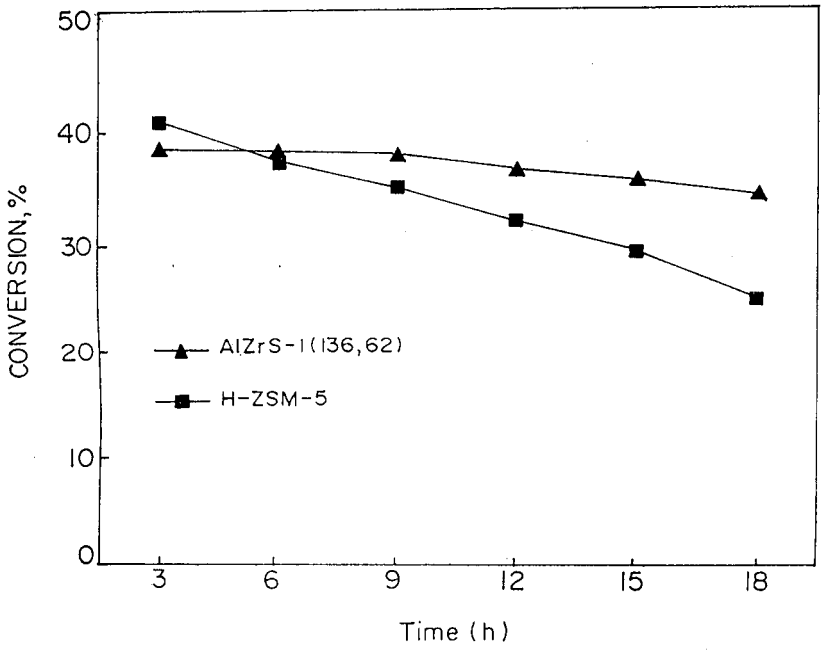

Fig 4.12 Variation of conversion with time on stream in o-toluidine isomerization.

4.6 CONCLUSIONS

Zirconium silicate with MEL and MFI framework can be synthesized using zirconium alkoxide. Both, zirconium source and template affect the precursor gel/solution, and, subsequently the purity of the ZrS-2 product and the amount of zirconium incorporation in the material. Only the samples synthesized using zirconium alkoxide and alcoholic TBAOH showed proportional increase in unit cell volume with increase in zirconium content.

The physico-chemical characterization by XRD, SEM, MAS-NMR, FTIR and adsorption studies indicate that Zr^{4+} and Al^{3+} can be incorporated simultaneously into the ZSM-5 structure. A shoulder (sh) at 970 cm^{-1} in the IR spectra in the framework region, a strong absorption band around 208 nm in the UV-Vis region, indicate that zirconium is incorporated in lattice framework of MEL and MFI structure. The Brönsted acid sites of ZrS-2 and AlZrS-1 samples are stronger than those of silicalite-2 and silicalite-1 respectively which are shown by the temperature dependent IR spectroscopy of chemisorbed pyridine.

ZrS-2 samples exhibited considerable catalytic activity in the hydroxylation of phenol, which further support the incorporation of Zr^{4+} in the MEL lattice. The catalytic activity of H-AlZrS-1 samples for o-toluidine isomerization showed less conversion compared to H-ZSM-5 increased m-isomer selectivity and catalyst life.

4.7 REFERENCES

1. Ulrike Ciesla, Stefan Schacht, Galen D. Stuky, Klaus K. Unger and Ferdi Schuth *Angew chem., Int. Ed. Engl.* 35(5) (1996) 541.

2. Notari, *B. Stucture-Activity and Selectivity Relationship in Heterogeneous Catalysis.* (eds. Grasselli, R. K. & Sleight, A. W: Elsevier, Amsterdam) 243, (1991).

3. Peter T Tanev, Malama Chibwe, & Thomas J. Pinnavaia. *Nature* 368, (1994) 321.

4 Lim, S and Haller, G. L. *Appl. Catal., A,* 188(1,2) (1999) 277.

5 Wei, Di; Chueh, Wei-Te and Haller, Gary L. *Catal. Today,* 51(3-4) (1999) 501.

6 Mahalingam Rathinam J, Badamali Sushanta K, Selvam Parsuraman., *Chem. Lett.,* (11) (1999) 1141.

7 Kornatowski J and Zadrozna G. *Proc. Int. Zeolite Conf., 12th,* Meeting Date 1998, Volume 3, 1577-1584. Edited by: Treacy, M. M. J. Materials Research Society: Warrendale Pa. (1999).

8 Luan Zhaohua, Maes Estelle M, Van der Heide, Paul A. W, Zhao Dongyuan, Czernuszewicz Roman S and Kevan, Larry., *Chem. Mater.*, 11(12) (1999) 3680.

9 Kovalenko A. S, Korchev A. S, Il'in V. G and Filippov A. P. *Theor. Exp. Chem.*, 35(3), (1999) 167.

10 Corma Avelino, Domine Marcelo, Gaona Jose A, Jorda Jose L, Navarro Maria T, Rey Fernando, Perez-Pariente Joaquin, Tsuji Junpei, McCulloch Beth and Nemeth Laszlo T. *Chem. Commun.* (20) (1998) 2211.

11. a) M. K. Dongare, P. Singh, P. P. Moghe, and P. Ratnasamy. Zeolites 11, (1996) 690., b) Occelli M. L, Biz S and Auroux A. *Appl. Catal., A,* 183(2) (1999) 231.

12. Bhavana Rakshe, Veda Ramaswamy and A. V. Ramaswamy., *J. Catal*., 163 (1996) 501.

13. Tuel A., S. Gontier., R. Teissier,. *J. Chem. Soc. Chem. Commun*. (1996) 65.

14. Vercruysse K. A, Klingeleers D. M, Colling T, Jacobs, P. A. *Stud. Surf. Sci. Catal., 117*(Mesoporous Molecular Sieves 1998, Elsevier Science B.V.) (1998) 469.

15. P. Meriaudeau, V. A. Tuan, L. N. Hung, F. Lefebvre and H. P. Nguyen., *J. Chem. Soc Fara. Trans* 93(23) (1997) 4201.

16. J.S. Reddy, R. Kumar and P. Ratnasamy, *Appl. Catal*. 58, (1990) L1

17. R. Fricke., H. Kosslick., V. A. Tuan., I. Grohmann., W. Pilz., W. Storek., G. Walther. *Stud, Surf. Sci. Catal.* 83, (1994) 57.

18. E. Duprey, P. Beaunier, M. A. Springuel-Huet, F. Bozon-Verduraz, J. Fraissard, J. M. Manoli, and J. M. Bregeault *J. Catal* 165 (1997) 22.

19 M. Decottignies, J. Phalippon and J. Zarzycki. *J. Mater. Sci* 13(12) (1978) 2605

20 M. A.. Combler, A. Corma and Perez-Periente *J. Chem. Soc. Commun.* (1993) 557.

21. Boccuti , M. R., Rao K. M., Zecchina. A., Leofanti. G., and Petrini. G. *Stud. Surf. Sci. Catal.* 48, (1989) 133.

22. Dang. Z., Anderson B. G., Amenomiya Y., and Morrow B. A,. *J. Phys. Chem*. 99, (1995) 14437

23 Vedrine J. C in " *Proceedings of the 6th international zeolite conference* " Eds: D. Oslon and A. Basio, Butterworth Guildford UK (1984) 497.

24. Simon Mark W, Nam Sang Sung, Xu Wen Qing, Sulb Steven L, Edwards John C, O' Young Chin Lin. *J. Phys. Chem* 96 (15) (1992) 6381.

25 Terry, Karl W, Lugmair, Claus G, Tilley, T. Don., *J. Am. Chem. Soc*., 119(41), (1997), 9745.

26. G. Bellusi, A. Carati, M. G. Clerici and A. Esposito *Stud. Surf. Sci. Catal*. 63, (1991) 421.

27. L. Forni, M. Pellozi, A. Giusti, G. Fornasari and R. Millini, *J. Catal*. 122, (1990) 44.

28. A. Thangaraj, R. Kumar and S. Sivasanker *Zeolites* 12 (1992) 135.

29. D. Trong On, S. Kaliaguine and L. Bonneviot, *J. Catal*. 157 (1995) 235.

30. K. Eichler, E. I. Leupold, H. Arpe and H. Baltes., U. S. Patent 4, 720, 583 (1988).

31. F.J. Weigert. *J. Org. Chem.* 52, 3296 (1987)

32. US Patent No. 4 283 571

33. Toray industries *Japan Kokai Tokkyo Koho* JP 8285330 (1982)

34. F. J. Weigert J. Org. Chem. 51, (1986) 2653.

5.1 INTRODUCTION

Aluminophosphate molecular sieves consist of alternating trivalent aluminum (Al^{3+}) and pentavalent phosphorous (P^{5+}) cations as the predominant occupants of the tetrahedral sites (M^{4+}). The resulting structure becomes neutral and therefore they are less attracted in industrial applications. Aluminophosphates are capable of incorporating many active metals in the framework. Attempts have been made to indroduce useful catalytic activity by chemical modification, adsorption or entrapment of catalytic species within the pore system[1]. However direct lattice substitution of equivalent or altervalent cations offers a mechanism for introducing ion exchange ability and acidic or basic centres. Hence di, tri and tetravalent cations which can adopt tetrahedral co-ordination could be incorporated during hydrothermal synthesis. These metal incorporated alumino-phosphates (designated as MeAPO-n) posses redox as well as acid centers, which are responsible for catalysis in oxidation and acid catalyzed reactions. Attempts have been made to introduce V^{5+}, Si^{4+}, Ti^{4+}, Cr^{4+}, Sn^{4+}, Fe^{3+}, B^{3+}, Co^{2+} and Mg^{2+} in various alumino-phosphate frameworks and are reported to alter their catalytic properties[2-9]. The introduction of transition metals, like V, Ti, Cr, Sn at substitutional sites in aluminophosphate (AlPO-n) frameworks are well documented[10-15], but similar studies on Zirconium containing $AlPO_4$-n molecular sieves are not well established[16-17].

Zirconia in its pure and modified form is an important material as catalyst and catalyst support[18], but owing to the difficulty in preparation as highly dispersed state with high surface area, it has limited industrial applications. Catalytic activity of ZrO_2 can be enhanced by promoting with sulphate anions (sulphated ZrO_2),[19-20] and by phosphate anions (phosphated ZrO_2).[21-23] Sulphated zirconia is nonporous, whereas many examples of phosphated zirconia are microporous, mesoporous or lammellar materials and have high surface area. Numerous studies are devoted to this problem, those on zirconium containing

microporous zeolites and mesoporous silica demonstrate that Zr^{4+} cation can be isomorphously substituted for Si^{4+} in high silica zeolites and mesoporous silicas[24-29]. Nevertheless, it also indicated that the presence of Zr in the catalyst enhances the life of the catalyst in reactions like skeletal isomerization of linear butenes[17] and isomerization of toludines[30]. Among the various interesting AlPO-n structures, the transition metal containing analogues of AlPO-5 and AlPO-11 are the most interesting and well studied.

The synthesis, characterization and catalytic properties of zirconium containing aluminophosphates with AlPO-5 and AlPO-11 structures are discussed here. The emphasis was given to the direct synthesis of Zr-AlPO-5 and Zr-AlPO-11 by hydrothermal method. The most important objective was to prepare well-defined zirconium containing aluminophosphates with AlPO-5 and AlPO-11 materials. These materials were characterized using physico-chemical techniques such as XRD, XRF, ^{27}Al and ^{31}P MAS-NMR, SEM, FTIR and sorption methods.

5.2 HYDROTHERMAL SYNTHESIS

The synthesis of transition metal containing alumino-phosphate molecular sieves can be carried out by two methods: by direct hydrothermal synthesis and by post synthesis modification. The hydrothermal synthesis is the best way to obtain a material with high dispersion of metal ions compared to post synthesis method. The Zr containing AlPO-5 and AlPO-11 molecular sieves in the present investigation were prepared using hydrothermal method. They were synthesized using aluminum isopropoxide (AlP), orthophosphoric acid (OPA), and zirconium propoxide (ZrP) as aluminum, phosphorous and zirconium source respectively. Triethyl amine (TEA) and di-n-propylamine (DPA) were used as templates for AlPO-5 and AlPO-11 structures respectively.

5.2.1 Synthesis of Zr-AlPO-5

Zr-AlPO-5 with different Zr content were prepared from the gel composition 1.5R: $x$$ZrO_2$: Al_2O_3: P_2O_5: $33H_2O$, where x was 0.04 - 0.1 and R was triethylamine (TEA). The method used for the synthesis of Zr-AlPO-5 samples is schematically shown in Fig. 5.1.

In a typical synthesis, 20.8g of aluminum isopropoxide and 80g of dry isopropyl alcohol (IPA) were mixed together and stirred at 60^0C for 1 h. Then 0.66g zirconium propoxide(ZrP) with 20 g of IPA was added slowly to the above mixture under vigorous stirring and the mixing was continued for 45 min. The solution was heated to remove the IPA before adding 11.5g of orthophosphoric acid along with 30g of water. After 1 h, 7.6g TEA was added slowly and stirring was continued for another 1 h. The composition of the precursor gel was 0.04 ZrO_2: Al_2O_3: P_2O_5: 1.5TEA: $33H_2O$. The homogeneous gel was then transferred into a PTFE lined stainless steel autoclave and kept for crystallization at 200^0C for 4-5 days. After complete crystallization, the white solid was recovered by filtration and was washed several times with deionized water and dried in oven. The samples thus obtained were calcined in air to remove the template by heating slowly to 600^0C and holding it for 8 h. Titanium containing AlPO-5 was also prepared using the same method described above except that titanium tetrabutoxide (TBOT) was added instead of zirconium alkoxide. The Zr source was not added in the gel so as to obtain pure AlPO-5. All the samples prepared were characterized by various physico-chemical techniques discussed in Chapter 2.

5.3 PHYSICO-CHEMICAL CHARACTERIZATION OF Zr-AlPO-5

5.3.1 X-ray diffraction

The XRD patterns of pure AlPO-5, Zr-AlPO-5 (0.04), Zr-AlPO-5 (0.08) and Zr-AlPO-5 (0.1) are presented in Fig.5.2 (a-d) respectively, which shows that all the samples have AFI (AlPO-5) topology and do not have any crystalline impurities. These

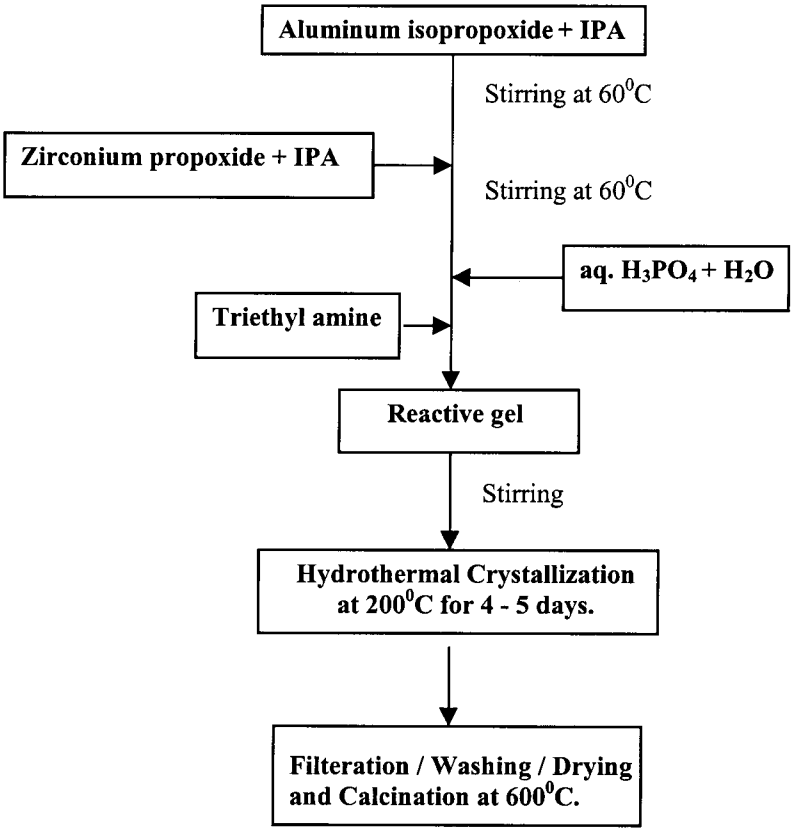

Fig. 5.1 Schematic representation of synthesis of Zr-AlPO-5 samples.

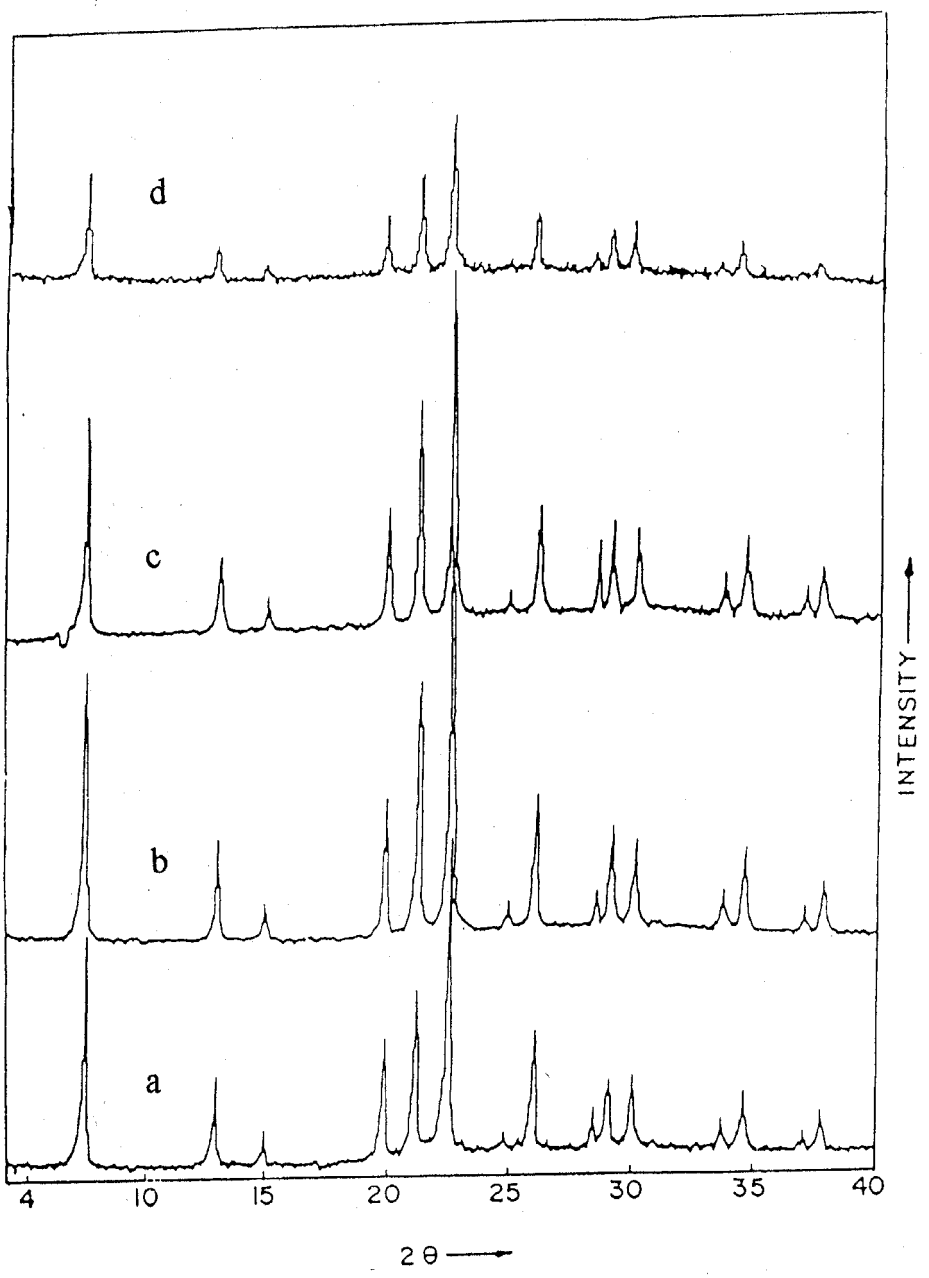

Fig. 5.2 Schematic representation of synthesis of Zr-AlPO-5 samples.

patterns are similar to those reported in the literature[11]. The intensity of the peaks in the product with high zirconium content (Fig.5.2, d) is lower, indicating some loss of crystallinity.

The physico-chemical properties of AlPO-5 and Zr-AlPO-5 samples are presented in Table-5.1 and the unit cell volumes calculated are presented in Table-5.2. The volume increased from 1366(Å)^3 for pure AlPO-5 to 1372(Å)^3 for Zr-AlPO-5 (0.08) samples. In the sample containing higher zirconium [e.g. Zr-AlPO-5(0.1)] the increase was not proportional to zirconium content, indicating the limited incorporation of zirconium in the lattice.

5.3.2 Chemical composition

The chemical compositions were determined by XRF method and the results are given in the Table-5.1. In case of Me-APOs, the elemental analysis poses always a question, whether the metal ion is substituted for the Al or P or for both because, the amount of metal ion in the solid is comparatively very less than both Al and P together. Therefore it is difficult to draw a conclusion from the chemical analysis alone about the substitution pattern. In the case of Zr-AlPO-5 samples, the Zr content in the solid was always lower than in the reactive gel and the Al/P+Zr ratio was near to 1. This indicated that the substitution of Zr for P in the lattice was predominant over the pair wise substitution of two Zr for one Al and one P cation.

The Pauling's minimum radius ratio concept[31], which is useful in predicting the potential incorporation of an element into zeolite-based lattice is of limited value for predicting the substitution in microporous AlPOs. Elements not normally predisposed to tetrahedral co-ordination with oxygen and situated largely outside the preferred range for tetrahedral co-ordination ($0.225 < \rho < 0.414$) can also be incorporated, for example Ti^{4+} and V^{4+}/V^{5+} containing molecular sieves. Their successful incorporation is ascribed to the

Table 5.1

The physico-chemical characteristics of AlPO-5 and Zr-AlPO-5 samples with different zirconium content.

Sr. No.	Sample*	Composition of crystalline phase	BET surface area (m^2/gm)	Adsorption wt%	
				Water	Cyclohexane
1.	AlPO-5	$Al_{12.02}P_{11.98}O_{48}$	395	22.1	8.8
2.	Zr-AlPO-5 (0.04)	$Al_{12.01}P_{11.82}Zr_{0.17}O_{48}$	340	20.3	9.1
3.	Zr-AlPO-5 (0.08)	$Al_{12.0}P_{11.64}Zr_{0.36}O_{48}$	342	21.4	9.0
4.	Zr-AlPO-5 (0.1)	$Al_{11.96}P_{11.58}Zr_{0.46}O_{48}$	316	20.6	8.9

*The number in parenthesis indicates the ZrO_2 moles in reacting gel.

Table 5.2

Unit Cell parameters of AlPO-5 and Zr-AlPO-5 samples

Sample	Unit Cell Parameters (Å)		Unit Cell Volume $(Å)^3$
	a = b	c	
AlPO-5	13.7020	8.4018	1366.0
Zr-AlPO-5 (0.04)	13.7206	8.4021	1369.7
Zr-AlPO-5 (0.08)	13.7283	8.4091	1372.5
Zr-AlPO-5 (0.1)	13.7239	8.4065	1371.1

flexibility of phosphate frameworks[32] and the unique possibility offered in AlPOs to extend the coordination sphere of the element with additional ligands besides the oxo bridges of the framework.

5.3.3 Scanning electron micrograph

The typical morphologies obtained from the gel with different zirconium content are shown in Fig 5.3 (a-c). The SEM photographs reveal that pure AlPO-5 (Fig.5.3a) crystallized in the form of hexagonal rods of irregular size, ranging from 0.5 to 3.0 μm, while the morphology of Zr-AlPO-5 (Fig 5.3, b-c) significantly changed depending on the Zr content. They consist of bundles of needle like crystals with no sharp edges.

5.3.4 Adsorption studies

Adsorption properties of Zr-AlPO-5 samples are presented in Table-5.1. BET surface area and the amount of H_2O and cyclohexane adsorbed are comparable to reported values[33]. These values show that the materials are highly crystalline without any

amorphous matter occluded in the pores. This is contrary to the findings of Meriaudeau[17] et. al, where in incorporation of Zr in SAPO-11 resulted in Zr species occluded in the pores. It is also observed that for Zr-AlPO-5 samples, N_2 adsorption is considerably less than that of AlPO-5, even-though water and cyclohexane adsorption values are comparable. This can be due to the difference in the interaction of N_2 molecules with the surface. The possible reason[16] could be the condensation of N_2 around the zirconium centers, which could hinder and stop the diffusion and sorption of N_2. Thus it might indicate a framework incorporation of Zr ions in Zr-AlPO-5 samples.

5.3.5 ^{31}P and ^{27}Al MAS-NMR spectroscopy

^{31}P and ^{27}Al MAS-NMR spectra of calcined samples are presented in Fig.5.4 (a-d). The values of the chemical shift, -30.8 ppm for ^{31}P and 36.78 ppm for ^{27}Al are the typical

(c)

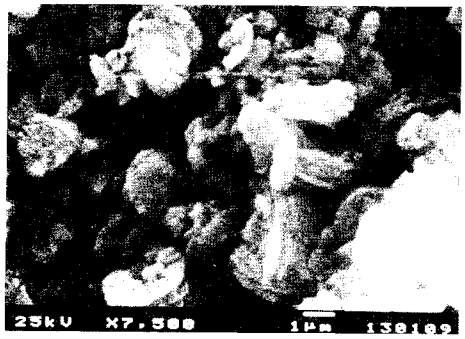

(b)

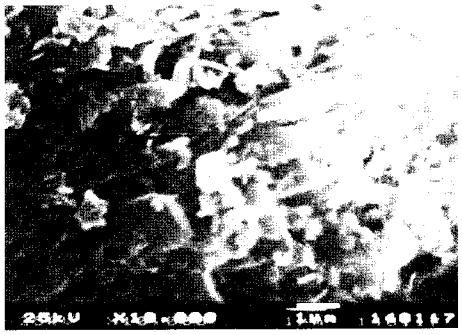

(a)

Fig. 5.3 The SEM photographs of a) AlPO-5, b) Zr-AlPO-5 (0.04) and c) Zr-AlPO-5 (0.08)

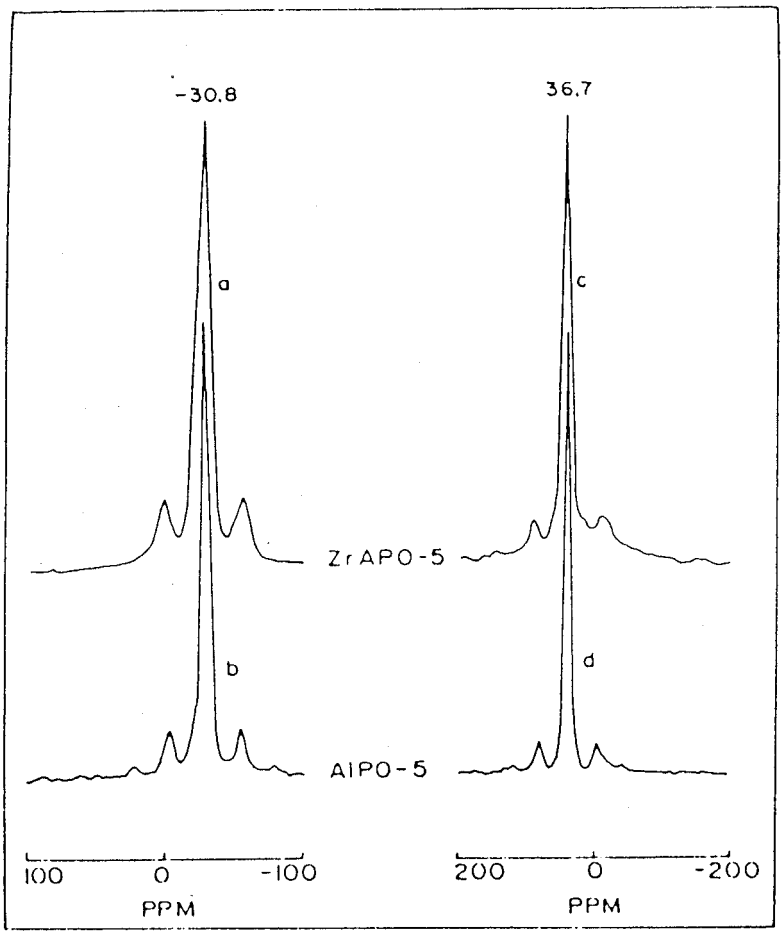

Fig. 5.4 ^{31}P (a,b) and ^{27}Al (c,d) MAS NMR spectra of AlPO-5 (b,d) and Zr-AlPO-5 (0.04) (a,c).

of AlPO-5 structure reported[5,34]. There are no additional lines in the spectrum, which indicates the absence of extra-lattice Al and P species in the samples.

5.3.6 FTIR spectroscopy

FTIR spectra in the framework vibration region are recorded in the Fig. 5.5 (a-d). Absorption bands are observed at around 490, 562, 622 cm^{-1} due to vibrations of double ring, at 706, 732, 1042(sh) cm^{-1} due to symmetric stretching and at 1136, 1257(sh) cm^{-1} due to asymmetric stretching vibrations of AFI structure. Though there is not much variation in the nature of the spectra of Zr-AlPO-5 and pure AlPO-5, a shoulder appears in the spectrum of Zr-AlPO-5 at 1042 cm^{-1} the intensity of which increases on increase in Zr content. This band is absent in the spectrum of pure AlPO-5. Similar band was also observed in the spectrum of Titanium containing AlPO-5[35], which was attributed to the insertion of Ti in the framework. Therefore in the case of Zr-AlPO-5 also, the band at 1042 cm^{-1} may indicate the presence of Zr in the AlPO-5 lattice.

5.3.7 FTIR spectra of hydroxyl region

FTIR spectra of surface hydroxyl groups of all samples are presented in Fig. 5.6 (a-c). There are only low intensity bands at 3790, 3740 cm^{-1} and a strong band at 3680 cm^{-1} in the spectrum of AlPO-5. They are assigned to terminal Al-OH (3790, 3740) and P-OH (3680) groups on the external surface of AlPO-5. The band at 3680 cm^{-1} was observed[21,36-38] on the amorphous zirconium phosphate co-gel also, which was attributed to the isolated OH groups bonding to the surface through (i) more than one Zr cations, and ii) a single P cation. This band is less pronounced on the surface of pure ZrO_2, wherein it is due to the bridging hydroxyl groups, Zr-(OH)-Zr. The absorption bands at 3790, 3740, 3680, 3655 and 3610 cm^{-1} are observed for Zr-AlPO-5 samples, (Fig.5.6b). The additional bands at 3655 and 3610 cm^{-1}, which are not found on AlPO-5 should therefore be related to the presence of Zr ions in AlPO-5 structure. These bands cannot be due to hydroxyl

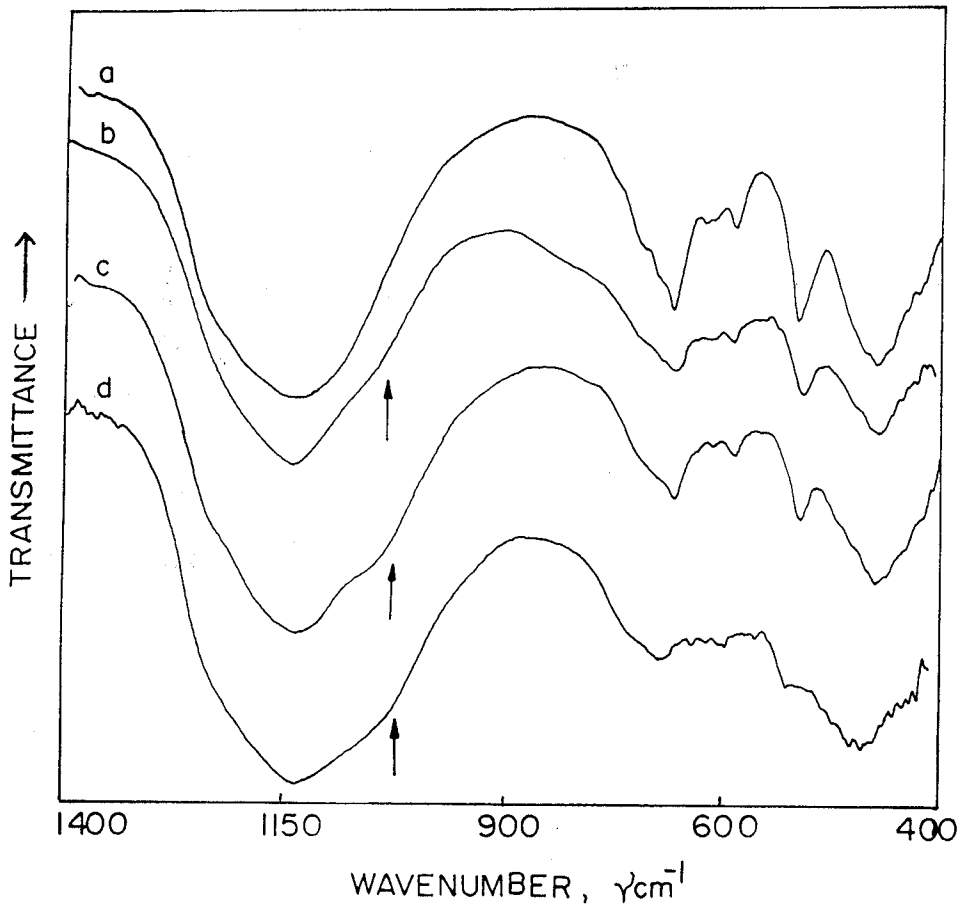

Fig. 5.5 FTIR spectra of a) AlPO-5, b) Zr-AlPO-5 (0.04), c) Zr-AlPO-5 (0.08) and d) Zr-AlPO-5 (0.1)

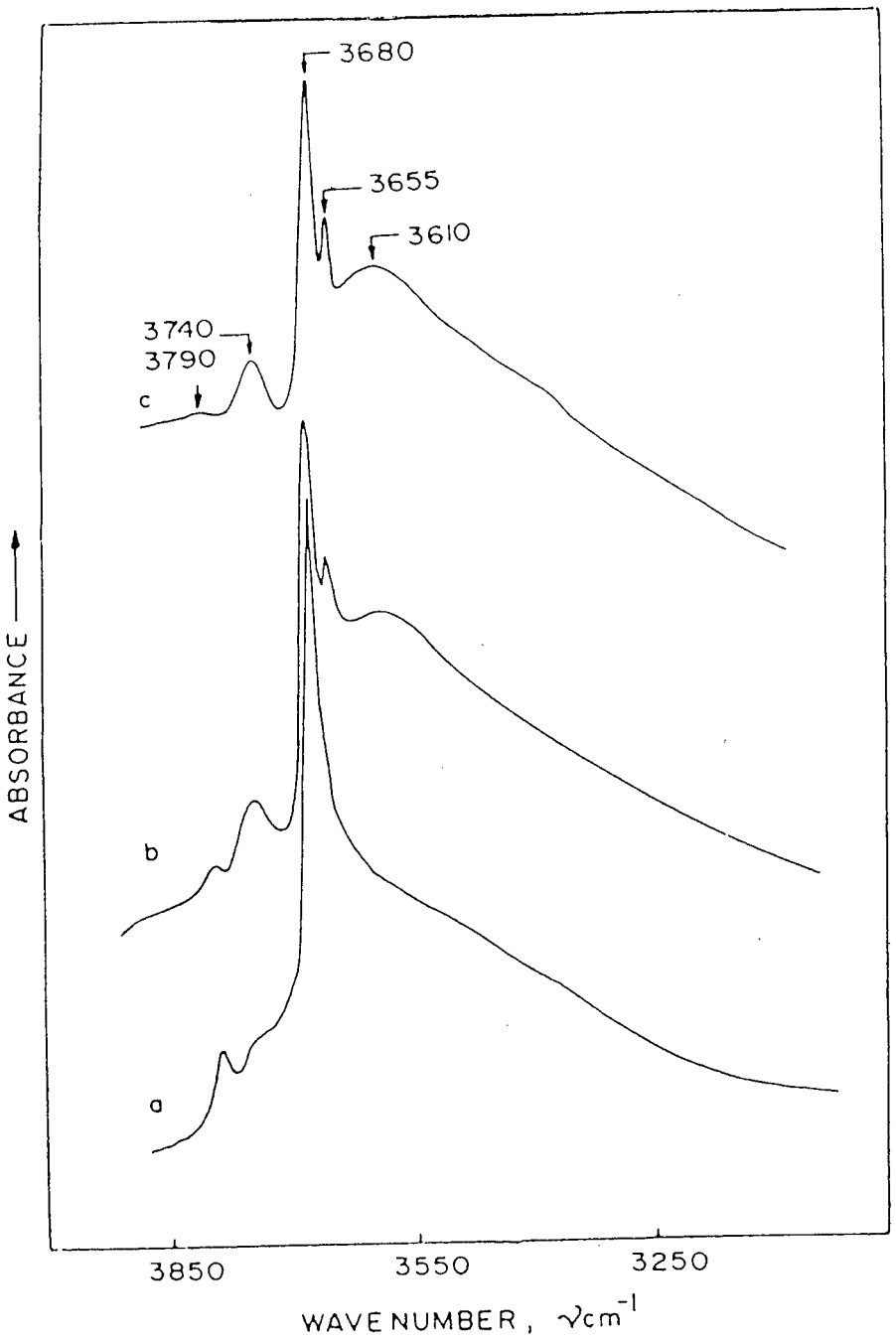

Fig. 5.6 FTIR spectra of surface hydroxyl groups of a) AlPO-5, b) Zr-AlPO-5 (0.04) and c) Zr-AlPO-5 (0.08)

groups of extra-lattice P or Al species because they are not detected in MAS-NMR spectroscopic studies. The intensity of these bands increases with increase in Zr content. They probably arise due to the partial substitution of P or P+Al pair by Zr cations in AlPO-5 lattice, which should generate bridging hydroxyl groups Zr(Al)-(OH)-Zr or Zr-(OH)-Al.

Such bridging hydroxyl groups should be acidic and their frequency should depend on the location in the pore structure of the material. For SAPO-5, these bridging hydroxyl groups [Si-(OH)-Al] are located in the 12-ring main channel and 8-ring side pockets[39]. They give bands one at high frequency (HF) 3625 and another at low frequency (LF) at 3525 cm^{-1}. Such HF and LF bands are also observed on SAPO-37 and zeolite type Y, which have dual pore structure. Therefore the band at 3655 and 3610 cm^{-1} can also be assigned to such HF and LF bands similar to SAPO-5 material.

5.3.8 FTIR spectra of chemisorbed ammonia

The nature of these -OH groups were further studied by FTIR spectra of chemisorbed NH_3. In Figure 5.7, difference FTIR spectra of Zr-AlPO-5 sample after adsorption of NH_3 at 50, 100, 150, 200, and 250^0C are presented in the range 4000-2800 cm^{-1}, which is O-H and N-H stretching region. The bands due to O-H stretching at 3680, 3655 and 3610 cm^{-1} appear as negative bands and new bands due to N-H stretching of NH_4^+ appear at 3370, 3340, 3287 and 3220 cm^{-1}. As the chemisorbed NH_3 is desorbed at increasing temperatures, intensity of the bands at 3680, 3655 and 3610 cm^{-1} increases, while that of bands of N-H stretching decrease in intensity. Therefore the bands at 3680, 3655 and 3610 cm^{-1} are definitely due to acidic -OH groups. A clearly defined isobestic point is visible at 3513 cm^{-1}. In the case of SAPO- molecular sieves[40], the protonated NH_3 (NH_4^+ species) interact with anionic oxygen of the framework via two protons, there by producing two different types of N-H stretching vibrations, one type belonging to free

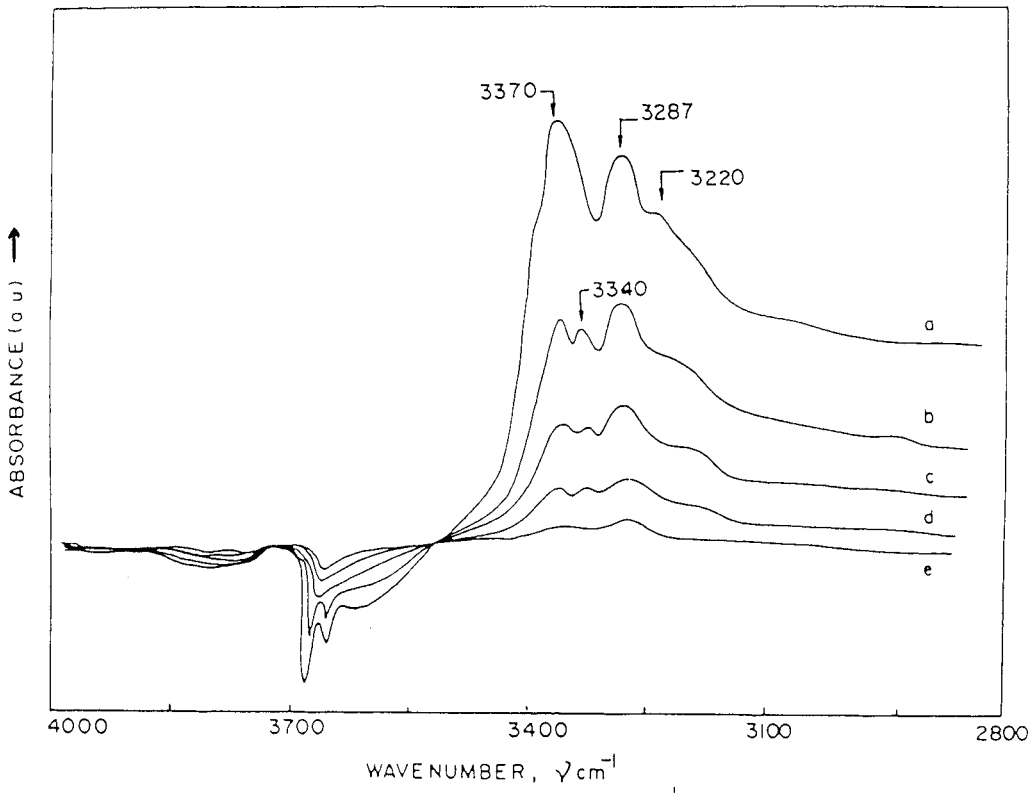

Fig. 5.7 FTIR difference spectra (4000-2800 cm^{-1}) of chemisorbed ammonia on Zr-AlPO-5(0.08) sample at a)50, b)100, c)150, d)200, and e)250^{0}C.

N-H bonds and another type belonging to N-H bonds involved in hydrogen bonding. The two pairs of bands at 3370, 3340 and 3287, 3220 cm^{-1} observed for Zr-AlPO-5 can also be ascribed to these two types of N-H stretching vibrations of adsorbed NH_3. The smaller shifts of these bands to lower frequencies indicate that the interaction between NH_4^+ protons and the framework oxygens of Zr-AlPO-5 are weaker than that of SAPO-40.

The Fig. 5.8 represents difference spectra of Zr-AlPO-5(0.08) sample in the region of N-H deformation vibrations. The spectra show two bands at 1620 and 1440 cm^{-1}, which decrease in intensity almost simultaneously upon increasing the sample temperature upto 250^0C. Where as in pure AlPO-5, the intensity of these bands (Fig. 5.8, f-h) is lesser and almost disappears at 150^0C. These two bands are ascribed to co-ordinatively bound NH_3 and protonated NH_3 (NH_4^+ species) on Lewis and Brönsted acid sites of Zr-AlPO-5 samples respectively.

5.3.9 Temperature programmed desorption of ammonia

The TPD of NH_3 curves for AlPO-5 and Zr-AlPO-5 are presented in Fig. 5.9. All the adsorbed NH_3 on AlPO-5 desorbed below 200^0C indicating the absence of strong acid sites on the surface where as some NH_3 is retained on the surface of Zr-AlPO-5 even upto 300^0C indicating that the Zr incorporation modifies the acidity of AlPO-5 making it stronger. In Ti-AlPO-5, Ulagappan et. al[17] have reported the possibility of substitution of Ti for Al or P in AlPO-5 structure. Similarly, if Zr replaces some of P or Al+P in AlPO-5, stronger acid sites are generated as has been already detected by FTIR and TPD of ammonia. But if two Zr cations replace a pair of Al + P cations in the lattice, no new acidic sites can be generated.

5.3.10 Catalytic activity in m-xylene isomerization

The isomerization and disproportionation of m-xylene has long since been used to characterize the pore size of molecular sieves and to distinguish the medium pore from the

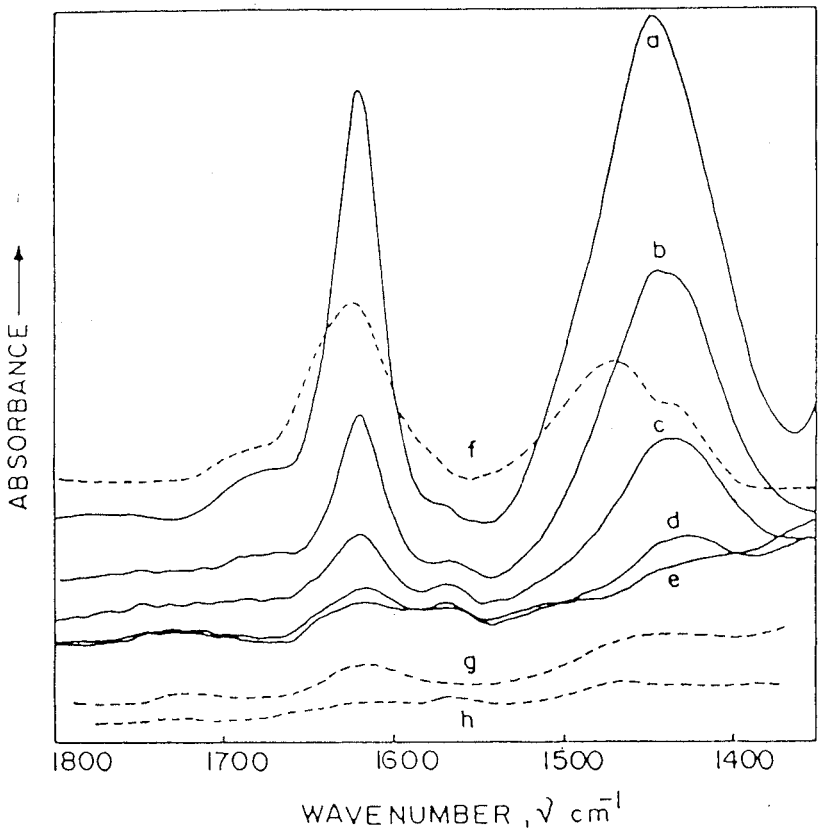

Fig. 5.8 FTIR difference spectra (1800-1350 cm^{-1}) of chemisorbed NH_3 on Zr-AlPO-5(0.08) sample at a)50, b)100, c)150, d)200, and e)250^0C; and $AlPO_4$-5 at f)50, g)100 and h)150^0C respectively.

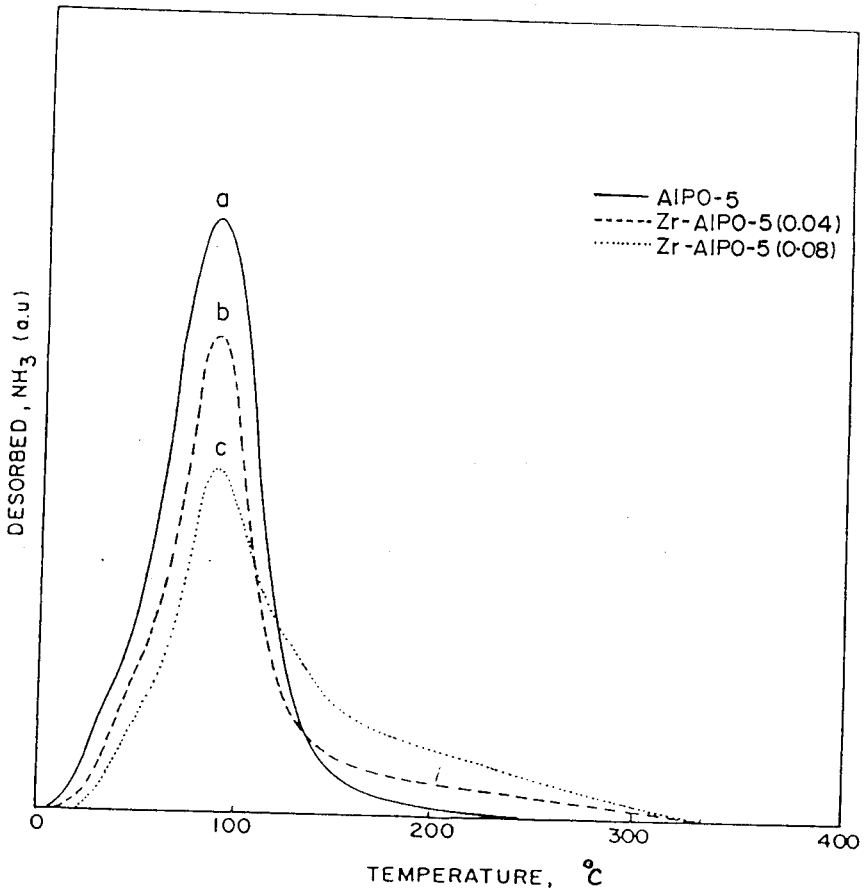

Fig. 5.9 The TPD of NH_3 chemisorbed on a) AlPO-5, b) Zr-AlPO-5 (0.04) and c) Zr-AlPO-5 (0.08)

large pore materials[41,42]. The shape and dimensions of the intracrystalline cavities in molecular sieves with 10- and 12-membered rings is an important factor in determining the product selectivities in the conversion of m-xylene. The activity in the isomerization and disproportionation of m-xylene also depends on their acidic strength. The type of metal ion (Al, Fe, B, Ti, etc) at lattice position is also an important factor that determines the acidity.

There are many papers on catalytic activity of metal substituted molecular sieves because of their considerable acidic properties. Studies on catalytic activity of Zr containing molecular sieves are very few, like oxidation reactions using H_2O_2[26], oxidation of cholesterol[43], o-toluidine isomerization[30] and skeletal isomerization of linear butenes[17], nevertheless they also showed that Zr incorporation in the micropores improves the life of the catalyst significantly. Catalytic activity of Zr-AlPO-5 for positional isomerization of m-xylene was studied as a test reaction. The reaction was carried out at 350-550^{0}C keeping WHSV-2 h^{-1}. The conversion of m-xylene at 450^{0}C for all the catalysts namely AlPO-5, Zr-AlPO-5(0.04), Zr-AlPO-5(0.08), Zr-AlPO-5(0.1) and Ti-AlPO-5 are presented in the Table-5.3. The variation in conversion with temperature is plotted in Figure 5.10,a. Increase in conversion is correlated with the zirconium content in the samples. As the zirconium content increased in the lattice, enhancement of acidity and activity was observed except for the sample with highest zirconium content [Zr-AlPO-5(0.1)]. On increasing the temperature from 500^{0}C to 550^{0}C, conversion increased from 56 % to 62 % for Zr-AlPO-5 (0.08), whereas it decreased from 23 % to 7 % for AlPO-5. AlPO-5 is expected to deactivate very fast similar to mordenite because of unidimensional pore system[44]. The decrease in activity of AlPO-5 and Zr-AlPO-5 (0.1)

Table-5.3

m-Xylene isomerization on AlPO-5 and Zr-AlPO-5 samples.

Catalyst ⇒ Product Distribution ⇓	AlPO-5	Zr-AlPO-5 (0.04)	Zr-AlPO-5 (0.08)	Zr-AlPO-5 (0.1)	Ti-AlPO-5 (0.08)
Benzene	0.02	0.059	0.14	0.02	0.12
Toluene	1.64	2.71	5.47	0.32	3.87
p-Xylene	4.81	9.639	9.97	1.28	8.28
m-Xylene	87.55	76.11	66.43	95.53	73.4
o-Xylene	3.83	8.31	8.74	1.31	8.17
Σ Xylenes	96.19	94.059	85.14	98.12	89.85
135 TMB	0.2	0.418	1.38	0.8	1.24
124 TMB	1.75	2.445	6.31	0.29	3.92
123 TMB	0.17	0.29	0.89	0.06	0.81
Σ TMB	2.12	3.153	8.58	1.15	5.97
HBF*	0.03	0.019	0.67	0.39	0.19
m-xylene Conv. (α %)	12.45	23.89	33.57	4.47	26.6
p-x/o-x	1.25	1.16	1.14	0.97	1.01

* High boiling fractions.

Experimental conditions
Feed: m-xylene
Temp: 450 ^{o}C,
WHSV: 2h^{-1}
Pressure: 1 atm.

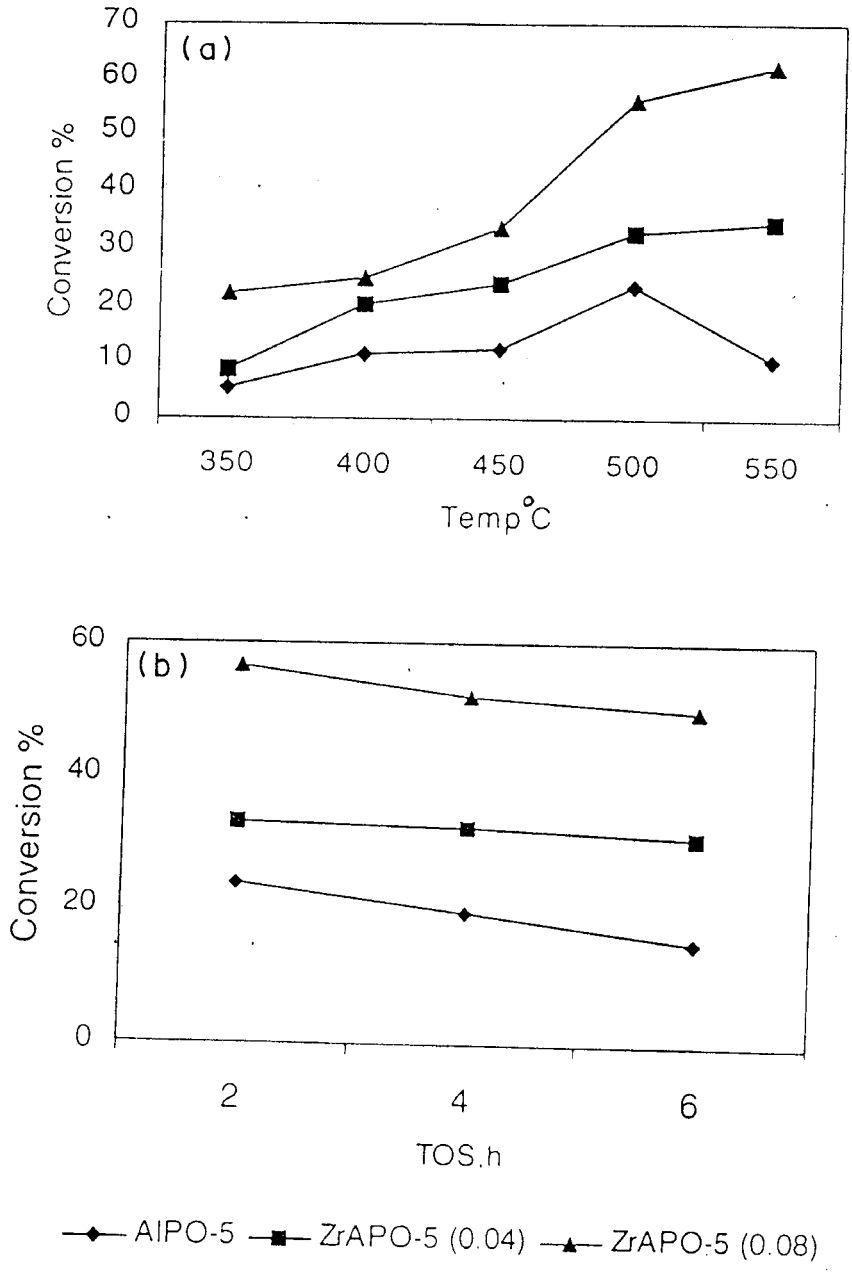

Fig. 5.10 The effect of a) temperature and b) time on stream on the conver m-xylene (at 500^0C) on Zr-AlPO-5.

may be due to the deposition of coke on the external surface and blocking of the pore mouth or channels.

In the medium pore molecular sieves, p-xylene is formed preferentially due to its relatively faster diffusion (10^4 times), but in the case of AlPO-5 molecular sieves being large pore variety (d = 0.8nm) the distribution of xylenes is expected to be thermodynamically controlled. In the present study, the p/o-xylene ratio was found to be in the range 1-1.2 suggesting that there was no diffusional restriction on xylene isomers in case of Zr-AlPO-5 containing low amount of zirconium and for AlPO-5 samples. The plot of the catalytic activity with time on stream for AlPO-5, Zr-AlPO-5(0.04) and Zr-AlPO-5(0.08) for 6 h is presented in the Fig. 5.10,b. The stability in the reaction was found to be better for Zr-AlPO-5 samples as compared to AlPO-5.

In addition to isomerization, m-xylene undergoes bimolecular disproportionation to form toluene and isomers of trimethyl benzenes(TMB) supporting the fact that diphenyl methane type of transition state was formed during the course of the reaction, which is represented schematically in Fig. 5.11. The disproportionation and isomerization activity was consistent, expected from the availability of acid sites of different strength; the isomerization occurs on the acid sites weaker than those involved in the disproportionation reactions. The estimation of the distribution of the trimethylbenzenes (TMB) in the product is therefore a catalytic means of probing the pore system of 12-membered ring molecular sieves[45]. Among TMBs the selectivity for 1,2,4-TMB was maximum which can easily diffuse out from the channel compared to other TMBs.

5.4 SYNTHESIS OF Zr-AlPO-11

Zr-AlPO-11 samples containing different Zr contents were prepared hydrothermally using zirconium propoxide, aluminum isopropoxide, ortho phosphoric acid and di-n-propyl amine (DPA). Based on some preliminary experiments the following

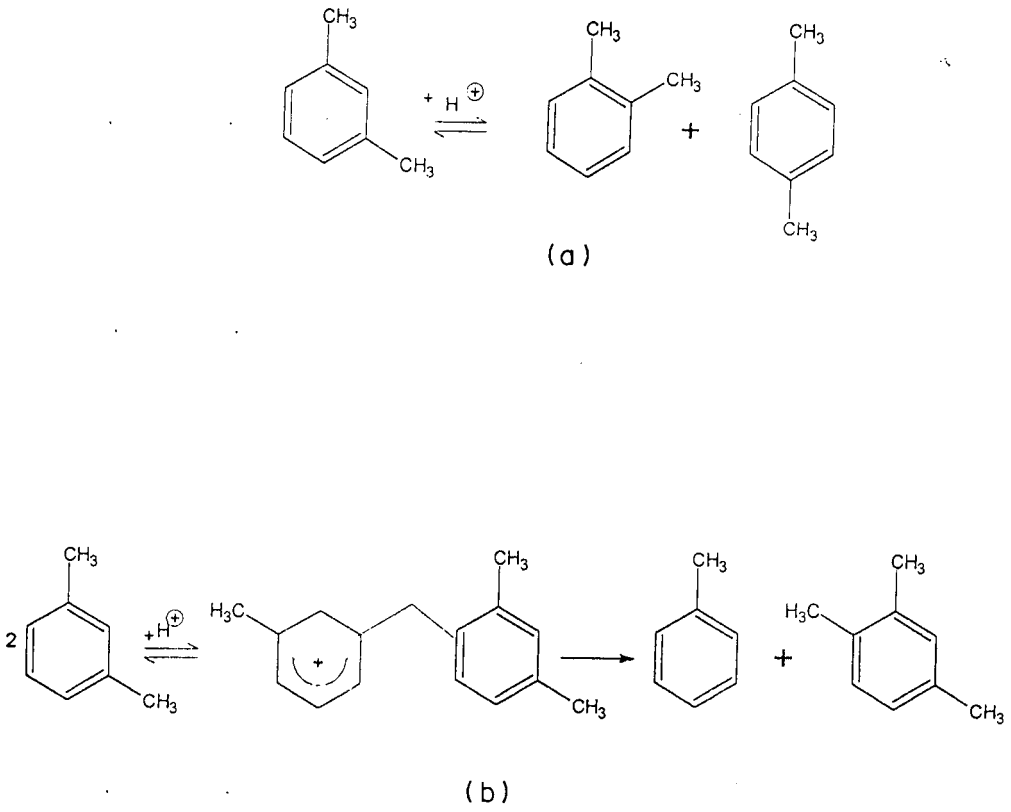

Fig. 5.11 Schematic representation of mechanism of m-xylene isomerization.

molar gel composition was used Al_2O_3: $xZrO_2$: (1-x/2)P_2O_5: DPA: 50 H_2O, where x varies from 0.03 to 0.1. In a typical synthesis, aluminum isopropoxide and zirconium propoxide in isopropyl alcohol were mixed together in a polypropylene beaker and stirred. The mixture was then heated to 60^0C while stirring to remove excess of alcohol and then cooled by ice before the addition of aqueous solution of ortho phosphoric acid. Finally, di-n-isopropyl amine was added as structure directing agent. A white gel was formed which was transferred to teflon lined autoclave and heated at 180^0C for hydrothermal synthesis for 4-5 days. After the hydrothermal crystallization, the sample was filtered, washed, dried and then calcined at 560^0C in air for 8 to 10 h. Zirconium free AlPO-11 and SAPO-11 samples were prepared using a standard procedure[46]. The synthesis of Zr-AlPO-5 samples is schematically represented in Fig. 5.12.

Platinum was loaded (0.5 wt %) on Zr-AlPO-11, SAPO-11 and pure AlPO-11 samples by wet impregnation with an aqueous solution of $Pt(NH_3)_4Cl_2$. The resulting materials were dried and reduced at 400^0C in flowing hydrogen prior to catalytic testing.

5.5 PHYSICO-CHEMICAL CHARACTERIZATION OF Zr-AlPO-11

5.5.1 X-ray diffraction

The XRD patterns of all the samples were identical to all the characteristic patterns of AEL topology[47] (Fig.5.13, curves a-d). It is observed from the patterns that the samples with low zirconium content are highly crystalline. The intensity of the peaks for samples with high Zr content decreased and required more time for complete crystallization. The unit cell parameters along with some other physicochemical properties are compiled in Table-5.4 and 5.5. The unit cell volume increased from 2093 $(Å)^3$ for pure $AlPO_4$-11 to 2102 $(Å)^3$ for Zr-AlPO-11(0.1) indicating the incorporation of Zr in the AlPO-11 lattice, but the increase was not proportional to the amount added in the synthesis.

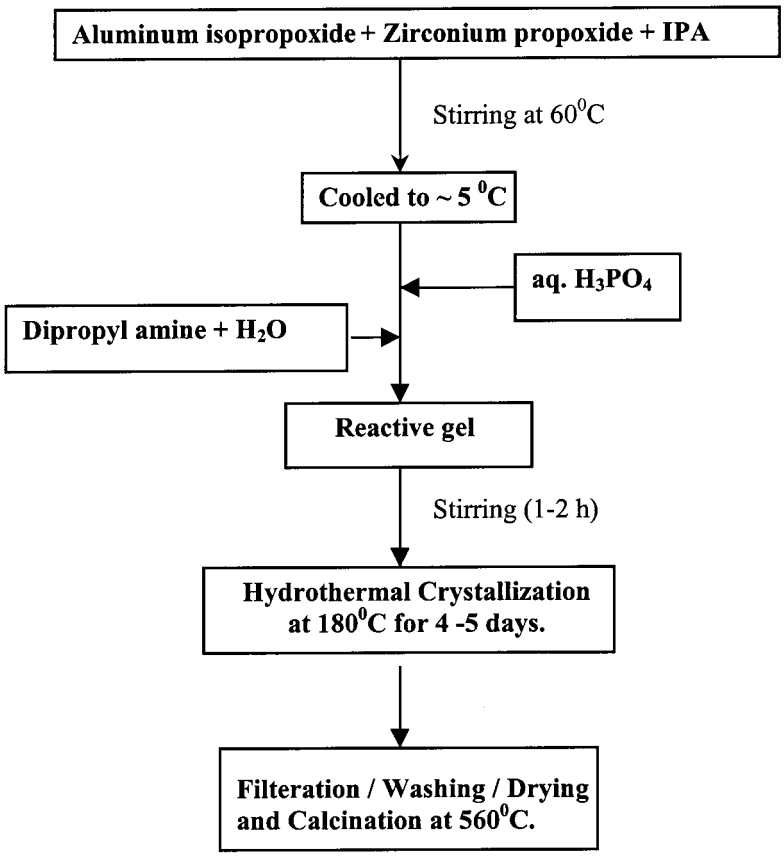

Fig. 5.12 Schematic representation of synthesis of Zr-AlPO-11 samples.

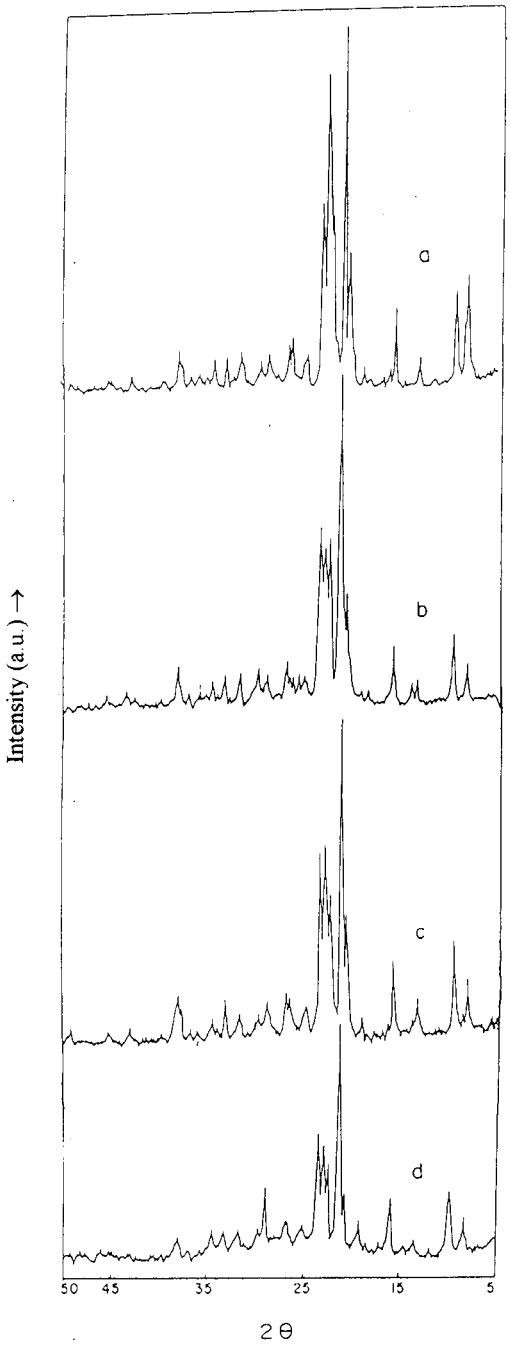

Fig. 5.13 XRD patterns of a) AlPO-11, b) Zr-AlPO-11(0.033), c) Zr-AlPO-11 (0.066) and d) Zr-AlPO-11 (0.1)

Table 5.4

The physico-chemical characteristics of AlPO-11, Zr-AlPO-11and SAPO-11 samples.

Sr. No.	Sample*	Composition of crystalline phase	BET surface area (m^2/g)	Adsorption wt%	
				Water	Cyclohexane
1.	$AlPO_4$-11	$(Al_{20.36}P_{19.64})O_{80}$	153	11.34	6.82
2.	Zr-AlPO-11(0.033)	$(Al_{19.92}P_{19.78}Zr_{0.30})O_{80}$	145	10.86	7.14
3.	Zr-AlPO-11(0.066)	$(Al_{19.90}P_{19.63}Zr_{0.47})O_{80}$	139	10.42	7.22
4.	Zr-AlPO-11(0.1)	$(Al_{19.78}P_{19.39}Zr_{0.83})O_{80}$	128	10.74	7.09
5.	SAPO-11(0.2)	$(Al_{19.70}P_{19.58}Si_{0.72})O_{80}$	165	12.37	6.93

* The number in parenthesis indicates the ZrO_2 moles in reacting gel.

Table 5.5

Unit Cell parameters of AlPO-11 and Zr-AlPO-11 samples

Sample*	Unit Cell Parameters (Å)			Unit Cell Volume $(Å)^3$
	a	B	c	
$AlPO_4$-11	13.3398	18.6381	8.4184	2093.05
Zr-AlPO-11(0.033)	13.3653	18.6391	8.4190	2097.31
Zr-AlPO-11(0.066)	13.3694	18.6404	8.4192	2098.16
Zr-APO-11(0.1)	13.3762	18.6492	8.4268	2102.11
SAPO-11(0.2)	13.3472	18.6446	8.4234	2096.19

5.5.2 Chemical analysis

The chemical composition of the Zr-AlPO-11 samples is shown in Table-5.4. It is observed that the Zr content in the solid was always lower than in the reactive gel. The chemical composition does not clearly indicate whether Zr is replacing both Al + P or only P in the lattice.

5.5.3 Scanning electron micrograph

The morphology and the particle size of the Zr-AlPO-11 samples are shown in Fig. 5.14 (a and b) The SEM photographs showed that the Zr-AlPO-11 crystallized in the form of agglomerates of irregular size, ranging from 1 μm to 5.0 μm.

5.5.4 FTIR spectroscopy

The FTIR spectra in the framework vibration region are recorded in the Fig. 5.15 (curves a-d). The spectra showed the characteristic absorption bands of AlPO-11 structure at around 1105, 704, 663 and 597 cm^{-1}. The nature of the spectrum of Zr-AlPO-11 and pure $AlPO_4$-11 are similar except that a low intensity absorption in the range of 1032 to 1037 cm^{-1} is observed in the spectrum of Zr-AlPO-11 samples. A similar band at around 1040 cm^{-1} is also observed in the spectrum of Zr-AlPO-5[48] and TAPO-11[35], which is attributed to the incorporation of Zr and Ti in the framework respectively. Therefore in the case of Zr-AlPO-11 also, this band can be attributed to the presence of Zr in AlPO-11 lattice.

5.5.5 ^{27}Al and ^{31}P MAS-NMR Spectroscopy

The ^{27}Al and ^{31}P MAS-NMR spectra of calcined Zr-AlPO-11(0.1) are presented in Fig.5.16 (curves a and b respectively). The chemical shifts at 37.6 ppm for ^{27}Al and -29.1 ppm for ^{31}P are typical of $AlPO_4$-11 structure[49-51]. No additional lines in the spectra are observed, which indicates the absence of any extra-lattice Al or P species associated with the samples.

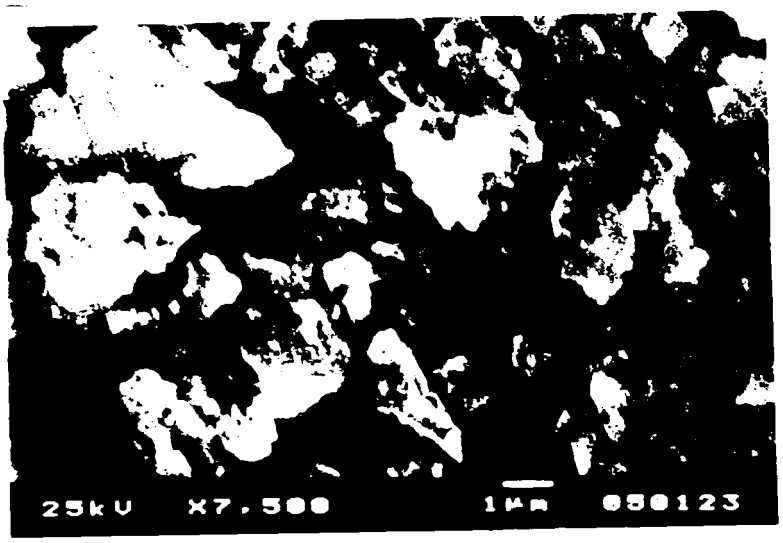

(a)

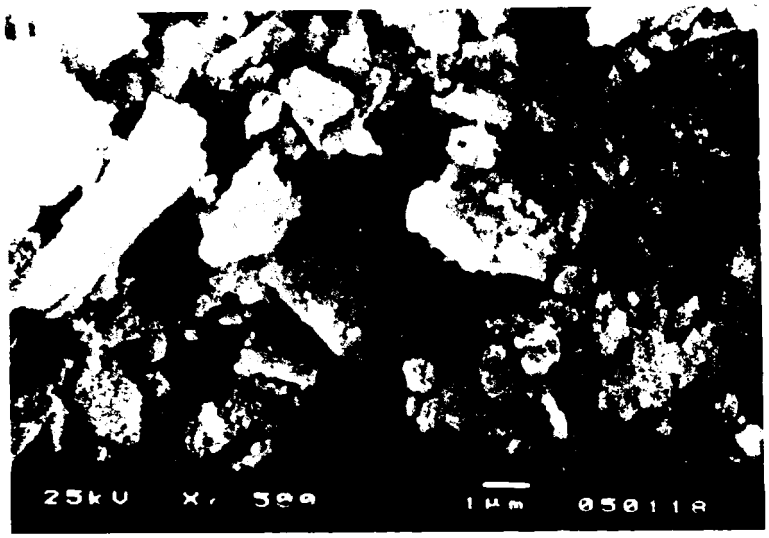

(b)

Fig. 5.14 SEM photographs of calcined a) Zr-AlPO-11(0.033) and b) Zr-AlPO-11 (0.066)

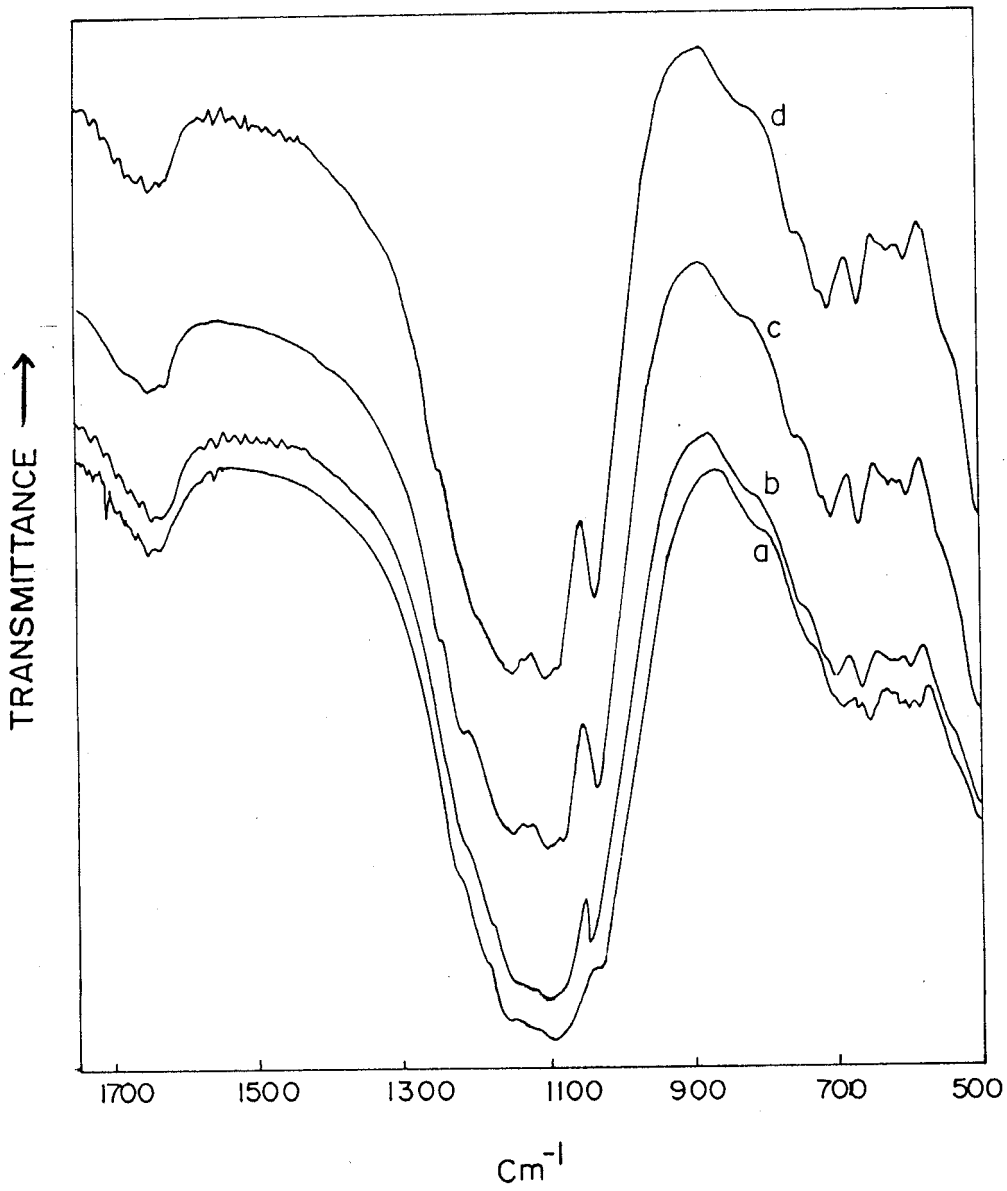

Fig. 5.15 FTIR spectra of a) AlPO-11, b) Zr-AlPO-11(0.033), c) Zr-AlPO-11 (0.066) and d) ZrAlPO-11 (0.1)

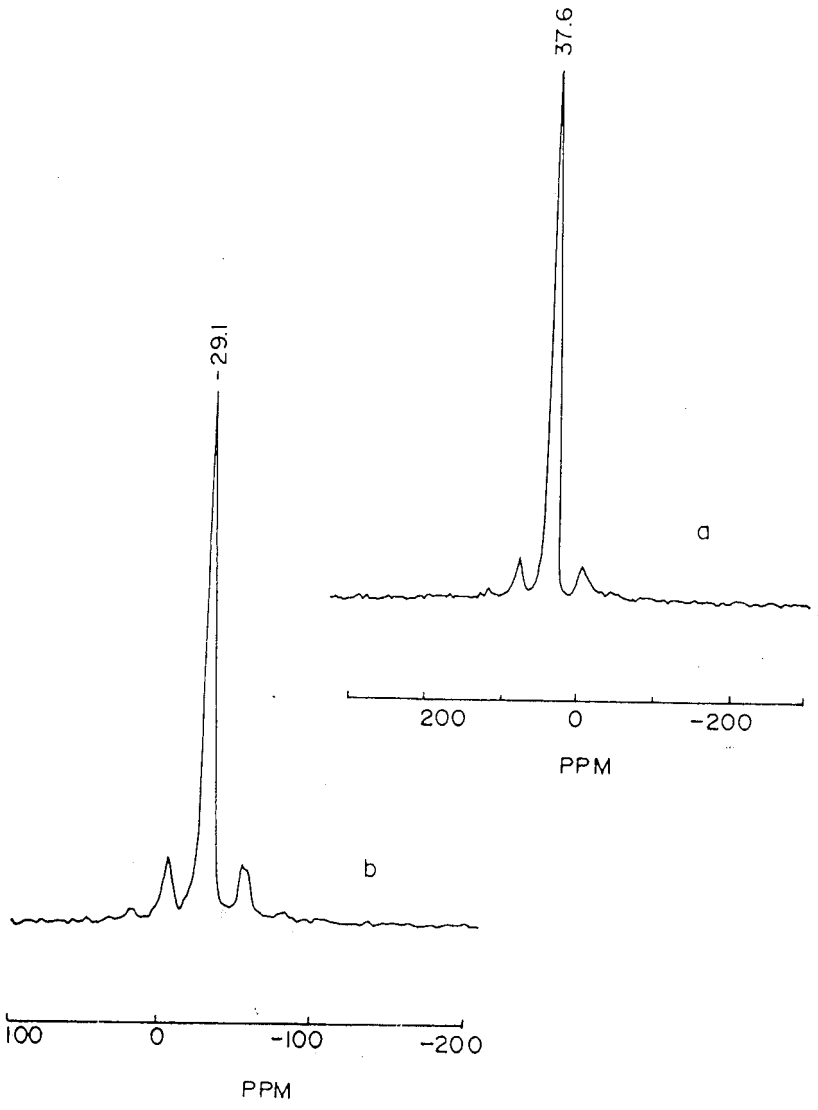

Fig. 5.16 The ^{27}Al and ^{31}P MASNMR spectra of calcined Zr-AlPO-11(0.1) sample (a and b respectively)

5.5.6 N_2 adsorption and BET surface area

The BET surface area, amount of H_2O and cyclohexane adsorption on Zr-AlPO-11 samples is presented in the Table-5.4. The values indicate that the samples are highly crystalline. Upon substitution of Zr in AlPO-11 lattice, the adsorption of N_2 and the surface area decreased. The possible reason[16] could be the condensation of N_2 around the zirconium centers, which could hinder and stop the diffusion and sorption of N_2. Similar observation was made in case of Zr-AlPO-5 samples as has been described previously. The results are in contrast to the findings of XRD, where in an expansion of unit cell volume of 9 $Å^3$ is observed.

5.5.7 Catalytic activity in n-hexane hydro-isomerization

The hydro-isomerization of light naptha is an industrially important process and is used in the production of high-octane gasoline blend stocks[52-53]. These reactions are generally carried over bifunctional catalysts, which often contains platinum. These reactions have already been studied over Pt-loaded zeolites, such as Pt-Y, Pt-Beta and Pt-Mordenite[54-56]. During the isomerization of n-paraffins, the shape selective molecular sieves suppress the formation of multi-branched isomers, which are more susceptible to hydrocracking thereby leading to higher isomer selectivity[57-58].

A process for lube dewaxing by wax isomerization has been developed at Cheveron[59]. A catalyst has been developed by loading platinum on the silicon substituted AlPO-11. The hydrogenation activity is balanced with acid activity, which exhibits high isomerization selectivity with high conversion and low selectivity for multiple branched isomers giving high catalyst stability. Such catalysts derived from some medium pore AlPO- molecular sieves are reported[60-61]. Work on the n-alkane isomerization over SAPO-5, SAPO-11, SAPO-31 and SAPO-41 has also been reported[62-64]. These studies have shown that the intermediate pore SAPOs make good isomerization catalysts.

Introduction of transition metals, like V, Ti, Cr and Zr at substitutional sites in aluminophosphate (AlPO-n) frameworks have also been reported to alter their catalytic properties. Therefore in this study, the activity of n-hexane hydroisomerization over Pt-Zr-AlPO-11 is also included.

The isomerization activity at the temperature of 300 and 325^{0}C are compiled in Table-5.6. The n-hexane conversion is higher on Pt/SAPO-11, where as the selectivity, for hexane isomers is better on Zr-AlPO-11. The product mainly consists of isomerized products such as 2,2 and 2, 3 dimethyl butanes (DMB), 2- and 3- methyl pentanes (MP) and cracked (C1-C5) products. It is observed from the table that the I/C (ratio of isomerized to cracked products) considerably decreases with increase in reaction temperature. The difference in the activity of these catalysts is probably due to their difference in acidity. The increase in conversion for Pt/SAPO-11 and Zr-AlPO-11 sample is due to the incorporation of Si and Zr respectively in the lattice, which gave rise to the formation of new acid sites. In the case of Pt/Zr-AlPO-11, the presence of Zr in lattice decreases cracking activity and favors isomerization there by increasing the I/C ratio.

5.6 CONCLUSIONS

Zr-AlPO-5 and Zr-AlPO-11 with different Zr content are synthesized and their physico-chemical characterization by XRD, SEM, MAS-NMR, FTIR and adsorption studies indicate that Zr can be incorporated in to the AlPO-5 and AlPO-11 structures. As a result of Zirconium substitution in AlPO-5 strcuture, bridging hydroxyl groups like Zr-OH-Al are generated. The Brönsted and Lewis acidity of the Zr-AlPO-5 is higher than that of AlPO-5. Therefore Zr-AlPO-5 shows better catalytic activity and stability in m-xylene isomerization.

Table-5.6

Catalytic activity of Pt/Zr-AlPO-11, Pt/AlPO-11 and Pt/SAPO-11 samples for hydroisomerization of n-hexane

	Pt/Zr-AlPO-11		Pt/AlPO-11		Pt/SAPO-11	
Product Distribution	300^{0}C	325^{0}C	300^{0}C	325^{0}C	300^{0}C	325^{0}C

n-hexane Conversion (%)	5.37	15.61	3.22	5.95	12.13	33.34
Cracking (C)	0.079	0.185	0.52	0.79	0.28	1.61
Isomers[a] (I)	4.843	13.76	2.60	4.8	10.67	28.38
Others[b]	0.448	1.66	0.10	0.36	1.18	3.35
Cracking (%)	1.47	1.185	16.15	13.39	2.28	4.83
Isomers (%)	90.19	87.96	80.77	80.72	88.00	85.12
I/C[c]	61.30	74.22	5	6.03	38	17.61

Conditions: WHSV= 1, H_2/n-hexane = 4, time on stream =1h.

a: Isomers of n-hexane such as
2,2 and 2, 3 dimethyl butanes (DMB), 2- and 3- methyl pentanes (MP)

b: Aromatic $C6^+$ compounds

c: Ratio of n-hexane isomerized / n-hexane cracked.

The catalytic activity of Pt-Zr-AlPO-11 for n-hexane isomerization shows increased isomer selectivity compared to Pt-AlPO-11. The increase in I/C is attributed to the presence of zirconium in the lattice, which decrease the cracking and favor isomer selectivity.

5.7 REFERENCES

1. Pyke D. R, Whitney P, and Haughton H., *Appl. Catal.* 18, (1985), 173.

2. Johan A. Martens, Wim Souverijns and P. A. Jacobs in *Comprehensive Supramolecular Chemistry* (Volume Ed. G. Alberti and Thomas Bein) Elsevier Sci. Inc. 660 White plains road Tarry Town New York NY 10591-5153 USA.

3. C. Montes, M. E. Davis, B. Murray and M. Narayana *J. Phys. Chem.* 94 (1990) 6425.

4. B. Kraushaar, W.G.M Hoogervorst, R. R. Andrea, C. A. Emeis and W.H.J Stork *J. Chem. Soc. Faradays Trans*. 87(6) (1991) 891.

5 Kornatowski J, Sychev M, Finger G, Baur W.H, Rozwadowski, M. Zibrowius B. *Proc. – Pol.-Ger. Zeolite Colloq,* (1992), 20-6 (Edited by: Rozwadowski, Michal. Nicholas Copernicus)

6. Han Shuyun. *Shiyou Huagong* 21(12) (1992) 811.

7. Bao Shulin, Xu Qinhua, Zhang Fangliang *Wuji Huaxue Xuebao*,7(3), (1991)311.

8. Akolekar D. B. *Appl. Catal* A 171(2) (1998) 261.

9. Sheldon, R. A. *Stud. Surf. Sci. Catal.*110 (3rd World Congress on Oxidation Catalysis) (1997) 151.

10 S. H. Jhung and Y. S. Oh. *Appl. Catal.* 62 (1990) 61.

11. a)A, Tuel and Y. Ben Taarit *J. Chem. Soc. Commun* (1994) 1667, b)A.Tuel *Zeolites* 15 (1995) 228., c)Akolekar Deepak Bansilal, Ryoo Ryong *J. Chem. Soc., Faraday Trans.* 92(22) (1996) 4617, d)Zahedi-Niaki, M. Hassan, Joshi Praphulla N, Kaliaguine Serge *Stud. Surf. Sci. Catal.*, 105B (Progress in Zeolite and Microprobes Materials, Pt. B), (1997) 1013., e)Vinje, Kristin; Lillerud, Karl Petter., Stud. Surf. Sci. Catal., 84 (Zeolites and Related Microporous Materials), (1994) 227.

12. Mityamoto., Y. Iwamoto ., H. Matsuda and T. Inui *Stud. Surf. Sci. Catal*. 49 (1989) 1233.

13. J. D. Chen., J. Dakka., E. Neeleman and R. A. Sheldon *J. Chem. Soc. Commun* (1993) 1379.

14 B. M. Weckhnysen and R. A. Schooheydt. *Zeolites*. 14 (1994) 360.

J. D. Chen and R. A. Sheldon. *J. Catal.* 153 (1995) 1.

15. Eswaramoorthy M, Jebarathinam N John, Ulagappan N,

Krishnasamy V. *Catal. Lett.* 38(3,4) (1996) 255.

16 J. Kornatowski, M. Rozwadowski, W. Lutz, M. Sychev. G. Pieper, G. Finger, and W. H. Baur. Zeolite Science (1994): Recent Progress and Discussions. *Stud. Surf. Sci. Catal.* 98 (1994) 13.

17 P. Meriaudeau, V. A. Tuan, L. N. Hung, F. Lefebvre and H. P. Nguyen., *J Chem. Soc., Faraday Trans.,* 93(23) (1997) 4201.

18 K. Tanabe, T. Yamaguchi, *Catal. Today* 20 (1994) 185

T. Yamaguchi, *Catal. Today* 20 (1994) 199.

19 D. A. Ward and E. I. Ko, *J. Catal,* 150, (1994) 18.

20 C. Morterra, G. Cerrato, F. Pinna, M. Signaretto and G. Strukul, *J. Catal*,

149, (1994) 181.

21 R. A. Boyse and E. I. Ko. *Catal. Lett.* 38 (1996) 225.

22 G. Alberti, M. Casciola, U. Costantino, and R. Vivani, *Adv. Mater*. 8 No. 4 (1996) 291.

23 U. Ciesla, S. Schacht, G. D. Stuky, K. K. Unger, and F. Schuth. *Angew. Chem. Int. Ed. Engl*. 35 (1996) 541.

24. D. A. Young U.S Patents 3 329 480 and 3 329 481 (1967)

25. H. Baltes, H. Litterer, E. I. Leupold, F. Wunder, Eur. Pat 77523 (1983) and Ger. Offen. De. 341 285 (1983)

26. M. K. Dongare, P. Singh, P. P. Moghe, P. Ratnasamy, *Zeolites* 11 (1991) 690.

27. Gui-Ru Wang, Xue-Qin Wang, Xiang-Sheng Wang and Shun-Xiang Yu, Stud. *Surf. Sci. Catal.* 83 (1993) 67.

28. B. Rakshe, Veda Ramaswamy. And A. V. Ramaswamy, *J. Catal,* 163, (1996) 501.

29. A. Tuel, S. Gontier, R. Teissier., *J. Chem. Soc. Chem. Commun* (1996) 651.

30. K. Eichler, E. I. Leupold, H. Arpe and H. Baltes., U. S. Patent 4, 720, 583 (1988).

31. Pauling L, *The Nature of Chemical Bond*, 3rd Ed, Cornell University 545, (1960).

32. Flanigen, E. M, Lok Brent M, Patton R. Lyle, Wilson Stephen T. *Stud. Surf. Sci. Catal., 28* (New Developments in Zeolite Science and Technology) (1986) 103.

33. S. G. Hegde. P. Ratnasamy. L. M. Kustov and V. B. Kazansky., *Zeolite*s 8 (1988) 137

34. D. Miller, E. John, B. Fahlke, G. Lawing, U. Haubenreisser, *Zeolites* 5 (1985) 53

35. N. Ulagappan and V. Krishanasamy., *J. Chem. Soc. Chem. Commun*. (1995) 373.

36. Z. Dang, B. G. Anderson, Y. Amenomiya and B. A. Marrow., *J. Phys. Chem*. 99 (1995) 14437.

37. P. A. Agron, E. L. Fuller Jr. And H. F. Holmes., *J. Colliod. Interf. Sci.*,

52 (1975) 553.

38. G. Busca, V. Lorenzelli, P. Galli, A. La, Gunestra and P. Patrono., *J.Chem. Soc. Faraday Trans.*, 83 (1987) 853.

39. S. G. Hegde. P. Ratnasamy. L. M. Kustov and V. B. Kazansky., *Zeolite* 8 (1988) 137.

40. B. Onida, Z. Gabelica, J. Lourenco and E. Garrone., *J. Phys. Chem.* 100 (1996) 11072

41. Csicsery, S. M., *J. Catal*., 108 (1987) 433.

42. Olson, D. H., and Haag, W. O., in "Catalytic Materials: Relationship between structure and reactivity ". ACS. Synp. Ser. No. 248 (1984) 275.

43. Vercruysse, K. A.; Klingeleers, D. M.; Colling, T.; Jacobs, P. A. *Stud. Surf. Sci. Catal*., 117 (Mesoporous Molecular Sieves) (1998) 469.

44. V. R Choudhary, D. E. Akolekar, *J. Catal.* 103(1991) 115.

45. J. Perez-Periente, E. Sastre V. Fornes, J. A. Martens, P. A. Jacobs, A. Corma *Appl. Catal* 69 (1991) 125.

46. a) B. M. Lok. C. A. Messina, R. L. Patton, R. T. Gajek, T. R. Cannan and E. M. Flanigen U.S. Patent 440 871 (1984), b) Alfonzo, M., Goldwasser, J., Lopez, C. M.; Machado, F. J.; Matjushin, M.; Mendez, B and Ramirez de Agudelo, M. M. *J. Mol. Catal. A: Chem*., 98(1) (1995) 35.

47. Bennett J. M. Dytrych W. J. Pluth J. J. Richardson J. W., Jr. and Smith J. V. *Zeolites,* 6(5) (1986) 349

48. M. K. Dongare, D. P. Sabde, R. A. Shaikh, K. R. Kamble and S. G. Hegde *Catalysis Today* 49 (1999) 267.

49. Blackwell, C. S.; Patton, R. L. *J. Phys. Chem.*, 92(13) (1998) 3965.

50. Barrie Patrick J, Smith Mark E and Klinowski, Jacek. *Chem. Phys. Lett*. 180 (1-2) 6, (1991).

51. Bennett J. M, Richardson J. W Jr. Pluth J. J and Smith, J. V. *Zeolites*, 7(2), 160 (1987).

52. Cusher N. A, Greenouch P, Rolfe J. R. K, ans Weiszman J. A. In Chap-5 "*Handbook of petroleum refining"*.

53 Refining Handbook, *"92, Hydrocarbon Processing"* 71, 195, 1992.

54. Leu L. J, Hou, L. Y, Kand, B-D, Li C, Wu, S-T and Wu J. C. *Appl Catal* 69, 49, 1991.

55. Guisnet M, Fouche V, Belloum M, Bourneville, J. P and Travers C. *Appl. Catal* 71, 283 (1991).

56. Chen J. K, Martin A. M, Kim Y. G and John V. T *Ind. Eng. Chem. Res*. 27, (1988) 401.

57. Ernst S. Weitkamp J, Martens J. A and Jacobs P. A. *Appl. Catal A: Gen*. 48, 1989, 137.

58. Martens J. A, Jacobs P. A and Weitkamp J, *Appl. Catal A: Gen*. 20 (1986) 239.

59. S. J. Miller. *Microporous Materials.* 2 (1994) 439.

60. Miller S.J, U. S. Patent, 4 689 138 (1987)

61. Miller S.J, U. S. Patent, 4 859 311 (1989)

62. Campelo J. M. Lafont F. and Marinas J. M. *J. Catal.* 156(1), (1995) 11.

63. Parlitz, B. Schreier E. Zubowa H. Eckelt R. Lieske E. Lischke, G. And Fricke, R. *J. Catal.,* 155(1) (1995) 1.

64. Meriaudeau P. Tuan V. A. Nghiem V. T. Lai S. Y. Hung L. N. and Naccache, C. *J. Catal.* 169(1), (1997) 55

SUMMARY

The present work was undertaken to study the incorporation of Ti and Zr cations in some microporous zeolites and alumino-phosphate materials. In view of the emerging prospects in industrial use, the isomorphous substitution of Ti^{4+} and Zr^{4+} ions in the lattice of MFI, MEL, AFI and AEL structures were selected for this study. Importance was given to the study of hydrothermal synthesis of these molecular sieves. The influence of various synthesis parameters on the nature of the product was analyzed using different physico-chemical techniques. In the initial part of this presentation, information available in the literature is reviewed and the general method of preparation of these molecular sieves is discussed with special reference to Ti and Zr incorporated microporous materials.

The synthesis of Ti containing molecular sieve with MFI structure (TS-1) using ethyl silicate-40(ES-40), a new silica source for zeolite synthesis is presented. Two different methods for the synthesis were used, which differed in the sequential addition of Ti alkoxide and tetrapropyl ammonium hydroxide (TPAOH). In each of the methods, samples with different Si/Ti ratios were prepared by varying the amount of titanium source (TBOT). The ^{29}Si and ^{1}H liquid NMR spectroscopy of TEOS and ES-40 showed that TEOS contained only monomeric silicate species, while ES-40 contained a variety of silicate species, including polymeric species containing Si-O-Si linkages. The ^{29}Si liquid NMR spectra were studied to understand the re-organization of silicate species in the precursor solution. The predominant emergence of Q^3 species, which are known to be the precursor for pentasil zeolites were observed when ES-40 was used as the source of silica. Therefore the rate of crystallization using ES-40 was faster than that of TEOS. The chemical composition of the product was determined by XRF method. It revealed enrichment of titanium in the product compared to that in the reactive gel. The XRD patterns of the crystalline TS-1 samples by both the methods I and II were identical to that

for TS-1 prepared using TEOS and showed orthorhombic symmetry before and after calcination. An increase in the unit cell volume was observed, which indicated the incorporation of Ti in the silicalite framework. The crystallites of samples prepared using ES-40 were cuboid in nature and of 0.1 to 0.2μm in size, which were smaller than those obtained using TEOS. The surface area by BET method and water, n-hexane and cyclohexane adsorption indicated that the products were highly crystalline and free from occluded impurities. The UV-Vis diffuse reflectance spectroscopy for samples prepared using method-I and low Ti containing samples prepared by method-II showed an intense band in the range 205-215nm indicating efficient Ti incorporation. The FTIR spectra of TS-1 samples prepared by method-I and method-II showed a characteristic band around 960 cm^{-1}, the intensity of which increased with the increase in the Ti content in the sample. The catalytic activities of various TS-1 catalysts prepared using ES-40 and TEOS in the oxidation of phenol and anisole using dilute H_2O_2 as oxidant were also studied. The TS-1 prepared using ES-40 showed high oxidation activity.

The synthesis, characterization and catalytic properties of zirconium-substituted silicate and alumino-silicate with MEL and MFI topology are presented in Chapter 4. Among the various TBAOH and zirconium sources used for the synthesis of Zirconium silcalite-2 (ZrS-2), only the samples prepared using alcoholic TBAOH and zirconium propoxide were found to be highly pure. On the contrary, the samples prepared from other sources of zirconium in combination with any type of TBAOH contained extra-lattice impurities. The samples prepared using zirconium alkoxide and alcoholic TBAOH showed proportional increase in unit cell volume with increase in zirconium content compared to the samples prepared using inorganic salts of zirconium. The samples prepared using other zirconium salts showed a limited lattice expansion. A shoulder (sh) at 970 cm^{-1} in the IR spectra in the framework region and a strong absorption band around 210 nm in the

UV-Vis region indicated that zirconium is incorporated in framework of MEL structure. As a result of zirconium substitution in MEL lattice, stronger Brönsted acid sites are generated compared to pure silicalite-2. ZrS-2 samples exhibited considerable catalytic activity in the hydroxylation of phenol, which further supported the incorporation of Zr^{4+} in the MEL lattice.

The crystalline alumino-silicate samples containing zirconium (AlZrS-1) with various Si/Zr and Si/Al ratios were prepared by the hydrothermal method. The XRD patterns of AlZrS-1 showed that the samples were crystalline and matched with that of ZSM-5 framework. The AlZrS-1 samples also showed increase in the surface area. The UV-Vis spectra for the H-AlZrS-1 with high Si/Zr and Si/Al ratios showed a single broad absorption band at 208 nm, where as H-AlZrS-1 with low Si/Zr and Si/Al ratios showed additional band in the region 258nm. The IR spectra in the framework vibration region exhibited a shoulder (sh) at 964 cm^{-1} in case of all AlZrS-1 samples, which is attributed to Si-O-Zr asymmetric stretching vibrations arising from the substitution of Zr in the framework. The FTIR spectroscopic studies of pyridine adsorption showed a decrease in the Brönsted and Lewis acid strength of the H-AlZrS-1 samples as a result of zirconium incorporation in ZSM-5 structure. The catalytic activity of H-AlZrS-1 samples for o-toluidine isomerization showed less conversion compared to H-ZSM-5 but increased m-isomer selectivity and catalyst life.

The synthesis, characterization and catalytic properties of zirconium containing aluminophosphate molecular sieves with AlPO-5 and AlPO-11 structures are discussed in Chapter 5. AlPO-5 and AlPO-11 molecular sieves with different Zr content were synthesized. The physico-chemical characterization by XRD, SEM, MAS-NMR, FTIR and adsorption studies indicate that Zr is incorporated in the AlPO-5 and AlPO-11 structures. As a result of Zirconium substitution in AlPO-5 and AlPO-11 structure,

bridging hydroxyl groups like Zr-OH-Al are generated. The amount of H_2O and cyclohexane adsorption on Zr-AlPO-5 and Zr-AlPO-11 samples indicated that the samples were highly crystalline. Upon substitution of Zr in AlPO-11 lattice, the adsorption of N_2 and the surface area decreased. The FTIR study of chemisorbed ammonia indicated that the Brönsted and Lewis acidity of the Zr-AlPO-5 was higher than that of AlPO-5. Therefore Zr-AlPO-5 showed better catalytic activity and stability in m-xylene isomerization. The catalytic activity of Pt-Zr-AlPO-11 for n-hexane isomerization showed increase in isomer selectivity compared to Pt-AlPO-11.

The following are the salient features of the present work.

1. It is possible to prepare highly pure TS-1 samples using ES-40 as the source of silica. The advantages of ES-40 are high rate of crystallization, high yield, better incorporation of Ti, smaller and uniform distribution of crystallite size and comparable activity in aromatic hydroxylation. ES-40 is comparatively much cheaper than TEOS and the process optimized here shows the commercial feasibility for the production of TS-1 catalyst.
2. Isomorphous substitution of zirconium in MEL and MFI structure is observed. ZrS-2 samples are active for hydroxylation of phenol. The catalytic activity of zirconium substituted ZSM-5 samples (H-ZrAlS-1) for o-toluidine isomerization is found to be superior to H-ZSM-5.
3. Zirconium containing alumino-phosphates with AFI and AEL topology can be prepared hydrothermally. The physicochemical characterization of these materials reveals that Zr occupies the tetrahedral position in the framework. As a result of zirconium incorporation, stronger Brönsted acid sites are generated Zr-AlPO-5 is found to be active in m-xylene isomerization and Pt/Zr-AlPO-11 samples show good activity and selectivity in n-hexane hydroisomerization.

4. It is possible to prepare Ti and Zr incorporated redox zeolites and microporous aluminophosphates in an industrially feasible manner by carefully choosing starting materials and adopting a proper preparation method.